DYNAMIC STUDIES ON THE BEARING CAPACITY OF PILES

Vol. 1

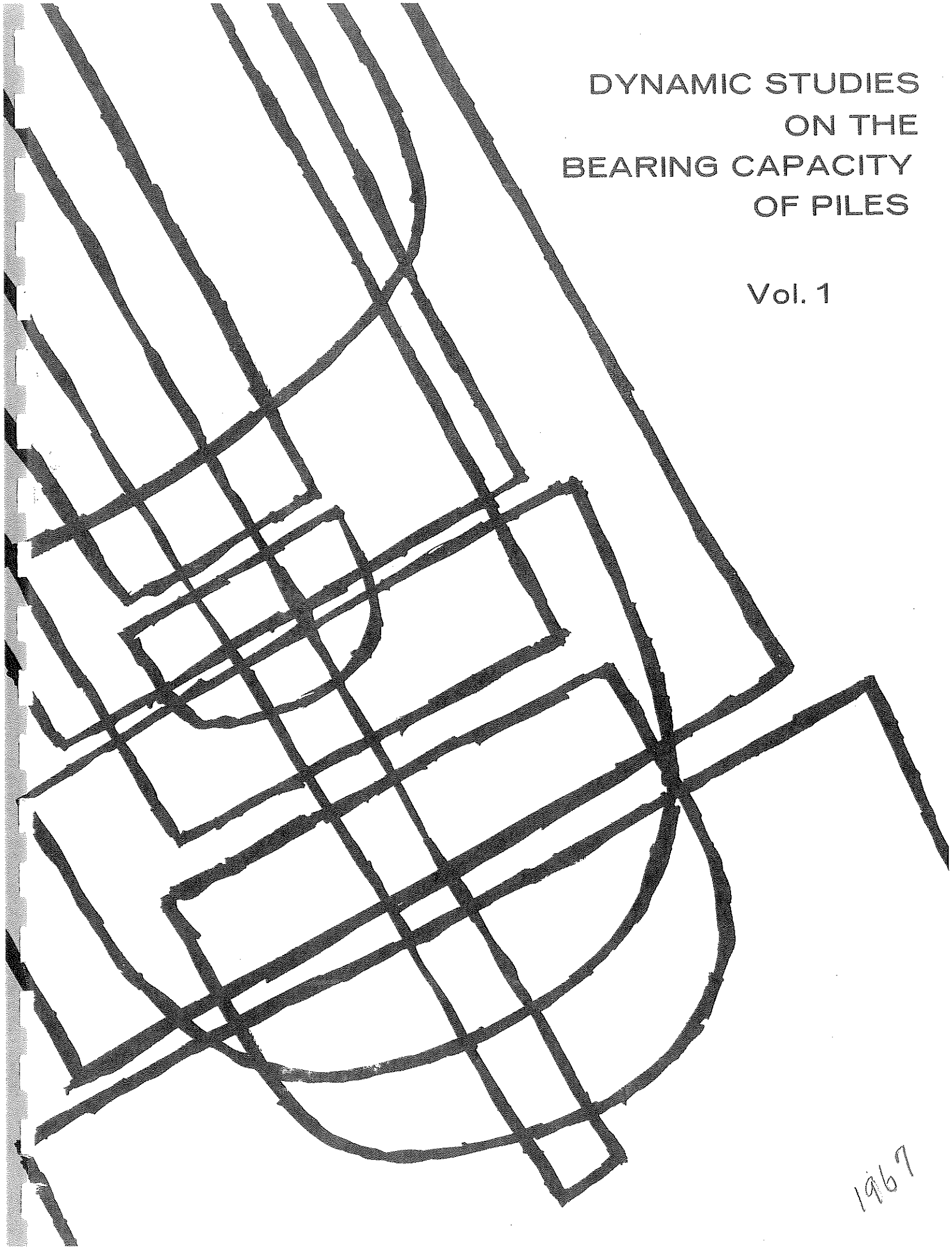

1967

DYNAMIC STUDIES ON THE BEARING CAPACITY OF PILES

Final Project Report

July 30, 1967

by

G. G. Goble

R. H. Scanlan

J. J. Tomko

Case Institute of Technology

This Research was sponsored by the Ohio Department of Highways and the Bureau of Public Roads. The opinions, findings, and conclusions expressed in this publication are those of the authors and not necessarily those of the State or the Bureau of Public Roads.

ABSTRACT

Developments in electronic instrumentation during the past few years make it possible to consider acceleration, velocity and force measurements of high-frequency phenomena such as occur during pile driving. Equipment has been developed to record acceleration and force near the top of a pile. Records have been made during the driving of a number of full scale steel pipe piles which were later load tested. Small scale piles were also driven and tested.

A theory relating dynamic measurements and static capacity is proposed. This theory has sufficient simplicity for use on a routine basis. Good correlation between the static capacity determined by the proposed theory from the dynamic record and the static capacity measured by load tests was attained. The proposed theory was also applied to dynamic records measured elsewhere with satisfactory results. This theory can not be expected to give a good measure of bearing capacity if the strength changes after driving. Therefore, it is suggested that the proposed theory be applied to records obtained by redriving piles in soils where strength gain is expected.

A literature survey was conducted with particular emphasis on experimental results. Analytical studies are reported which use both a humped mass and a continuous model of the pile.

As a secondary goal, results from fast and slow static load tests are reported and compared.

ACKNOWLEDGEMENTS

The project reported here was supported by the Ohio Department of Highways and the Bureau of Public Roads. The cooperation and advice on technical matters of P.Eckart, R. Dowalter, R. Grover, R. Ibos and A. Anderson, all of the Ohio Department of Highways, contributed substantially to the sucess of the project. In administrative matters the assistance of C.R. Hanes, Ohio Department of Highways was appreciated.

The analysis of the Michigan results was performed by W. S. LaPay. The efforts in equipment design and development of D. D. Bubb, J. P. Budlong and W. T. Thompson are acknowledged. F. Rausche assisted in the preparation of the report.

The assistance of National Engineering and Contracting Company in providing heavy equipment to perform load tests on model piles was particularly appreciated. The Horvitz Company and Arcole Midwest Corporation were construction contractors for the full scale test piles.

The authors are indebted to Dr. R. H. Nara for the original ideas leading to this work.

TABLE OF CONTENTS

CHAPTER 1

INTRODUCTION

The prediction of the bearing capacity of piles is a problem which has plagued Civil Engineers since antiquity. This problem has been studied for the past two hundred years. The general philosophy behind many studies has been that there is a high probability that information is generated during driving which can yield a measure of the static bearing capacity. Until recently, due to the high frequency dynamic effects, generated by the driving operation, permanent set was the only measurement which could be made reliably. This limitation led to the use of the energy approach upon which the numerous pile formulas are based.

Developments in electronic instrumentation and transducers in the past few years make it possible to consider making acceleration, velocity and force measurements of high frequency phenomena and to hope to make such measurements on a routine basis. The present project developed from the conviction that certain dynamic parameters must relate to static bearing capacity and that recent developments in electronic devices make possible (and practical) the measurement of these parameters. The purpose of the project was to study the relationship between selected dynamic parameters and static bearing capacity.

Based on a study of the experimental results obtained in

this project a simple force balance theory is proposed. This theory is presented in Chapter 2. Correlation of the theory with experimental results of both full scale and reduced scale piles and with piles tested elsewhere is given in Chapters 3 and 5.

A portion of the project was concerned with a literature review. The important results of this review giving experimental data are presented in Chapter 3. The apparatus used in tests performed in the project is described in Chapter 4.

The simplified model used in the study is based on an assumed rigid pile. It is possible that this assumption can lead to erroneous results in some extreme cases. Therefore, efforts have also been devoted to the study of the soil-pile system with an assumed elastic pile. One phase of this effort uses a continuous elastic pile with greatly simplified boundary conditions. The preliminary portion of this effort is reported in Volume II. Further work in this direction is required for more realistic boundary conditions.

Another effort used the elastic pile assumption with the model for the pile consisting of many discrete masses interconnected by springs. Thus, considerable freedom was possible in the selection of the boundary conditions and also in the treatment of soil and pile properties. This study is also discussed in Volume II.

A number of "static" load tests were conducted in connection with this project. It became apparent that this area also requires further study. Data was obtained using a number of different loading

rates and methods. While this topic was not the primary one for study, useful information was obtained and is reported.

The experimental results obtained in this project and elsewhere support the proposed simplified analytical model. This description of pile behavior has sufficient simplicity for application in practice. Experience with the electronic equipment indicates it will be possible to develop the devices necessary for routine application of the method. Further experimental results are necessary to verify the theory and define limitations.

CHAPTER 2

SIMPLIFIED ANALYTICAL MODEL

Consider the pile to be a rigid body struck by a time-varying hammer force, F(t). Consider further that the total earth resistance, R, on the pile is also a function of time; R will oppose F. Newton's equation then governs the situation, where m is the mass of the pile and the acceleration, a, is a function of time:

$$F - R = ma \qquad 2.1$$

The action of the forces is shown in the free body diagram of Figure 2.1.

Now it may be assumed that R takes the form of a series in the velocity, v, of the pile:

$$R(t) = R_0 + R_1 v + R_2 v^2 + R_3 v^3 + \ldots \qquad 2.2$$

where R_0, R_1, R_2 etc. are constants (Poncelet's Law). The first of these constants, R_0, represents the static bearing capacity of the pile, since it is equal to the earth resistance when v = 0. Therefore, in the dynamic equation 2.1 above, it becomes very desirable, in seeking the static value, R_0, of R, to ascertain values of F and a at that instant when v is zero.

To this end the instrumentation employed (an accelerometer and a strain gage at the top of the pile) is such as to visualize the dynamic, time-varying values of both F and a. Since $\frac{dv}{dt} = a$,

or

$$v = \int_0^t a \, dt \qquad 2.3$$

it is possible to know v from the integration of an accelerometer record giving a. The value of F is obtained from a knowledge of the strain in the pile through strain-gage measurements or from strain measurements on a transducer. F is related to time-varying strain, $\varepsilon = \varepsilon(t)$, by

$$F = AE\varepsilon \qquad 2.4$$

where E is the modulus of elasticity of the pile material and A is the pile area.

The procedure for determining R_o is then to integrate a(t), find v(t), pick the point in time, t_o, where $v(t) = 0$, and read F and a at this point: $F = F(t_o)$, $a = a(t_o)$. At this point $R = R_o$, so that the force balance, equation 2.1, is:

$$F(t_o) - R_o = ma(t_o)$$

Hence

$$R_o = F(t_o) - ma(t_o) \qquad 2.5$$

In practice, $v = 0$ always occurs at a point in time where the acceleration is <u>negative</u> (deceleration) so that the practical calculation consists of the addition of an inertia term $ma(t_o)$ to a force term $AE\varepsilon(t_o)$. This sum is then taken as the desired approximation to the static resistance of the soil.

CHAPTER 3

SURVEY OF EXPERIMENTAL LITERATURE

A portion of the project was concerned with a literature investigation. The primary purpose of this work was to obtain experimental data which could be of use in verifying any theory which might be proposed. A bibliography of the papers reviewed is given in Volume II of this report. The only useful experimental data found, from the standpoint of this study, is contained in tests reported in references 3.1 and 3.2. The results of these tests will be reviewed briefly with emphasis on their application to this project.

In connection with the literature study a review of all dynamic driving formulas was made and is discussed briefly in Volume II. A more detailed discussion is contained in reference 3.3.

Eiber (Ref. 3.1) made acceleration measurements during the driving of small scale piles in sand in the laboratory. He applied the basic idea presented in Chapter 2. However, he measured acceleration only and considered the total moving mass (hammer, capblock and pile). In equation 2.1 F is zero and the resistance at zero velocity is equal to the inertia force of the total mass of the system. Acceleration records usually have a very jagged character. Therefore, a small difference in the location of the time of zero velocity can lead to a substantial difference in the magnitude of

the acceleration. This problem was partially overcome by smoothing the acceleration record. Smoothing was accomplished by integrating the acceleration record and then obtaining the slope of this curve in the region where its ordinate is zero.

Eiber's work was useful in exploring the general feasibility of the application of equation 2.2 and the practicality of the measurements. The experimental results cannot be used for verifying equation 2.5 because force measurements are not available.

The Michigan study (Ref. 3.2) of the performance of pile driving hammers and piles provided the only results found in the literature which could be applied in the work reported here. A number of full scale piles were driven under controlled conditions at three different sites. Of primary interest were the force and acceleration measurements made on piles which were later load tested statically. Force measurements were made with a strain gage force transducer introduced into the driving system between two driving caps as shown in Figure 3.1. An accelerometer was attached to the force transducer and oriented along the axis of the pile. Force and acceleration were recorded and published in the project report. Records of static load tests were also reported.

It is possible that there were energy losses between the transducer and the pile due to impact. It should also be noted that tension forces will not be measured by the transducer so that any portions of records showing a tension force have no meaning. However, in applying the proposed theory the point of zero velocity

always occurs prior to the force record indicating a tensile force. Acceleration records were obtained from a single accelerometer mounted at the edge of the base of the force transducer. Any motions due to bending or rotation of the pile will give an output which is different than the motion at the centerline of the system.

The load testing procedure used in the Michigan Test was different from either of the two procedures used in the tests reported here. In the Michigan tests increments of load were applied at 30 minute intervals and held constant during this period. Some of their tests were carried to very large settlements (in excess of 12 inches). Their results indicate that the pile continued to gain strength slowly with a "strain hardening" effect. Load tests conducted according to the procedures outlined in Chapter 4 did not show this effect.

The data published in reference 3.2 was analyzed using the theory proposed in Chapter 2. The results are given in Table 3.1.

Correlation for the piles driven at Muskegon was fair. LTP-2, LTP-6 and LTP-9 were 12-inch pipes and LTP-3 was a 12-inch fluted tapered pile. LTP-2 and LTP-3 were both imbedded about 58 feet in loose sand. LTP-6 and LTP-9 were driven 128 feet through about 60 feet of loose sand and the remaining length through layers of sand, silt, and some clay all with varying amounts of organic material present. All piles were load tested after the elapse of some time. It should be noted that the load test value in every case exceeds the dynamic prediction.

The correlation on the Detroit piles was less satisfactory. LTP-1 was an open end pipe pile driven into soft clay. This pile was load tested three hours after driving and at three later times up to ten days after driving. The load capacity shown is that at the end of driving. The remaining Detroit piles all driven through the soft clay into hardpan did not correlate as well as might be expected. Perhaps a portion of this discrepancy can be attributed to the increase in capacity with time due to "set-up".

The soil at the Belleville site consisted of 45 feet of stiff-to-firm clay overlying 14 feet of silt and fine sand with clay laminations. Under these layers was a hard till clay. LTP-1 was an open ended 12-inch pipe pile which was load tested immediately after driving and subsequently five additional times, the last 51 days after driving. The capacity varied from 60 tons to 105 tons. The soil was removed from the inside of this pile by jetting. LTP-3 was a fluted-tapered pile driven through the clay into the sand and silt layer. LTP-5 was a 12-inch pipe pile and LTP-6 was an H-pile. They were both driven to about the same depth as LTP-3. The correlation of LTP-1 was quite good. In this case the load test was made about 4 hours after the completion of driving. All the other piles were tested several days after driving (LTP-6 was tested 41 days later).

It should be noted that the Muskegon piles were driven after the others and less difficulty was encountered with instrumentation. However, all of the acceleration records were

adjusted to assure that the maximum displacement calculated by double integration of the acceleration was the same as that which was taken while driving.

CHAPTER 4

EXPERIMENTAL STUDY

4.1 Introduction

In applying the theory proposed in Chapter 2 it is necessary to measure acceleration, velocity and force at the top of the pile. At the time of initiation of the project it was not clear what information would be required. However, if acceleration and force measurements are available many other parameters can be calculated.

Given the goal of measuring force and acceleration near the top of the pile the type of instrumentation becomes fairly clearly defined. However, the development and use of this instrumentation on a routine basis is not a simple task, particularly in view of the conditions on a pile driving project (dust, steam, oil spray and time urgency). Instrumentation design requirements for the acceleration channels were set at a frequency limit of 1000 cps with acceleration up to 500 g. The same frequency requirements were designed into the force recording system although it appeared less critical than for the acceleration channels. It was desired to obtain some kind of strip recording to provide a complete permanent time record of the phenomenon.

4.2 Dynamic Recording Equipment

Initially it was desired to make both acceleration and strain measurements by easily attachable transducers. The

acceleration measurement caused no problem since acceleration transducers are commercially available in a wide variety of types. In this case the Kistler model 808A piezoelectric accelerometer was selected for its wide band width and linearity up to 8000 cps. The accelerometer characteristics are given in Table 4.1 and it is shown with its attachment device in Figure 4.1.

A block diagram of the instrumentation used in recording the signal from the accelerometer is shown in Figure 4.2. A Kistler Model 568 Universal Electrostatic Charge Amplifier and a Kistler Model 567 Power Amplifier were used in amplifying the accelerometer output to drive the light beam galvanometer of the Honeywell Visicorder. The Visicorder has a top recording speed of 80 inches per second on the time base, making a 1000 cycle trace quite readable. The galvanometer was linear up to 1000 cps. Thus, there is a difference between the frequency response limits of the accelerometer and the galvanometer, the accelerometer having a much higher natural frequency.

A check on the calibration of the acceleration signal was accomplished by carefully turning the axis of the accelerometer through 180 degrees resulting in an output of $\pm$ 1 g. The sensitivity of the charge amplifier was then adjusted to give a convenient recording deflection. Knowing the gain setting used when recording, the acceleration necessary to obtain a particular galvanometer deflection could be determined.

Some difficulties occurred in developing this instrumentation

system. The primary difficulty was encountered when a zero shift occurred on the acceleration record. Investigation with an oscilloscope showed that very large accelerations associated with high frequency vibrations caused overloading of the charge amplifier. These accelerations had a rise time too fast for the galvanometer to follow. This problem seldom occurred with the full scale pile because of the mechanical filtering effect of the driving cap. The problem was avoided with the model pile by placing a wooden block and a rubber cushion between the hammer and the pile end. These acted, in effect, as low-pass mechanical filters.

Considerable difficulty was encountered in attempting to develop a strain transducer which could be easily attached to the side of the pile. In the early part of the project experimentation was conducted on a proposed device. It was impossible, using this device, to obtain reproducible results for either static or dynamic conditions. In order to expedite the main goals of the project, work on this device was discontinued until the late stages of the project. In the mean time strain measurements were made from strain gages applied directly to the pile. The fundamental difficulty with the strain transducer under development was finally diagnosed to be excessive stiffness, resulting in large forces being transmitted to the attachment pens, thus, causing yielding to occur at these points. Flexible strain transducers are presently being designed and evaluated with regards to sensitivity, reproducibility, and frequency response limitations.

All of the strain data reported here were obtained from strain gages attached directly to the pile. Four gages were used with pairs connected in series to cancel out the effects of cross bending, and two strain records were recorded. This provided back-up records in case gages were damaged during handling and driving of the piles. Conditioning of the strain signal was accomplished with a Honeywell Carrier Amplifier Model 131-2Cr. Since the device is basically a full bridge instrument three legs of the bridge were built into the termination box and only a single active gage was used. The strain transducers under development will make use of a four arm bridge and hence increase the output from the transducer.

The strain gages were all epoxy-backed, foil resistance gages manufactured by Micro-Measurements, Inc. The waterproofing procedure was usually as follows: After attaching the lead wires using a terminal strip, the gage was coated with W.T. Bean Gagecote number one and the ends of the lead wire with Gagecote number two. The entire assembly was then coated with a very thick coating of Gagecote number five. This system provided both waterproofing and mechanical protection.

The recording instrumentation is shown in Figure 4.3. This instrument package could be driven by either a small portable generator or line power.

All of the equipment was mounted in a small truck. This system made it possible to visit a full scale pile site on short notice. Figure 4.4 shows the recording setup at a model pile site.

A sample of a typical record taken from a model pile is shown in Figure 4.5.

4.3 Model Pile Driving Equipment

To test out the proposed theory it was necessary to obtain as much data as possible. Since full scale test piles would be driven infrequently on Ohio Highway Department projects and driving conditions would be those associated with the usual construction conditions and not particularly conducive to trial and proving of electronic equipment, small scale piles were tested. Consideration of the use of laboratory conditions versus small piles driven in the field led to the selection of field sites. Driving and measurements would be simpler in the laboratory but the assembly of field soil conditions would be substantially more difficult and open to question. The selection of the pile size and pile material was based on practical considerations. No attempt was made to model any existing piles or classification of piles. The pile was considered to be a full scale structural system.

Standard 2-1/2 inch, nominal diameter steel pipe was selected to represent the pile. The pipe was cut into five foot sections and threaded internally for a distance of three inches at each end. Splices were made with a hollow externally threaded steel plug. Figure 4.6 shows a detail of the connection. This system provided the ability to drive different lengths of piles and made possible the use of a smaller driving rig.

The effect of the connections on the propagation of the stress wave in the pile was investigated in the laboratory prior to the field experiments. Two sections of pile, one ten feet long and one composed of two five foot sections connected as described above were used. An impact force was then applied to each pile and the accelerations were recorded. No significant change in the elastic wave as indicated by the character of the acceleration trace could be detected. Thus, it was assumed that the small scale pile system adequately duplicated the behavior of a single piece of pile or a pile composed of welded sections.

The bottom of the pile was plugged with a threaded cap shown in Figure 4.7. This cap was instrumented with strain gages as shown to provide a force transducer. The strain gage leads were taken up the inside of the pile to the instruments. The detail at the top of the pile is shown in Figure 4.8 and the termination boxes in Figure 4.9.

The pile was driven by means of a drop hammer. The driving rig, Figure 4.10 consisted of two 5 x 5 x 5/15 inch angles, 16 feet in length. For convenience and ease of transportation the angles were cut into eight foot lengths and field-bolted together. The angles were positioned as shown in Figure 4.1 so that they would serve as guides for the hammer. They were tied together at the top by an inverted channel, on top of which a pulley was mounted. The guides (angles) were also tied together at five foot intervals by 3" x 2-1.2" angles to provide added stability and insured

proper spacing. This driving system was held in the vertical position by guy lines. The system was erected in the field using the large, lightweight aluminum tripod shown in Figure 4.4.

The drop hammer consisted of an eight inch diameter steel cylinder weighing 166 pounds. Small angles bolted to the side of the hammer, held it in the guides and made it easily removable.

To prevent high frequency vibrations resulting from metal to metal impact, a cushion block was used. The cushion consisted of a wooden plug and rubber insulator inserted into a steel cap block. The driving cap block slipped into a brass bushing which was threaded into the top of the pile to protect the internal threads of the pile. The cap block provided alignment and held the top of the pile in position by means of a notched half inch steel plate fitting between the guide angles. The driving cap and its assembly is illustrated in Figure 4.8.

To maintain a constant drop height, the device shown in Figure 4.10 was constructed. It consisted of four 7/8 inch threaded rods eight feet in length, extending from the driving cap to a one-fourth inch aluminum plate at the top. The hammer was lifted to a three-quarter inch rod extending from the upper plate before being released. Since the assembly was attached to the driving cap it moved with the pile and provided a control of the drop height. The threaded rods provided adjustability of the drop height.

The hammer was lifted manually using a pulley arrangement with a mechanical advantage of two. The hammer was attached to the lower pulley with a electromagnet. The magnet can be seen in Figure 4.10. The hammer was lifted to the desired height and the current to the magnet was then shut off resulting in the release of the hammer. The magnet was then lowered, the current turned on, and the process repeated.

A check on the energy losses due to friction between the hammer and leads was performed in the laboratory. Photo cells were placed a measured distance apart in the driving leads near the driving cap. The hammer was then released from different heights and the time recorded for the hammer to pass between the two photocells. From this the velocity and the energy loss could be determined. The results of these tests are shown in Figure 4.11.

4.4 Model Pile Load Tests

Two types of load tests were used to determine static pile capacity, the Standard Ohio Highway Department load test (M.L. Test), and the constant rate of penetration test (C.R.P. Test).

The M.L. Tests were performed in accordance with the procedure specified by the Ohio Department of Highways (Ref. 4.1). In this procedure an initial load of 4/5 R is applied. The load R is determined from information obtained during driving using the equation

$$R = \frac{3F}{S + C_1} \qquad 4.1$$

where S is the penetration in inches per blow, C_1 is a coefficient varying from 0.10 to 0.30 depending on soil conditions and the type of cushioning used in the driving mechanism and F is wh for the case of single acting hammers. W is the weight of the striking parts of the hammer in pounds and h is the height of fall in feet.

An additional increment of load amounting to 1/5 R is applied after all measurable settlement has ceased. By measurable settlement is meant settlement of less than 0.01 inch in a 20 minute period.

Additional increments of load of 1/5 R are applied after measurable settlement ceases. The elapsed time between the end of measurable settlement and the application of an additional load increment is increased by one hour for each load increment. The settlements are measured upon application of the initial and incremented loads and at 20 minute intervals thereafter.

M. L. Tests were terminated when the ultimate load capacity of a pile was reached and not at the "failure load" as defined in the Ohio Department Specifications, Section 5-17.02. The ultimate load used in this context is defined as that load which results in an infinite set.

Upon completion of the conventional M.L. Test a C.R.P. Test was performed. Only a C.R.P. Test was performed immediately upon completion of driving. Also in some cases the M.L. Test was not performed after the wait period due to the time required for performance. The C.R.P. Test rate varied from 0.002 inches per

minute to 0.010 inches per minute depending upon previous tests of the same soil condition and the total set recorded from the M.L. Test, if one has been performed.

The C.R.P. Test was terminated when the ultimate load capacity of a pile was reached as defined in the case of the M.L. Tests.

The apparatus used for both the C.R.P. and M.L. Tests was the same. A 15-ton capacity hydraulic jack was used to obtain the desired force by manually jacking against a dead weight of approximately 25-tons or more (a piece of heavy equipment furnished by National Engineering and Contracting Co. or by the Ohio Department of Highways), thus eliminating the need for anchor piles. The applied load was recorded using a strain gage force transducer as shown in Figure 4.12.

The deflection or set of the pile was measured with four linear displacement potentiometers placed around pile at 90° apart and mounted to a reference frame fixed to the ground. This arrangement yielded an average set of the pile, taking into consideration any rotation of the pile resulting from eccentric loading. The displacement indicator used is shown in Figure 4.3.

The rate of penetration was controlled by a separate linear differential transducer mounted to the same reference frame when a C.R.P. Test was performed. The entire set-up of the load test apparatus for a model pile is shown in Figure 4.12.

4.5 Full Scale Driving

A number of full scale piles were tested during the course of the project. These piles were made available to the project by the Ohio Department of Highways in connection with bridge construction projects in Northeastern Ohio, and were piles which were later load tested. No provisions were made for such tests in contractural arrangements with contractors responsible for construction. Thus, project personnel were on the construction site with the cooperation of the contractor. This required that all measurements be made quickly and with a minimum interruption and disturbance to the contractor. Dynamic records were taken under two circumstances. When sufficient advance notice could be given by the contractor (through the Ohio Department of Highways inspector) the pile was instrumented a short distance below the driven end with strain gages and the pile was prepared for attachment of the accelerometer mounting. After the pile was placed in the leads the instruments were connected. Records were taken during the final blows. Frequently, records of test piles were not obtained due to the short notice of driving given by the contractor. Furthermore, if pile strength developed slowly as is commonly the case with some soils, measurements during driving cannot be expected to predict strengths not present. Thus, it proved useful to redrive the pile after load testing. In these cases instrumentation could be applied prior to driving and the contractor then suffered a minimal delay.

Recordings made during full scale tests included strain

records from two pairs of series strain gages and one or two accelerometers. A typical record is shown in Figure 4.13.

4.6 Full Scale Load Tests

The procedure used on the full scale piles with regard to M.L. Tests was similar to that used for model piles. The essential difference in the M.L. Test was that the load application was complete when an additional increment of load caused the settlement to exceed 0.02 inch per ton of load increment or when the total load exceeded 3R, and not when the ultimate load capacity was reached as defined previously in Section 4.4 of this report.

The measurement of load was accomplished by using a pressure gage on the hydraulic jack and the settlement was measured by one mechanical displacement gage.

These tests were conducted under the supervision of Ohio Department of Highways personnel. After the completion of the M.L. Test a C.R.P. Test was run on some of the test piles by project personnel. The rate of penetration differed on some tests and is given in the results.

For the C.R.P. Test all measurements made during the slow load tests were repeated. In addition, strain measurements were made from resistance gages installed near the top of the pile. From strains, pile loads could be calculated. Readings were taken from two pairs of gages. This load measuring system proved to be very sensitive. Comparative results are given in Chapter 5. Additional load was applied until failure occurred either by reaching the ultimate load capacity of the soil-pile interface or by yielding in the steel.

CHAPTER 5

RESULTS AND DISCUSSION

Based on the results obtained from this project the simplified analytical model presented in Chapter 2 shows promise in predicting ultimate static capacity. A more elaborate model following the general approach presented in Volume II, Chapters 3 and 4 may be necessary to define the limitations of the simplified model. It may be possible to use the results of elastic pile analytical studies to modify the simplified results for cases where realistic limits are exceeded. The elastic pile analytical studies are only in the initial stages and extensive further work must be done to obtain practical results.

5.1 Model Pile Dynamic Results

Using the instrumentation and driving system described in Chapter 4, small scale piles were driven into a medium coarse sand at a location made available by the Ohio Department of Highways near one of their active construction projects. The driving site was at West 14th Street and Abbey Road, Cleveland, Ohio. Piles were spaced not more than fifteen feet apart and not less than six feet apart. According to previous soil borings made under the supervision of the Ohio Department of Highways, the soil was classified as a well-graded sand. The physical characteristics of all model piles driven are shown in Table 5.1.

A summary of the results of model piles driven and load tested at this location is presented in Tables 5.2 and 5.3. Table 5.2 gives results of static capacity obtained by a C.R.P. Test compared to the dynamic prediction based on data obtained at the end of driving. The first column designates the depth to which the pile was driven below grade and its corresponding sequence number. For example, pile 15-3 means, the third pile of a series driven 15 feet below grade. The C.R.P. test was performed about three hours after the end of driving. Table 5.3 gives results of static capacity measured after a minimum three day waiting period compared with the dynamic prediction obtained by redriving after the load test. It should be noted that for pile 13-1, 15-1, and 15-2 redriving was not accomplished. Correlation must be attempted by comparing the dynamic prediction at the end of driving with the static strength after setup period. The necessary values are given in Table 5.2 and 5.3.

Complete data were not always obtained for the test piles reported in Tables 5.2 and 5.3. For the first three piles the test equipment and procedure was being developed. Some measurements were not obtained due to equipment malfunction. Also since the mathematical model was under development it was not yet decided what measurements would be required. Only a very limited number of M.L. tests were performed due to the time required for their performance.

The general procedure developed was: first the pile

was driven to the desired depth and dynamic measurements were taken during the last 10 blows, a C.R.P. Test was then performed as soon as possible. After waiting for at least three days, a M.L. Test was performed. Upon completion of this load test, a C.R.P. Test was performed, and immediately thereafter the driving rig was once again erected, the pile was struck about 10 times and dynamic recordings were taken. For piles 15-4 to 15-7 no load tests were performed immediately upon completion of driving due to lack of time.

By examining the results presented it can be seen that there is good agreement between the predicted load capacity and static load capacity. Based on the load tests performed no difference greater than 18% is found. It is clearly seen, however, that the long-term ultimate bearing of a pile cannot be reliably determined by measurements at the end of driving. The strength of the soil-pile interface builds up (or in certain circumstances may decrease) as time proceeds. However, a good prediction of final strength is obtained if the pile is restruck after it has been in the ground for some time as evidenced by the results given in Table 5.3. Corresponding to an increase in bearing capacity is a decrease in set per blow as shown in the last column of the table. It is interesting to note that the inertia contribution to the total dynamic bearing capacity of the pile is substantial; in some cases more than 50% of the total load capacity.

Shown in Figure 4.5 is a typical record of a model pile

taken in the field. The method of obtaining the results given in Tables 5.2 and 5.3 is as follows: The acceleration traces are replotted on graph paper to a convenient scale. The ordinate values are converted into units of acceleration, i.e. g's, from the calibration of the accelerometer. The abscissa scale on which the units are in milliseconds, is also adjusted for ease of analysis. This time-acceleration curve is then integrated to obtain the velocity of the pile as a function of time. At the point of zero velocity the values of acceleration and the corresponding force in the pile are obtained. These values and the geometric properties of the pile are substituted into equation 2.5. Corresponding to the first zero velocity point, the acceleration is negative because the pile is decelerating.

As a sample calculation consider model pile No. 15-3, blow number 1A that was obtained after a C.R.P. Test was performed on August 23, 1965. From Figure 5.11, the point of zero velocity (V=0) occurs at 7.7 milliseconds. The corresponding force and acceleration at this time are 13.6 kips and -66.0 g's respectively. The mass of the pile used in calculating the inertia force is that mass which lies between the location of the strain gages and the pile tip. For this case, the mass is 107.1/g as shown in Table 5.1. Substituting these values into equation 2.5 gives the predicted static bearing capacity

$$R_o = 13.6 - \left(\frac{107.1}{g}\right)(-66.0\ g) = 13.6 + 7.06 = 20.66 \text{ kips}$$

Curves giving the static and dynamic record for model piles will be discussed. These curves were carefully plotted from the original record and were used in determining the results presented in Tables 5.2 and 5.3. The results of test pile 13-1 are given in Figures 5.1 and 5.2. A number of blow records were actually examined to make sure the record obtained was typical. Both a C.R.P. and a M.L. Test were performed. Although the load displacement curves differ substantially they show nearly the same value for ultimate capacity.

Figures 5.3, 5.4 and 5.5 show the results of tests on pile 15-1. Successive records of acceleration and velocity are given in Figures 5.3 and 5.4. The similarity of these records shows the reproducibility of the results. Acceleration peaks are closely duplicated as is their time of occurrance. The velocity records show even better reproducibility. Their peak values and time of zero velocity are identical.

The results for pile 15-2 are given in Figures 5.6, 5.7 and 5.8. Figures 5.7 and 5.8 show the results of three C.R.P. Tests and one M.L. Test. There C.R.P. Tests were run at the same rate and repeat well. They show nearly the same maximum value as the M.L. Test.

Figures 5.9, 5.10, 5.11, 5.12, 5.13, and 5.14 show the results of tests on pile 15-3. Three changes in procedure are evident here. The pile tip force transducer was added. The pile was given a C.R.P. Test immediately after driving and it was redriven

after final load tests. Figure 5.12 indicates small increases in maximum velocity for the second blow as compared to the maximum velocity of the first blow shown on Figure 5.11. The time of zero velocity has become somewhat later for the second blow. For the load tests it is possible to separate side force and tip force. Comparing Figures 5.10 and 5.14 there is a increase of approximately 15% in bearing capacity. An M.L. Test was not run to save time.

The results for pile 15-4 are given in Figures 5.15, 5.16, 5.17, and 5.18. Again the velocity record on redriving shows an increasing peak and a later zero. An M.L. Test was not performed.

Figures 5.19, 5.20, and 5.21 show the results from pile 15-5. For unexplained reasons this pile had a substantially greater capacity than other piles in the same area. The same changes are noted in the velocity on redriving. An M.L. Test was attempted on this pile. At a load of 16 kips the compactor, which supplied the dead load for testing, shifted destroying the instruments. A load test was not made in view of the high predicted capacity.

Results for piles 15-6 and 15-7 are given in Figures 5.22 through 5.29.

5.2 Full Scale Piles

The piles tested were 12-inch diameter steel pipe piles having a variety of wall thicknesses and lengths and driven into

different soils as given in Table 5.4. The results are not nearly as complete as in the case of model piles because of lack of cummunication between contractor, state inspector, and pile project personnel and many other problems associated with field work. Nevertheless, the available results present a favorable picture considering the conditions in which they were obtained. The method used for determining the dynamic bearing capacity was the same as in the case of model piles. The ultimate static load capacities for each M.L. Test presented in Table 5.5 were determined by extrapolating the data obtained by Ohio Department of Highways personnel. In examining these results column six should be compared with either column 2 or 3 of this table.

Pile #138 was driven into silt and clay in "easy" driving conditions. The results obtained are presented in Figures 5.30, 5.31, 5.32. It is interesting to note that the dynamic record of Figure 5.30 shows that zero velocity was not reached until almost 20 milliseconds. This record was obtained during original driving and it predicts a much lower capacity than obtained in the load tests made several days later. It was not possible to arrange the redriving of this pile.

Pile #113 was the first full scale pile for which successful recordings were made. Results are shown on Figure 5.33 and 5.34. Figure 5.33 represents a dynamic record obtained during driving. Redriving of the pile was not attempted. Very good correlation is obtained between the dynamic prediction and the

static capacity. It might be expected that the sand in which this pile was driven would not show a large strength increase with time. A comparison of the dynamic records of Figures 5.30 and 5.33 shows substantially different behavior between the silt and clay of pile #138 and the sand of pile #113.

The results for pile #103 are given in Figures 5.35, 5.36, and 5.37. The only load test information available is from an M.L. Test. Dynamic records are given for two successive blows. The character of the records differs considerably. This could be due to a change in the input energy delivered to the pile. However, the predicted capacities in the two cases are 111.1 and 99.7 tons for the first and second blow, respectively.

Figures 5.38, 5.39 and 5.40 show the results from Pile #A of Wall #91A. In this case successive records give very similar results.

Thus, of the four piles for which records were obtained excellent correlation was obtained in three. The other case was a pile in a material which could be expected to gain substantial strength with time.

5.3 C.R.P. and M.L. Load Tests Results of Model Piles

The model pile work required the performance of a number of load tests. The standard Ohio Department of Highways load test procedure was used as a basis for the development of the test method. This type of test was very time consuming, requiring

several days for one pile and demanding 24 hour attention. In an attempt to reduce the time required for a load test a constant rate of penetration test was applied. The dual purpose of performing a C.R.P. Test in conjunction with the standard load test set by the Ohio Department of Highways Specifications was, first to compare the ultimate load capacity of each type of test and, second to see if there was any appreciable change in ultimate load capacity of a pile due to variation in the rate of penetration.

The results of two model piles in which a conventional M.L. and several C.R.P. Tests were performed are shown in Figures 5.2, and 5.8. The ultimate load capacity of both piles, designated as 13-1 and 15-2, obtained from the C.R.P. Tests are within engineering accuracy compared to the ultimate load capacity obtained from the M.L. Test. In both cases the results of the C.R.P. Tests are slightly higher, approximately 2.4%, than that obtained from the M.L. Test.

The "failure load" as specified by the Ohio Department of Highways Specifications for the M.L. Test cannot be related to a particular load for the C.R.P. Test. This difference is caused by the rate of penetration. In a conventional M.L. Test, the loading rate is so slow that sufficient time elapses for creep to be substantial. However, in a C.R.P. Test this effect is not nearly as pronounced; thus indicating that the soil-pile interface resistance force is stiffer than in the M.L. Test procedure.

It has been found that the rate of penetration is not a critical factor with regards to the ultimate load capacity of a pile as shown in Figures 5.5, 5.18, and 5.26 of piles 15-1, 15-4 and 15-6 respectively. The rate of penetration was almost doubled in the case of piles 15-1 and 15-4, and increased more than 5 times for pile 15-6 without any substantial change in ultimate load capacity. Also in Figures 5.14 and 5.26 of piles 15-3 and 15-6 respectively, the point force at the tip of the pile increases at a slower rate than the top force due to skin friction during the initial phases of a C.R.P. Test. This fact again suggests the time dependence in the so called elastic range of the soil when comparing the C.R.P. and M.L. Load Tests.

The reproducibility of the C.R.P. Tests shown in Figures 5.5, 5.7, 5.13, and 5.18 for piles 15-1, 15-2, 15-3, and 15-4 is very good even in the case where the rate was almost doubled. The results presented here of the C.R.P. Tests and the conventional M.L. Tests supports the use of a C.R.P. Test in the future as a replacement of the M.L. Tests. A C.R.P. Test yields more reliable information than a M.L. Test, with substantial time saving.

5.4 C.R.P. and M.L. Test Results for Full Scale Piles

A number of static load tests were performed on full scale test piles. These results are of interest not only to verify the proposed dynamic theory but also to study the problem of making a proper load test.

For pile #138 Figures 5.31 and 5.32 show results of two load tests. A M.L. Test was performed in the usual manner by Ohio Department of Highways Personnel. A C.R.P. Test was performed by project personnel at a rate of 0.022 inch per minute. Figure 5.32 show the similarity between the C.R.P. Test and that portion of the displacement occurring immediately in the M.L. Test. Figure 5.31 points out the difference in force measurement using the strain gages on the pile as compared with that of the hydraulic jack pressure gage. The sharp break in the load deflection curve in Figure 5.31 leads to the suspicion that the pile steel may have yielded instead of the soil. The stress in the pile at the point where the curve breaks is approximately 42 ksi.

The load tests performed on pile #175 are of interest. Figures 5.41, 5.42, and 5.43, represent the M.L. and C.R.P. load test results for this particular pile. The correlation between strain gage load measurement and pressure gage load measurement is poor. A comparison of the M.L. Test instantaneous displacement with the C.R.P. Test results shows good comparison. Figure 5.43 is of particular interest. In this drawing the applied load measured from the strain gages has been obtained by multiplying strain by the cross-sectional area of the pile and the modulus of elasticity of steel. The applied load from the strain gages continually increased indicating structural yielding of the pile at the particular point where the strain gages were located. Upon unloading the pile, there was a large residual strain, confirming yielding had occurred. It

should be pointed out that even if strain readings hold steady the pile steel could be yielding at another location.

The measurement of load under field conditions is not a simple task. The use of hydraulic pressure gages on the jacks can yield unreliable results for the following reasons:

1. Friction losses can be substantial.

2. The pressure gage is a very sensitive instrument. Calibration can be lost by the shocks it receives under normal construction usage.

3. Frequently, less than 30% of the gage range is used at full load. Thus, reading errors are increased.

Force transducers are available, using a strain gage measuring system, which are very accurate and reliable. However, the use of such a system for force measurement would undoubtedly be more expensive to the Department of Highways since contractors would have to acquire new and unfamiliar equipment.

CHAPTER 6

CONCLUSIONS AND RECOMMENDATIONS

Based on the results of this project the correlation between dynamic prediction and measured static capacity is promising. Further tests are necessary in a variety of soil types. Full scale tests are particularly important and useful. Any method of prediction of static capacity based on measurements obtained during driving can be expected to predict the capacity at the time of measurement. Estimates of strength change must be based on soil studies. The use of the system described here in connection with redriving appears to provide an accurate strength measure. Available results with widely differing response characteristics do not indicate any limits on the theory (in predicting existing strength). It is possible to develop electronic instrumentation to make this measurement on a rapid, routine basis. Thus, the strength of a substantial number of piles could be reasonably measured. Theoretical studies of an elastic pile can contribute to an understanding of the limitations of the proposed simplified theory.

The correlation of the Michigan tests with the proposed dynamic prediction was not as satisfactory. A substantial part of this lack of agreement is undoubtedly due to the strength change between driving and load testing. It should be noted that all of the Michigan data on acceleration were modified prior to its publication. The data was adjusted so that the maximum directly measured

displacement agreed with the maximum of the curve obtained by double integration of the acceleration record. The measured acceleration reported in this project are as recorded. Integration of these records resulted in essentially zero velocity. The failure of the Michigan records to meet the velocity check could effect their application in the proposed theory.

The effort required to develop the instrumentation system was greater than had been anticipated. Electronic devices for this purpose are commercially available but the construction and calibration of the total system with sufficient ruggedness and reliability to perform under field conditions was a challenging task. This instrumentation is now functioning with reasonable reliability.

The results of load tests indicate that the C.R.P. Test can be more accurately performed than the M.L. Test with considerable time saving. The load measured is the ultimate capacity and, hence, a different factor of safety is required in design than is used for the Ohio Department of Highways "yield load". The use of the C.R.P. Test with strain gage load cells would avoid many problems of accurate load measurement.

The wide variety of ultimate load capacities measured on model piles at a single site is disturbing to the concept of the single load test pile. These piles were quite closely spaced but their capacities differed widely. The use of the system proposed here would make practical the dynamic testing of many piles.

REFERENCES

3.1 Eiber, R. J. "A Preliminary Laboratory Investigation of the Prediction of Static Pile Resistances in Sand" Master's Thesis, Dept. of Civil Engr., Case Institute of Technology, 1958.

3.2 "A Performance Investigation of Pile Driving Hammers and Piles", Michigan State Highway Commission, Lansing, Michigan, March 1965.

3.3 LaPay, W. S., "Dynamic Pile Behavior - Literature Survey and Response Studies", Master's Thesis, Case Institute of Technology, 1965.

3.4 "Construction and Materials Specifications", State of Ohio, Department of Highways, Columbus, Ohio, Jan. 1963.

TABLE 3.1

PROPOSED THEORY APPLIED TO MICHIGAN RESULTS

Pile Designation	Soil Condition	Type of Pile	Embedded Length	Static Load Test Capacity*	Dynamic Prediction of Capacity
				tons	tons
Belleville:					
LTP-1	Clay	12" open end pipe	44	60	82
LTP-3	Clay-tip in very fine Sand and Silt	12" fluted-tapered	61	180	81
LTP-5	Clay-tip in very fine Sand and Silt	12" pipe	67	400	85
LTP-6	Clay-tip in very fine Sand and Silt	12 x 12 H	58	230	154
Detroit					
LTP-1	Clay	12" open end pipe	70	20	6.5
LTP-2	Clay	12" pipe	79	150	48
LTP-7	Clay	12" fluted-tapered	81	180	39
LTP-8	Clay	12 x 12 H	81	170	44
Muskegon					
LTP-2	Sand	12" pipe	58	100	60
LTP-3	Sand	12" fluted-tapered	58	60	59
LTP-6	3 Layers	12" pipe	128	255	102
LTP-9	1. Loose Sand 2. Soft Sed's Peat 3. Compact Sand	12" pipe	128	250	160

*This value is obtained from extrapolation of the load - settlement curve given for each pile. The value given is the plastic failure load.

**Load obtained from considering both pile wt. and plain driving cap and cushion assembly.

TABLE 4.1

Accelerometer Characteristics

Kistler 808A

Range	10,000 g
Resolution	0.01 g
Linearity (per cent of reading)	0.5%
Transverse sensitivity (less than)	5%
Repeatability and stability	0.2%
Temperature sensitivity	0.01%/°F
Temperature range	-320°F to + 500°F
Frequency response (5%)	near d.c. to 8000 cps
Resonant frequency (mounted)	40,000 cps
Weight (Approx.)	20 grams
Dimensions (Approx.)	0.5" hex x 1.1" long

TABLE 5.1

Physical Characteristics of Model Piles

(Crossectional Area of all Piles is 1.704 in.^{2})

Pile No.	Grade	Length of Pile in Feet Below Strain Gage at end of driving	Length of Pile in Feet Below Strain gages after C.R.P. or M.L. Test	Weight of Pile in lbs. End of driving	Weight of Pile in lbs. After C.R.P. or M.L. Test
13-1	13	16.5	-	95.5	-
15-1	15	18.5	-	107.1	-
15-2	15	18.5	-	107.1	-
15-3	15	18.5	18.5	107.1	107.1
15-4	15	18.5	18.5	107.1	107.1
15-5	15	18.5	18.5	107.1	107.1
15-6	15	18.5	18.5	107.1	107.1
15-7	15	18.5	18.5	107.1	107.1

TABLE 5.2

Comparison of Static Bearing Capacity with Dynamic

Prediction for Model Piles at the End of Driving

Pile Depth	Ultimate Static Capacity From C.R.P. Test lbs.	Dynamic Results at v = 0 m a(t_o) lbs.	F(t_o) lbs.	R_o = F(t_o) - ma(t_o) lbs.	Set/Blow inches
13-1	- - -	-1240	4080	5320	1/2
15-1	- - -	-3860	6050	9910	5/16
15-2	- - -	-4280	6110	10390	1/4
15-3	14800	-6000	7000	13000	1/4
15-4	- - -	-3430	6280	9710	5/16
15-5	- - -	-7820	7078	14898	1/4
15-6	- - -	-3110	6781	9891	3/16
15-7	- - -	-3750	6187	9937	3/8

TABLE 5.3

Comparison of Static Bearing Capacity with Dynamic

Prediction for Model Piles After Setup Period

Pile Depth	Ultimate Static Load Capacity From Load Tests in lbs. C.R.P. Test	M.L. Test	Dynamic Results at v = 0 $m\,a(t_o)$	$F(t_o) = AE\varepsilon(t_o)$	$R_o = F(t_o) - m\,a(t_o)$ in lbs.	Set/Blow in inches
13-1	8860	8650	---	---	---	---
15-1	11400	---	---	---	---	---
15-2	12900	12700	---	---	---	---
15-3	18300	---	-7060	13600	20660	1/8
15-4	10600	---	-5030	6280	11310	3/16
15-5	---	*16000++	-6830	21900	28730	1/16
15-6	12100	---	-4665	8878	13543	1/8
15-7	14000	---	-7060	9430	16490	1/8

* Dead weight system shifted causing breakage of equipment at this load.

TABLE 5.4

Physical Characteristics of Full Scale Piles Tested

All Piles were 12" Round Seamless Pipe Piles

Pile No. and Description	Type of Soil	Wall Thickness in inches	Cross-sectional Area in $in.^2$	Length of pile in ft. below Grade	Length of pile in ft. below Strain Gages	Weight of Pile in tons
138 of Pier 4 of Br. No. I-71-1826	Silt & Clay	0.179	6.67	85.0	110.0	1.25
113 North Pier of Br. No. Cuy. 21-1431	Sand	0.219	9.82	53.0	59.5	1.00
175 of Pier No. 5 of Br. No. Cuy I-71-1826	Silt & Clay	0.179	6.67	65.0	-	-
103 of Pier No. 2 of Br. No. Cuy 290-0040	Sandy Silt	0.210	7.83	74.0	74.0	0.99
A of Wall No. 91A of Br. No. Cuy. 90-1395	Sand & Silt	0.210	7.83	74.0	74.0	0.99

TABLE 5.5

COMPARISON OF STATIC CAPACITY WITH DYNAMIC RESULTS OF FULL SCALE

PILES BASED ON SIMPLIFIED ANALYTICAL MODEL

Pile Description and Location and soil condition.	Ultimate Static Load Capacity From Load Tests in Tons		Dynamic Results @ V=0		$R_t = F_{V=0} - m A_{V=0}$
	C.R.P. Test*	M.L. Test‡	$m A_{V=0}$	$F_{V=0}$=AEE	In Tons.
Pile #138 - Pier #4 of 2-71 BR. No. I-71-1826 (Silt and Clay)	135**	130-150	27.6+	31.9+	59.5+
Pile #113 North Pier Willow Freeway BR. No. Cuy-21-1431 Sand	---	100-120	18.0+	104.0+	122.0+
Pile #175 - Pier #5 BR. No. Cuy-71-1826 (Silt and Clay)	125**	110-130	---	---	---
Pie #103 - Pier #2 BR. No. Cuy.-290-0040 (Sandy silt)	---	98-110	36.6	74.5	111.1
Pile #A of Wall #91A BR. No. Cuy-90-1395 (Sand silt)	126.0	115-140	31.7	108.75	140.7

**These piles are believed to have yielded structurally. There was no evidence of soil-pile interface yielding based on the C.R.P. Test.

* C.R.P. Based on Strain Gage Results.

‡ Results extrapulated from Ohio Highway Department M.L. Tests.

+ Results obtained at the end of driving.

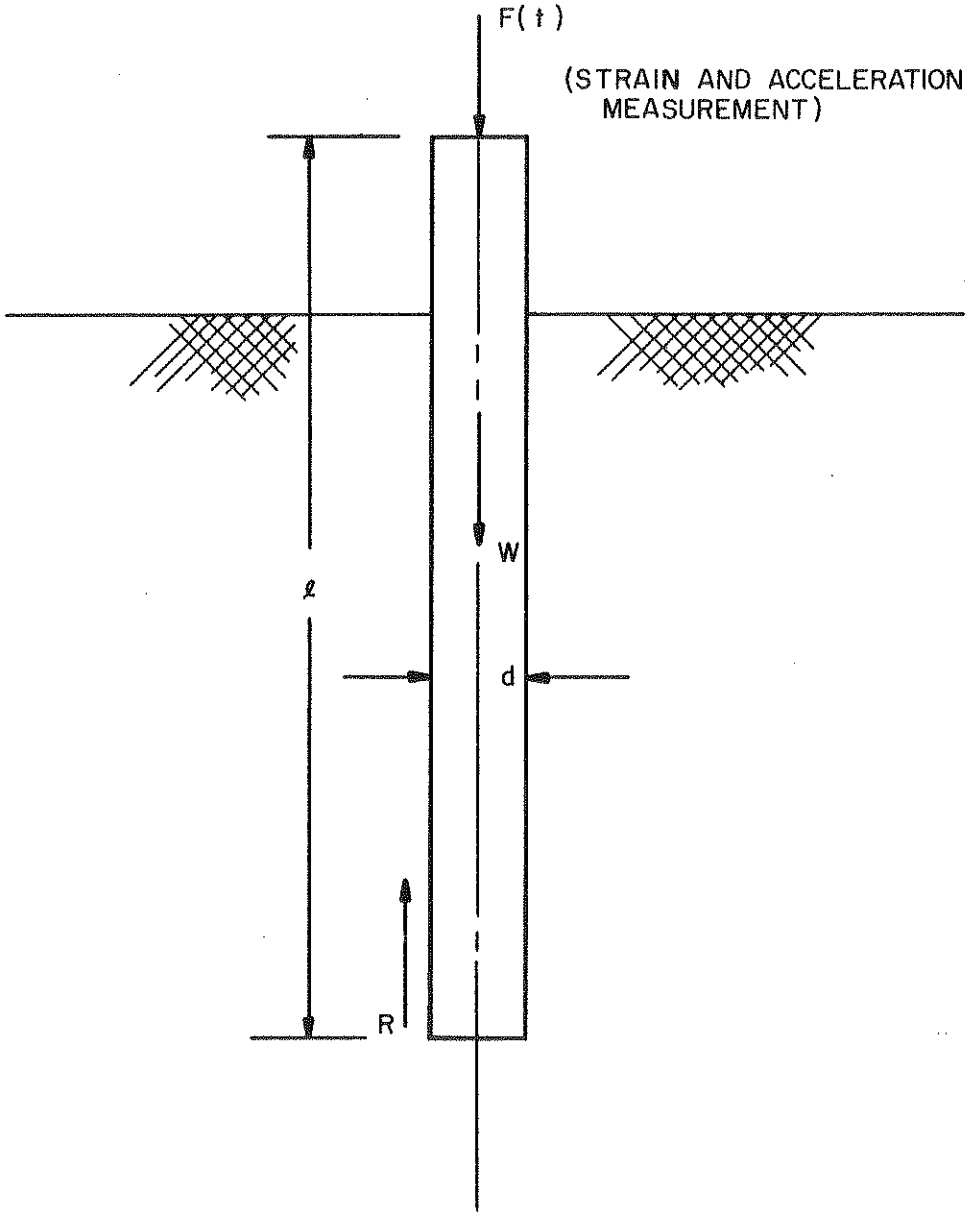

FIGURE 2.1

SIMPLIFIED ANALYTICAL MODEL

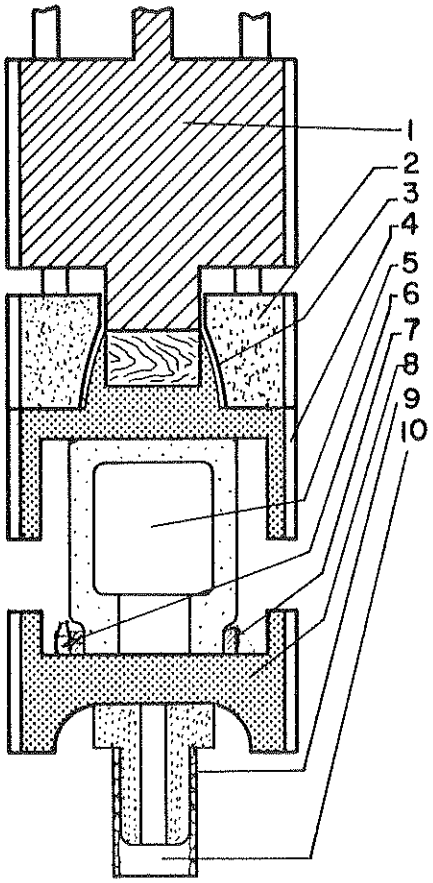

Ident. No.	Item
1.	Ram
2.	Hammer Base
3.	Oak Cushion and Two Steel Plates
4.	Vulcan Concrete Pile Driving Cap
5.	Load Cell
6.	Accelerometer
7.	Adapter Ring for Load Cell
8.	McKiernan-Terry Universal Drive Cap
9.	Pipe Pile Protector
10.	Pipe Pile

Figure 3.1

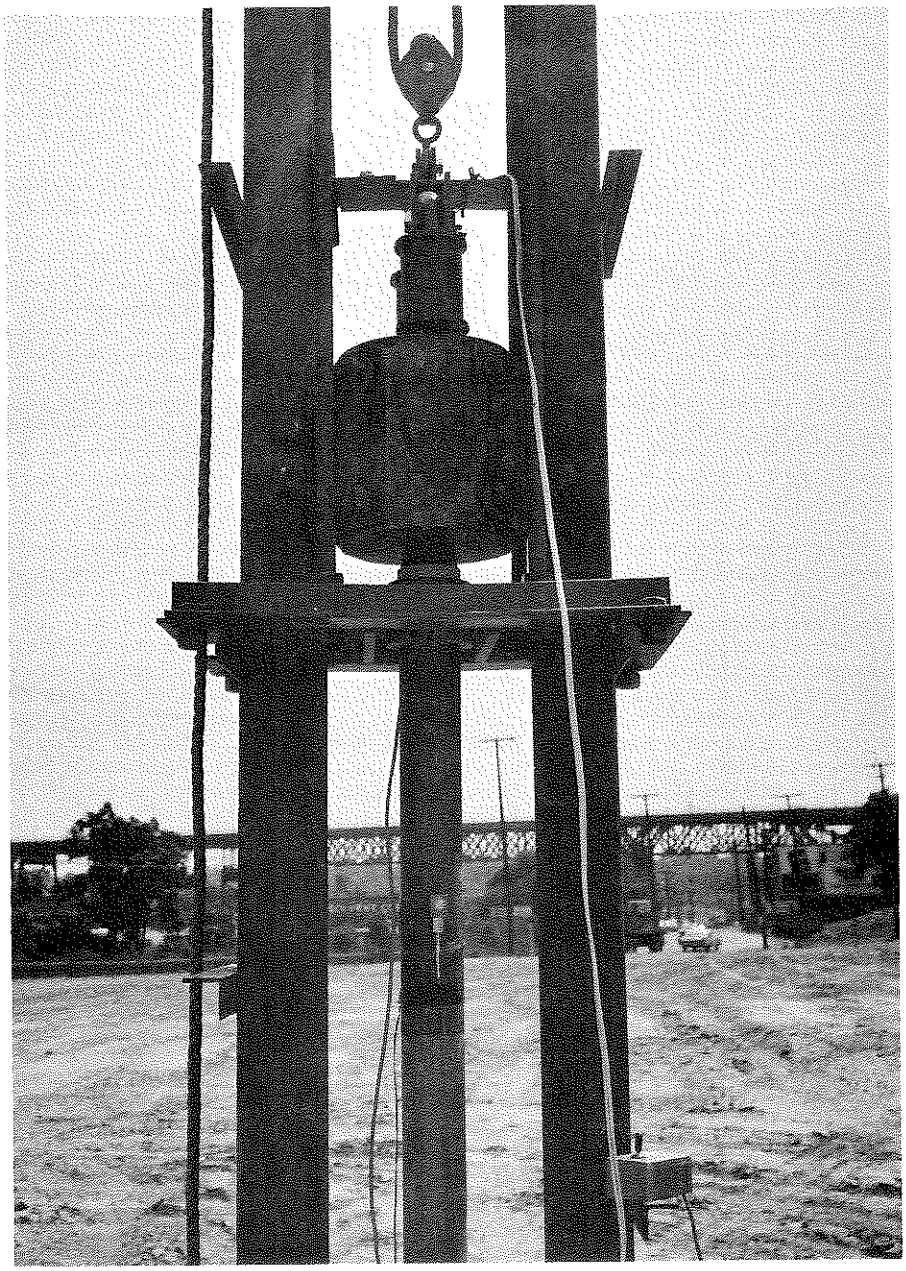

FIGURE 4.1

Accelerometer and its Attachment Device on Instrument Section

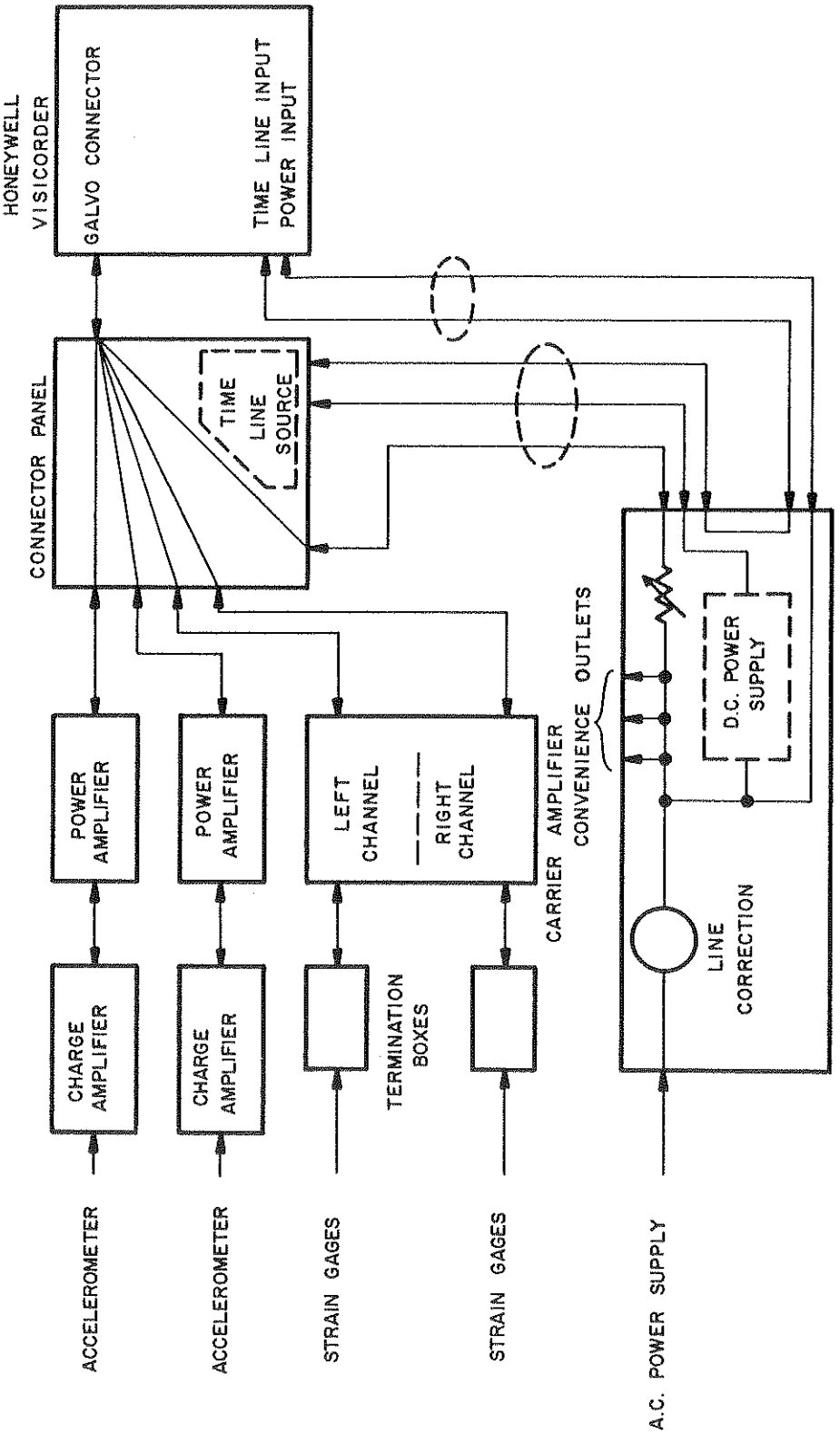

FIGURE 4.2

BLOCK DIAGRAM OF RECORDING INSTRUMENTATION

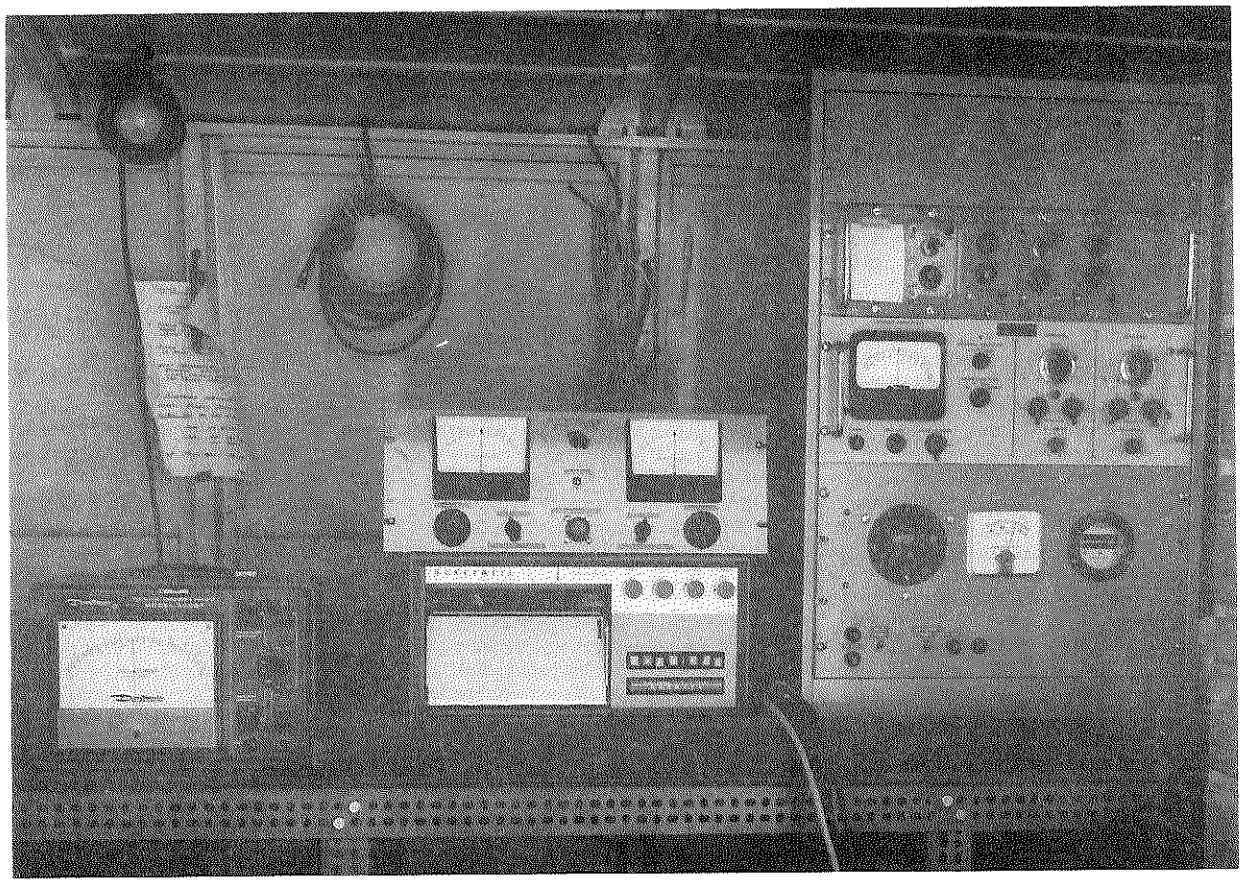

FIGURE 4.3

Differential Transformer and Null Bridge Indicator, Visicorder, and Containing Charge and Power Amplifiers, and Honeywell Carrier Amplifier

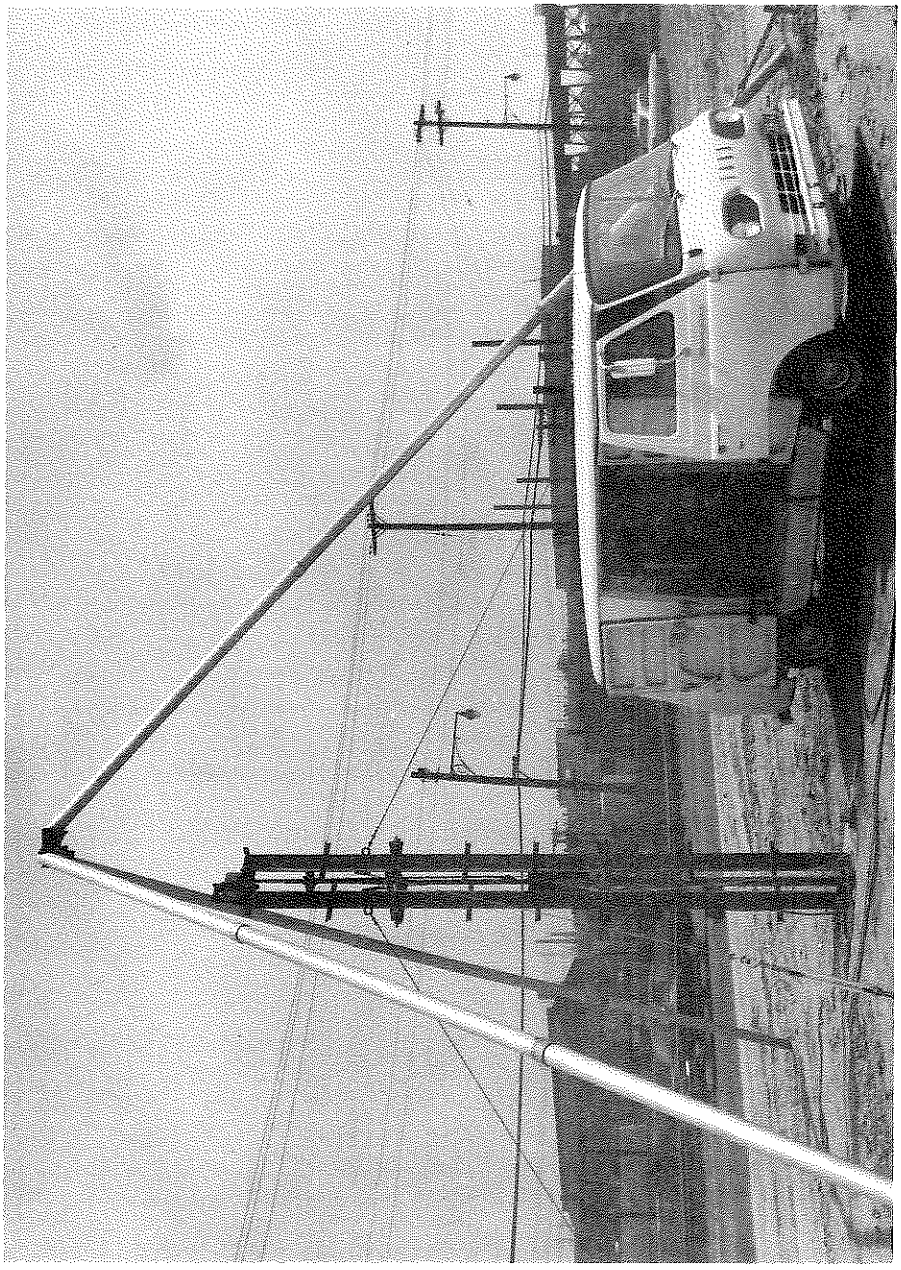

FIGURE 4.4

Pile Driving Rig and Tripod, and Instrumented Truck

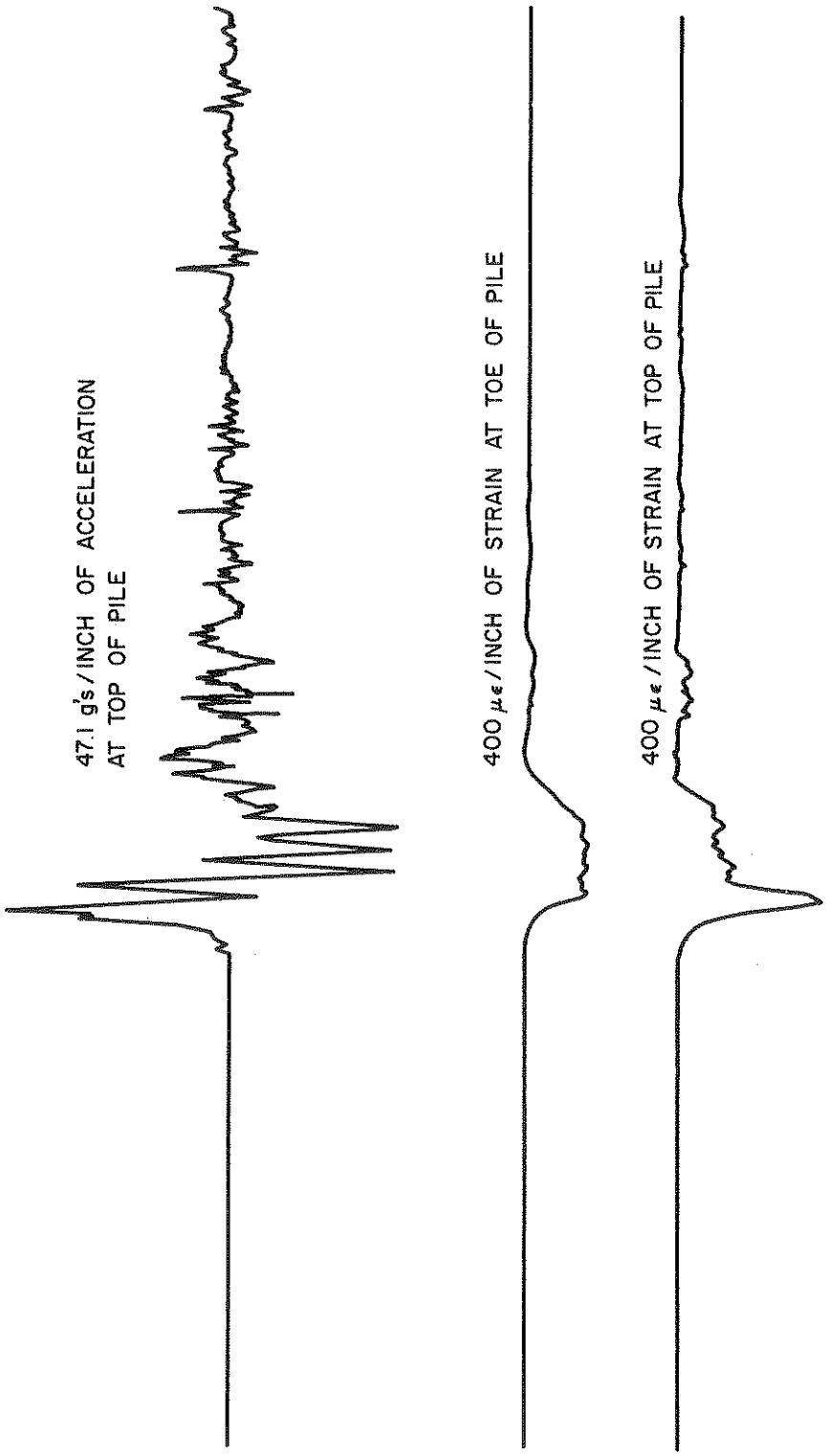

FIGURE 4.5

Typical Record Taken from a Model Pile

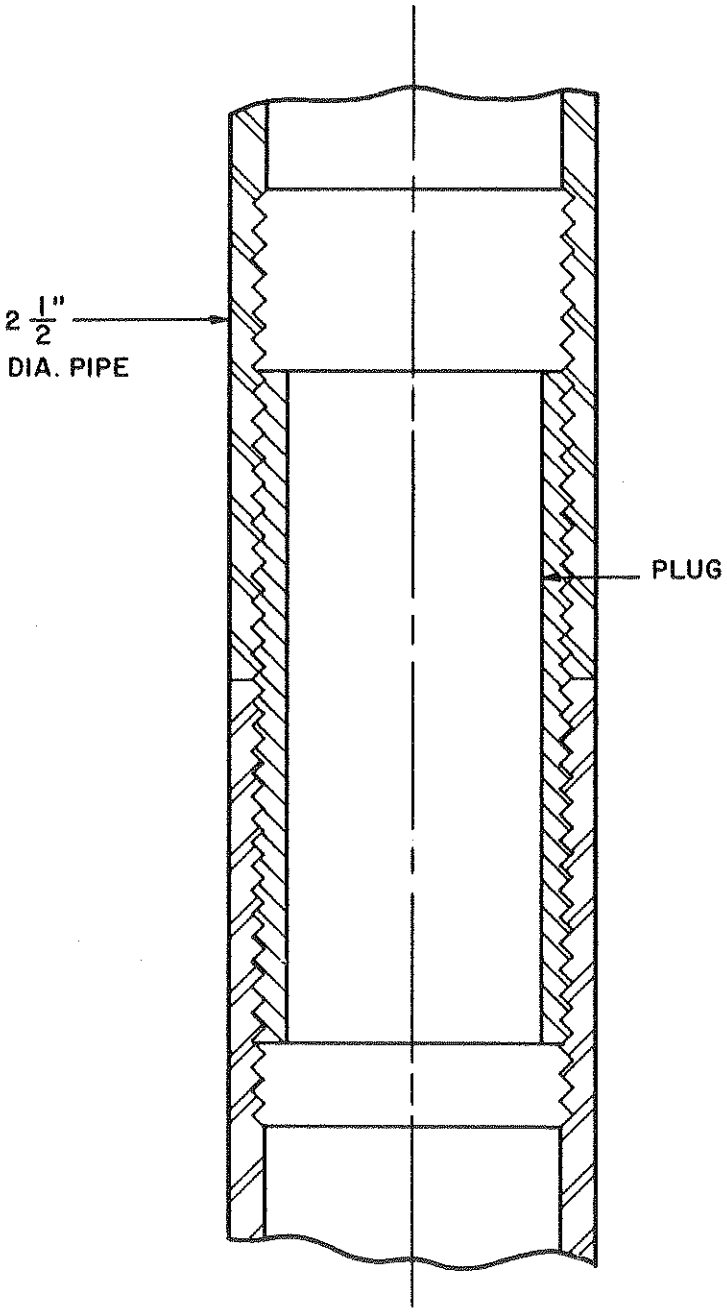

FIGURE 4.6

Model Pile Splice

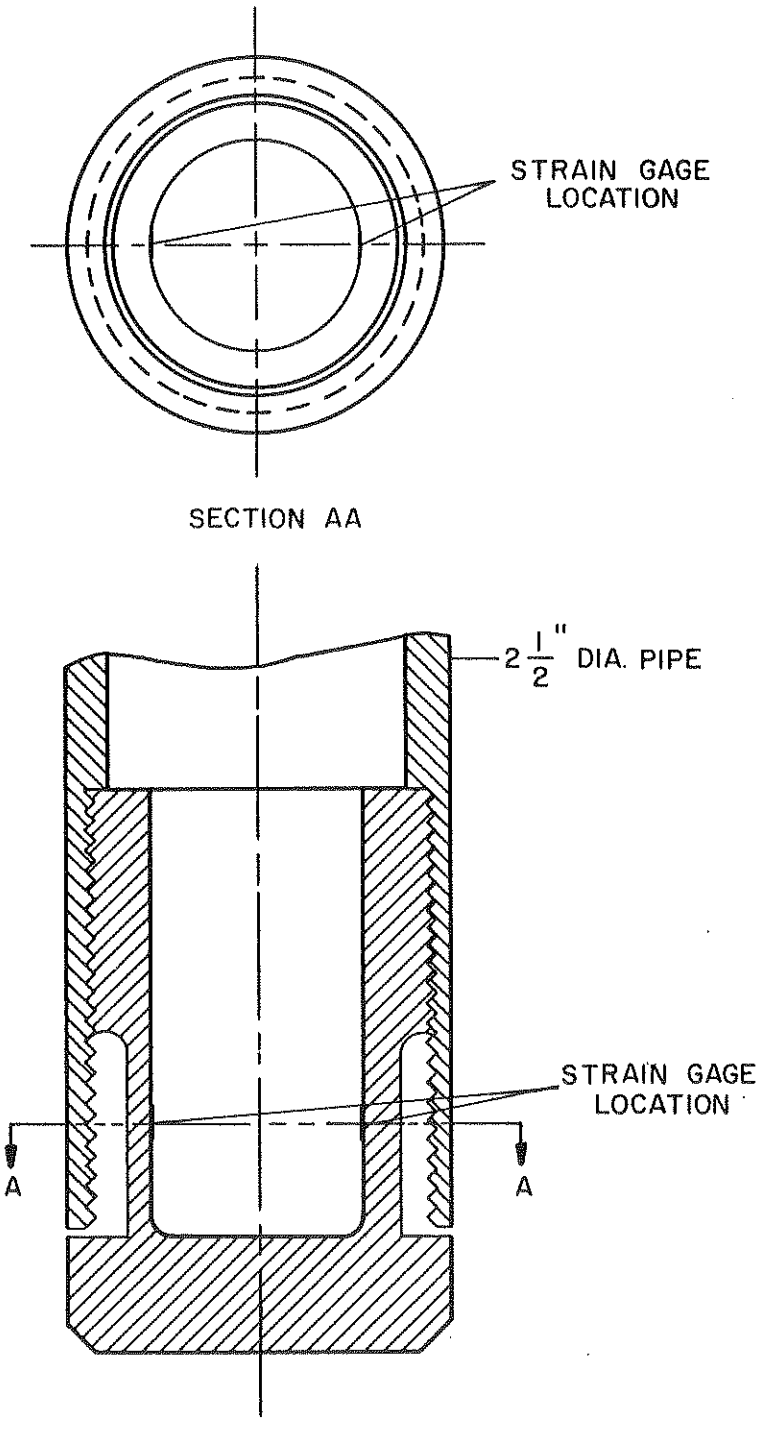

FIGURE 4.7

PILE TIP

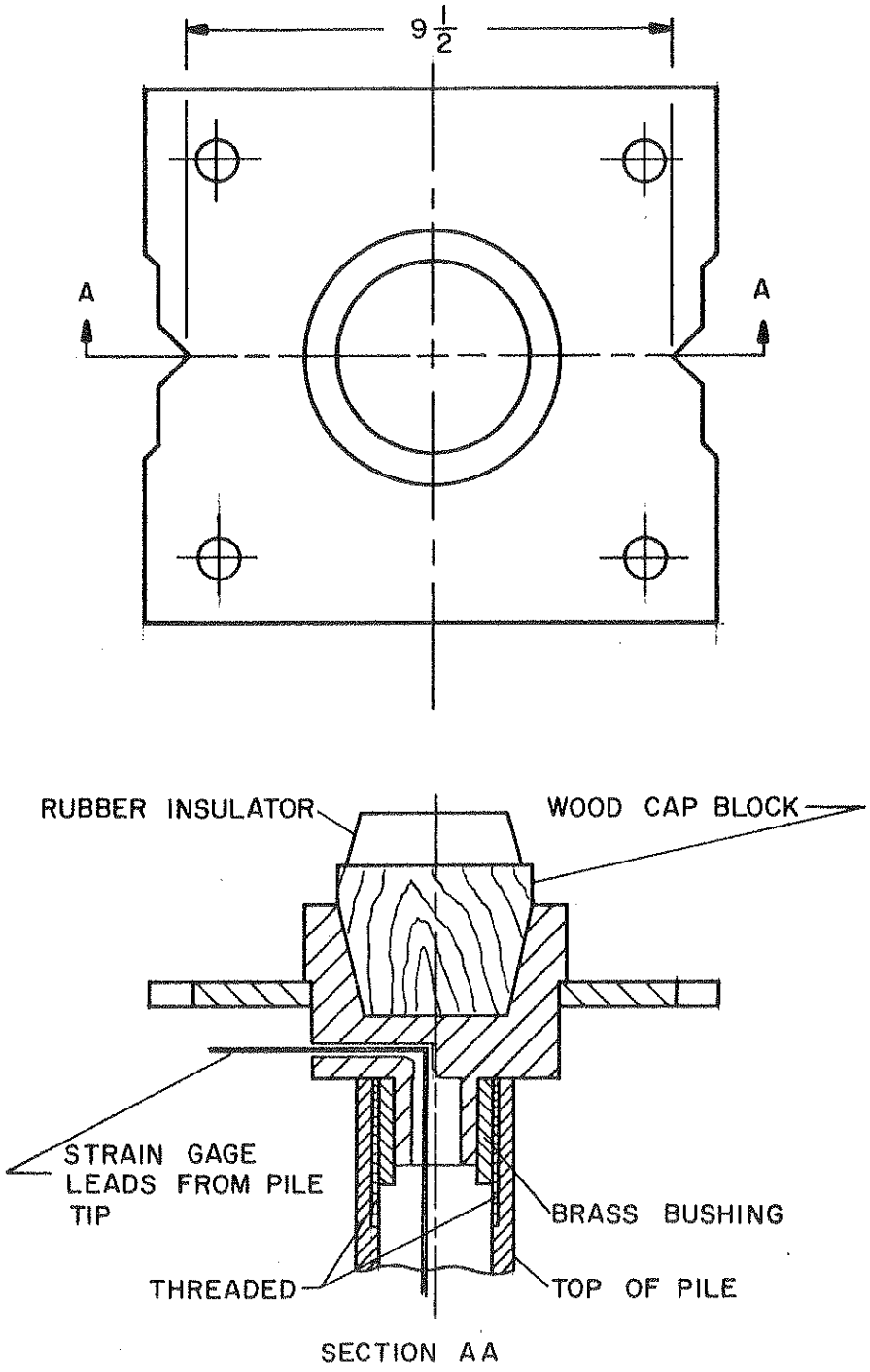

FIGURE 4.8

PILE DRIVING CAP DETAILS

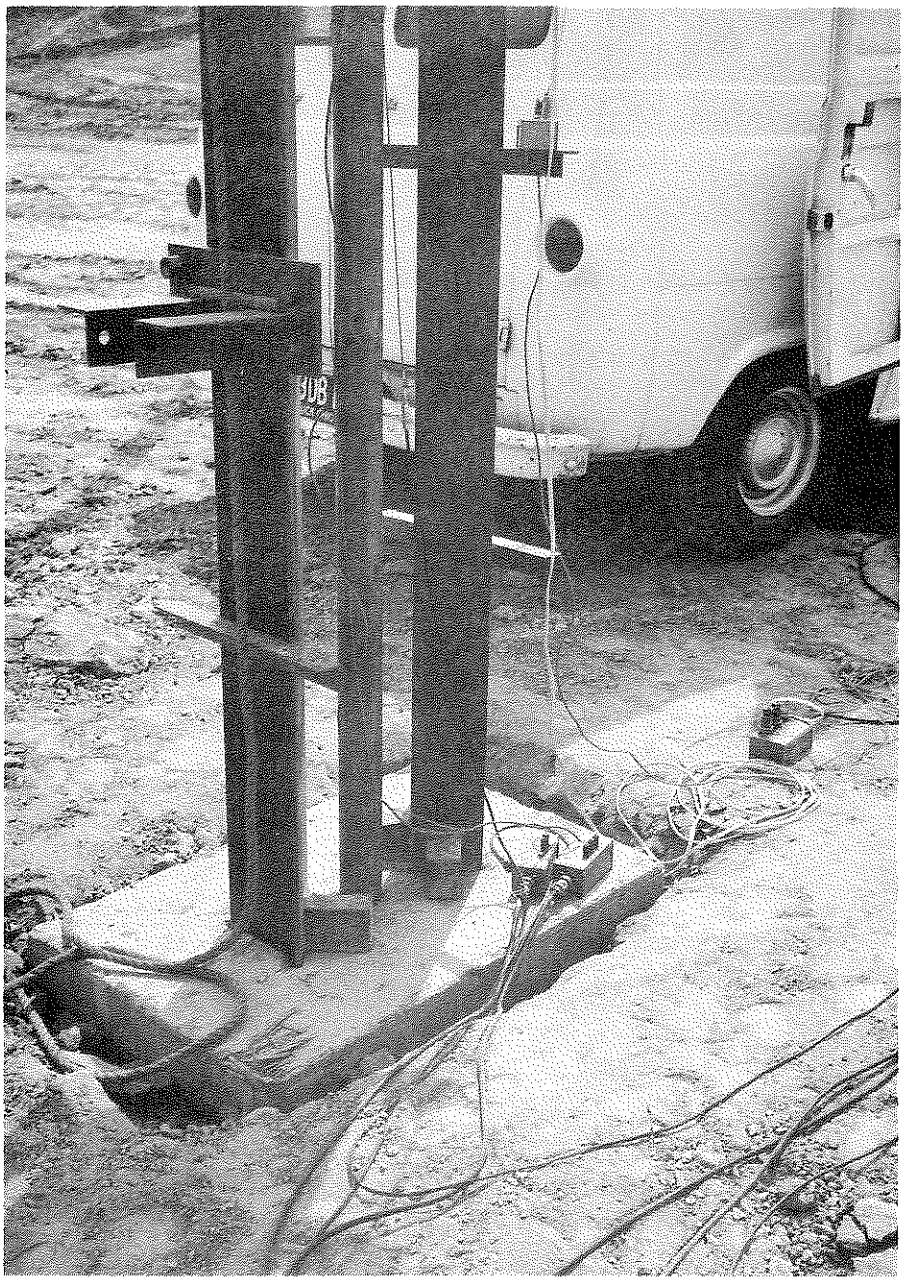

FIGURE 4.9

Termination Boxes

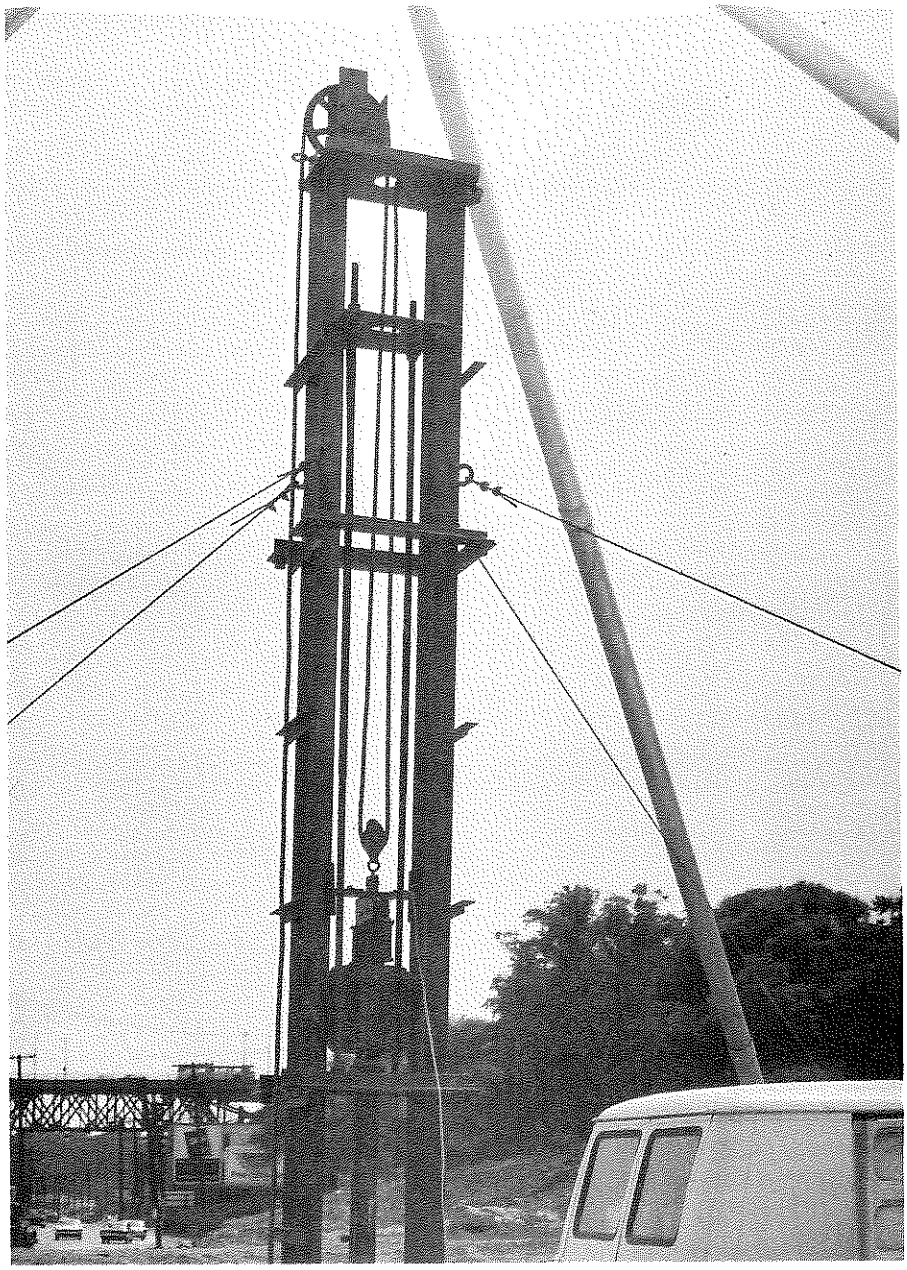

FIGURE 4.10

Model Pile Driving Rig

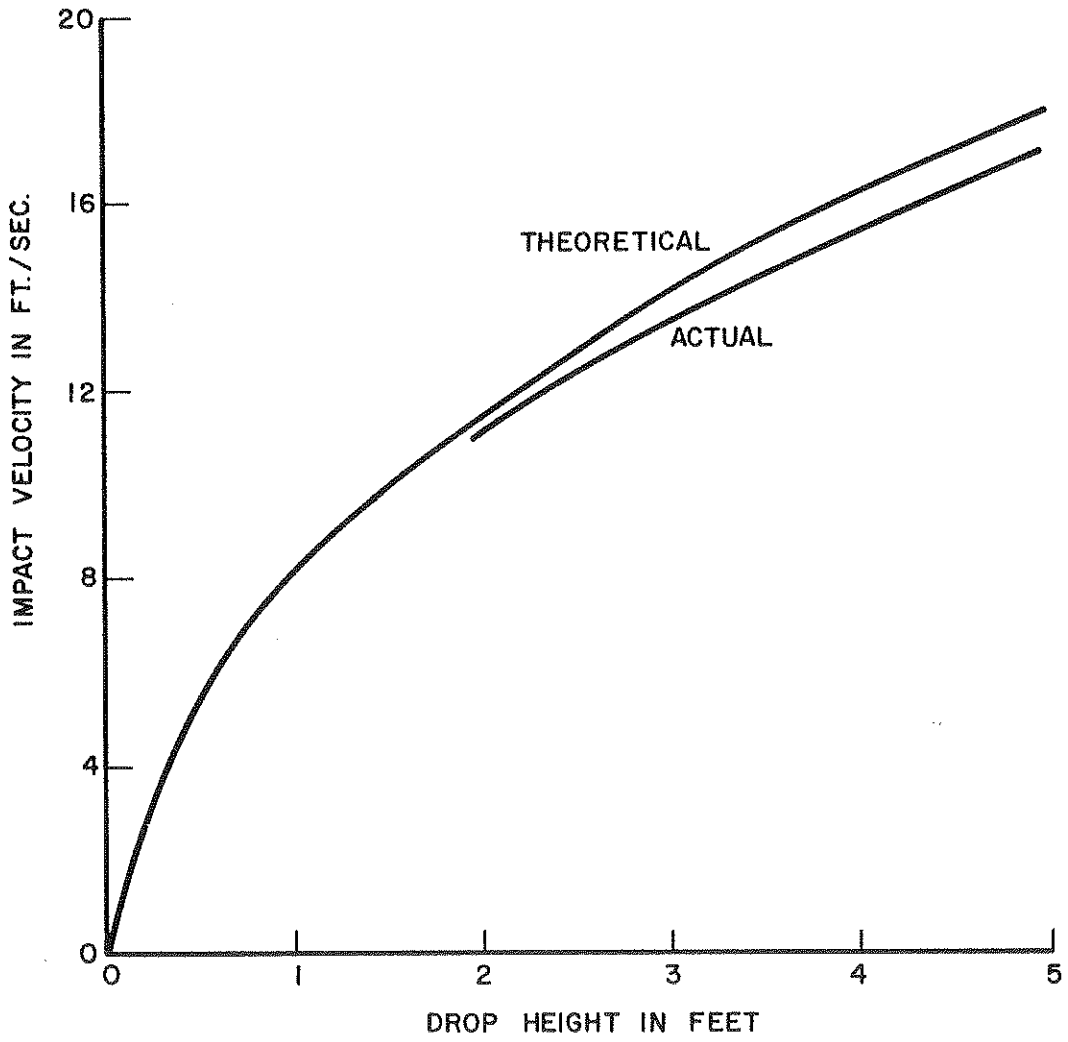

FIGURE 4.11

Energy Loss Calibration

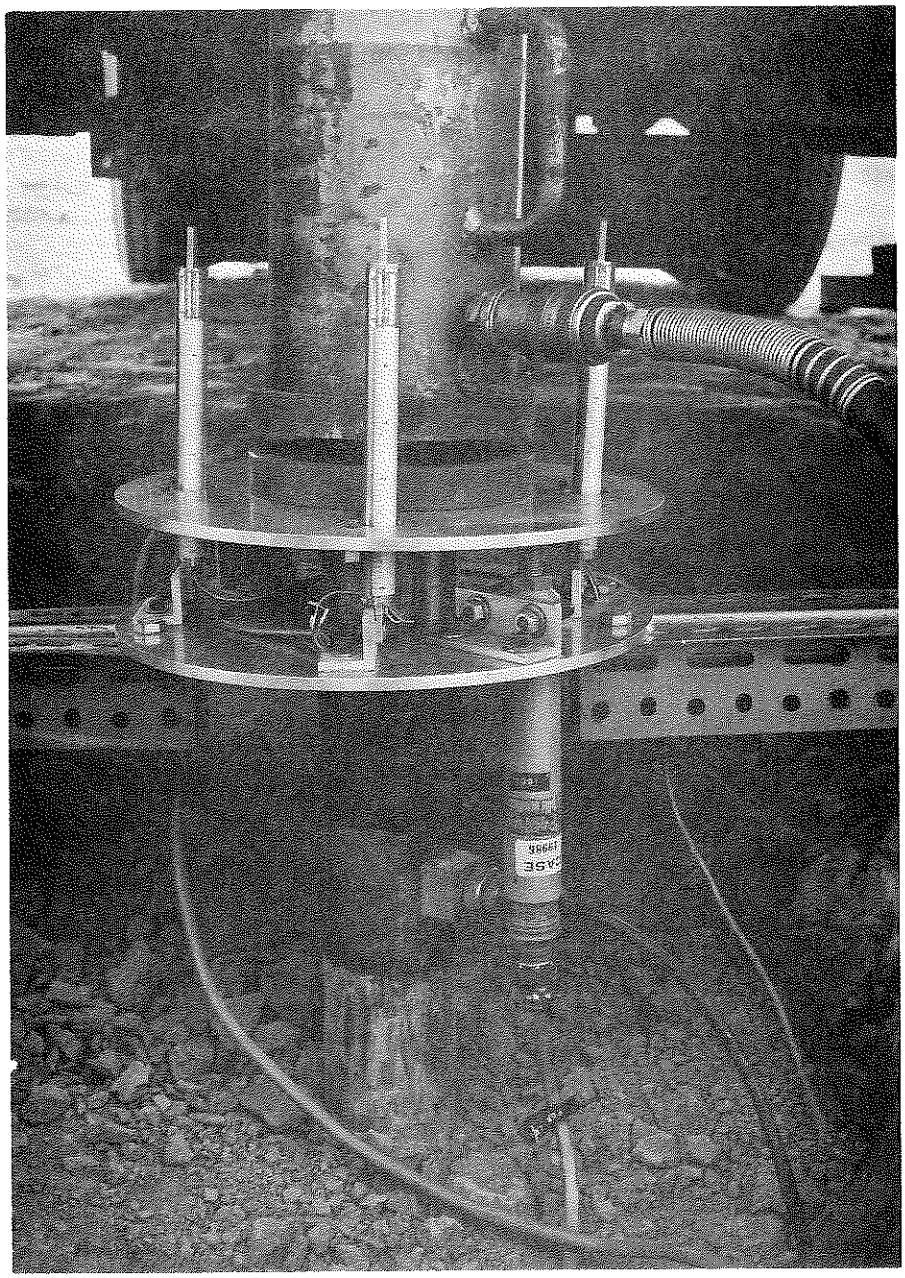

FIGURE 4.12

Model Pile Load Test Apparatus Showing Potentiometers, Transducer Section, and Hydraulic Jack

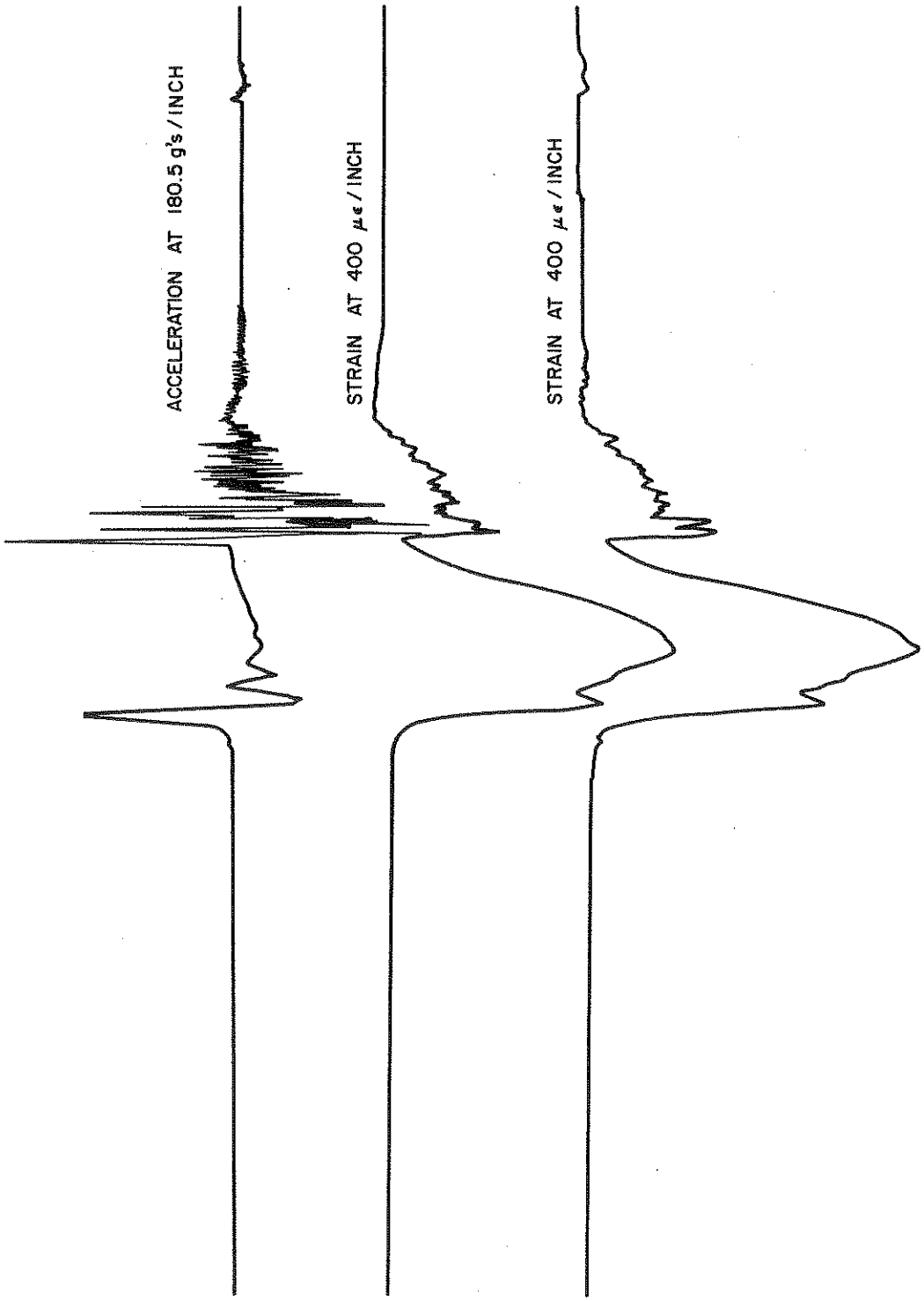

FIGURE 4.13

Typical Dynamic Record of a Full Scale Pile

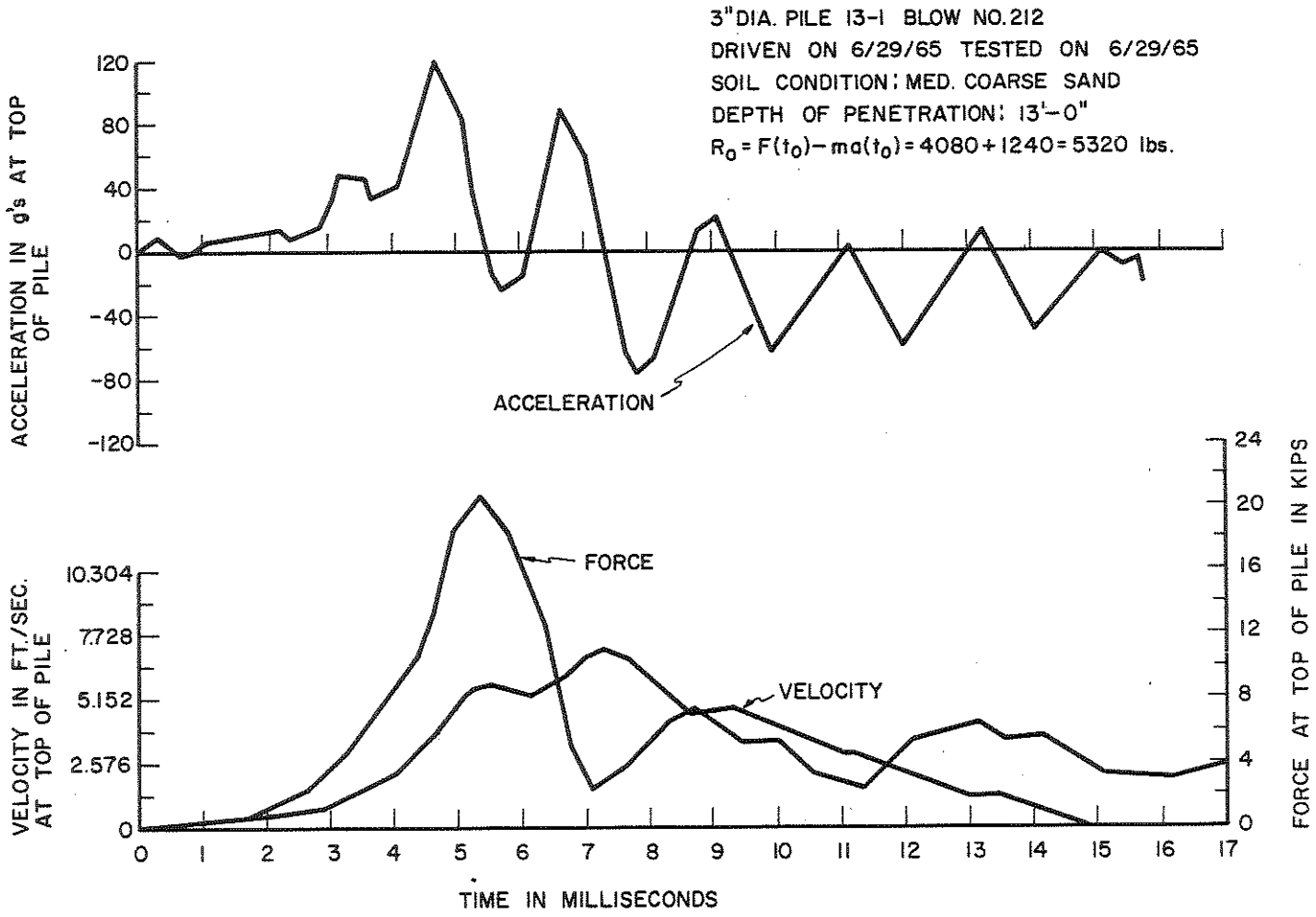

FIGURE 5.1

Dynamic Results of Model Pile No. 13-1
at the End of Driving, Blow No. 212

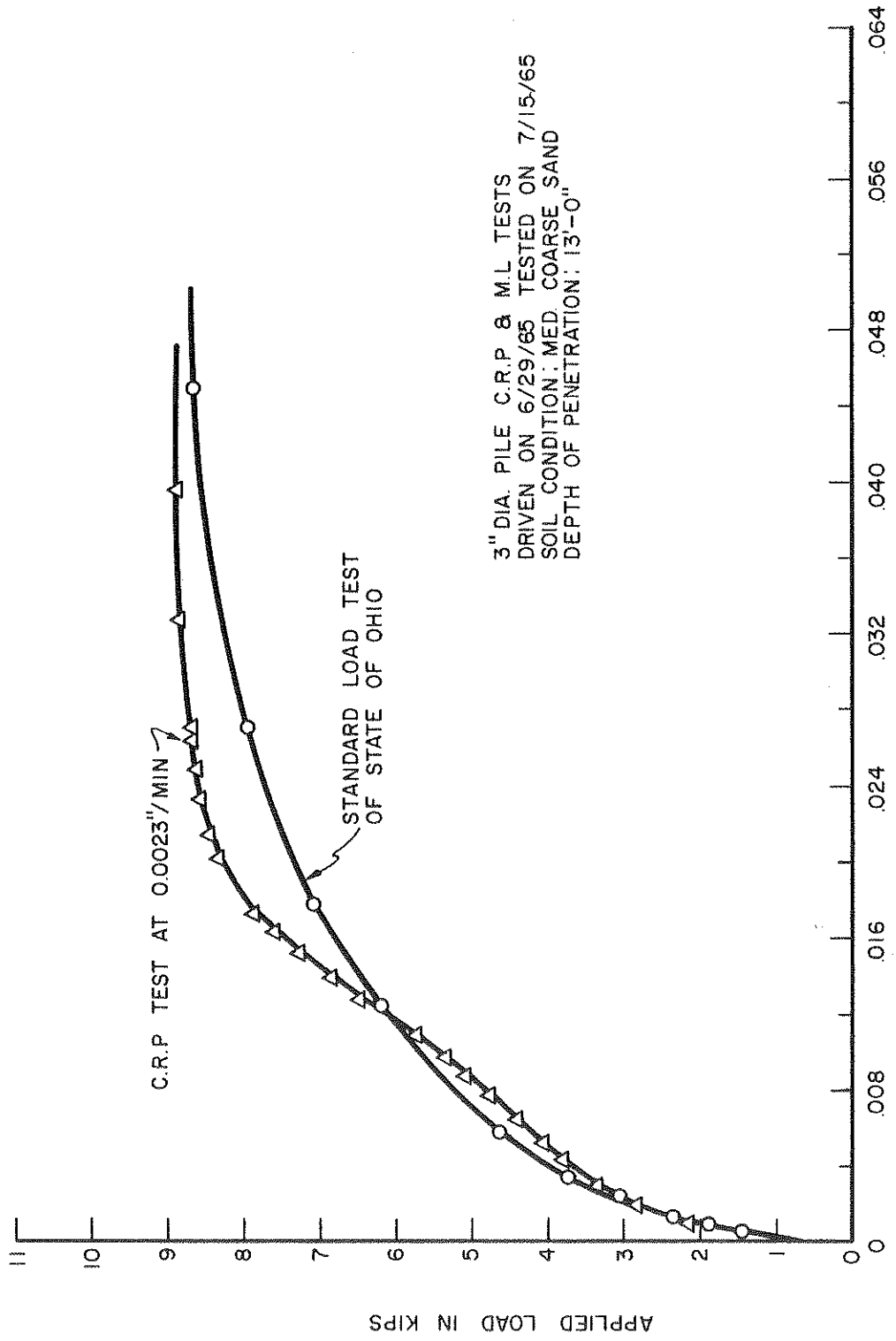

FIGURE 5.2

C.R.P. and M.L. Test Results of Model Pile No. 13-1

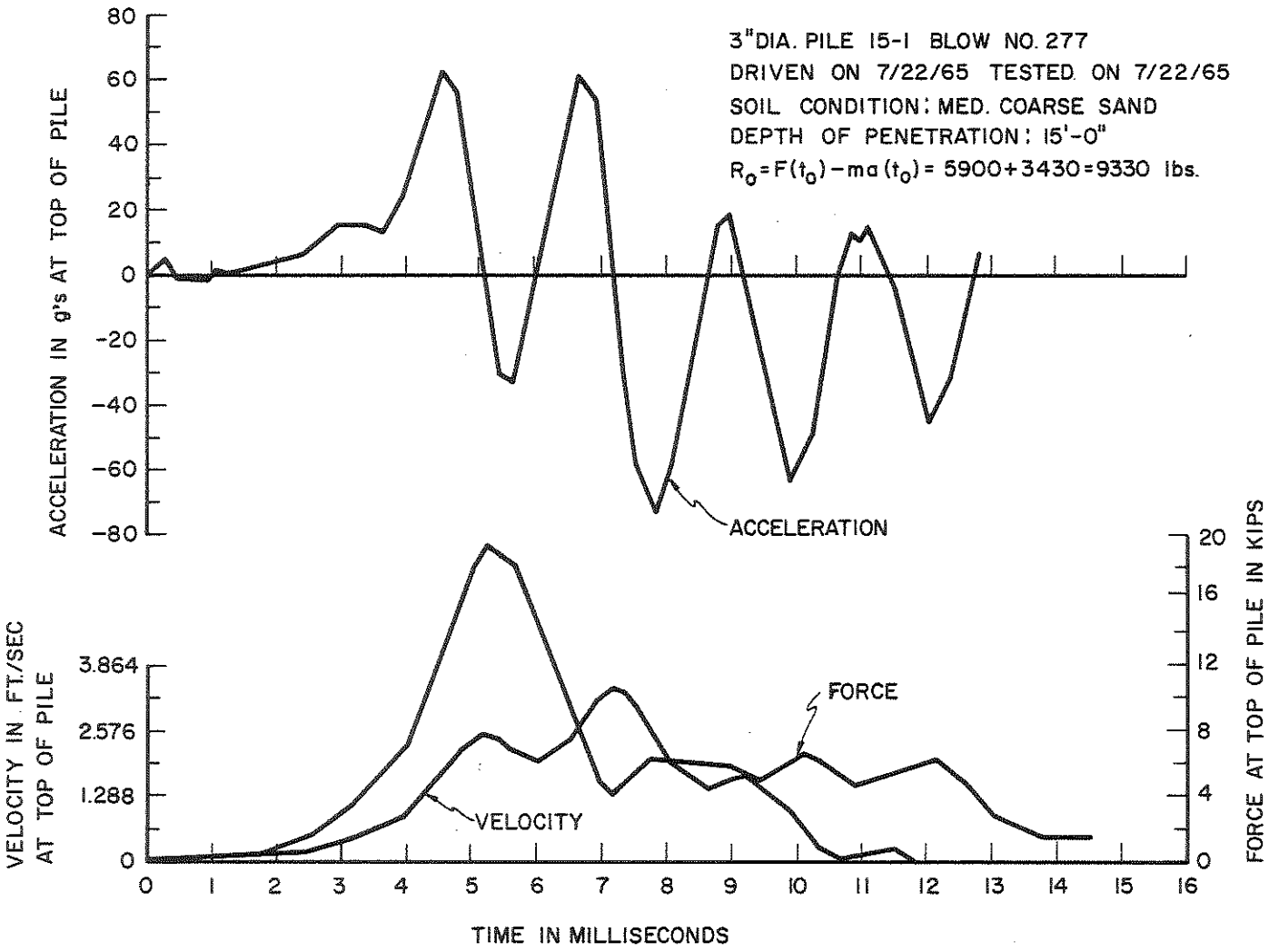

FIGURE 5.3

Dynamic Results of Model Pile No. 15-1 at the End of Driving, Blow No. 277

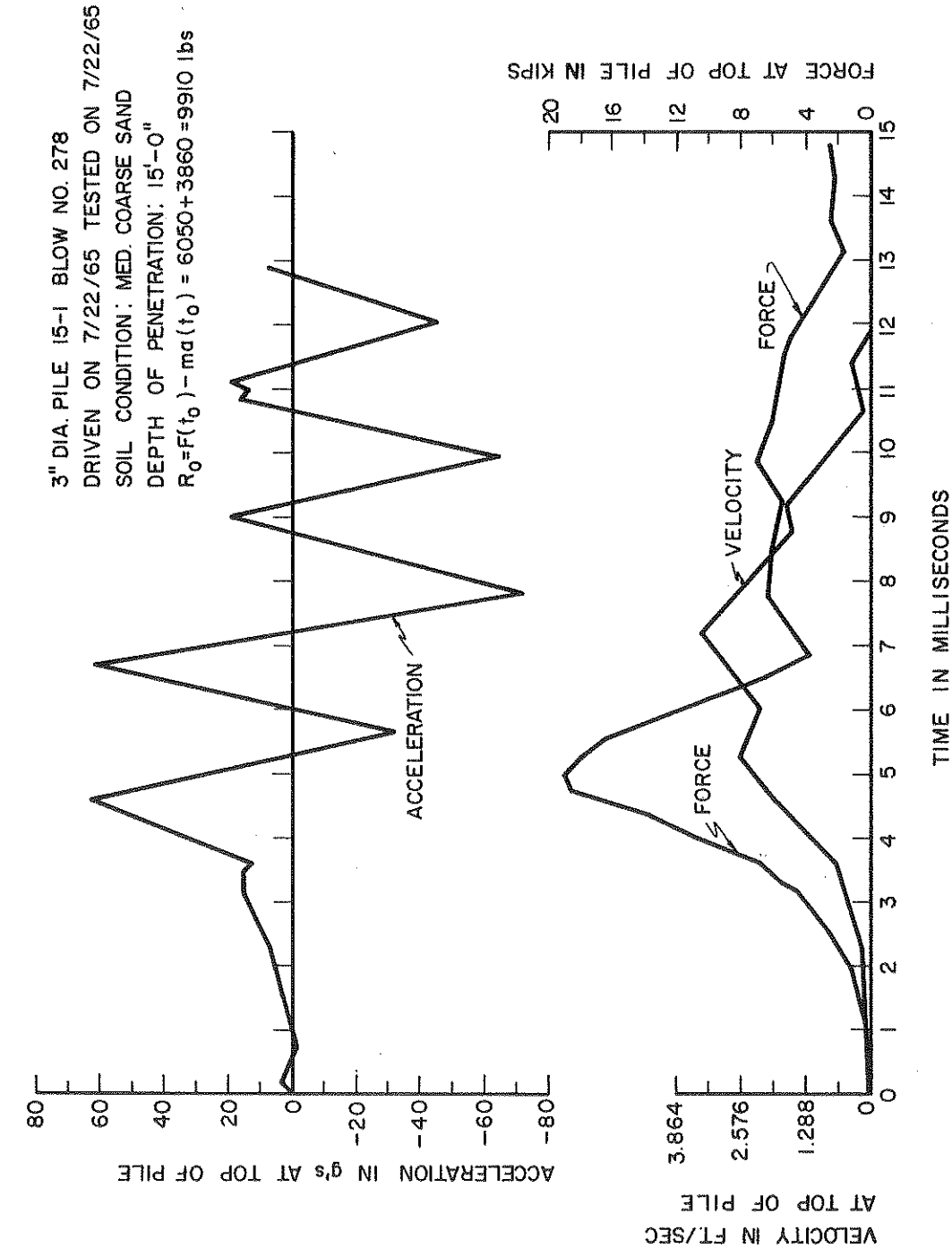

FIGURE 5.4

Dynamic Results of Model pile No. 15-1 at the end of Driving, Blow No. 278

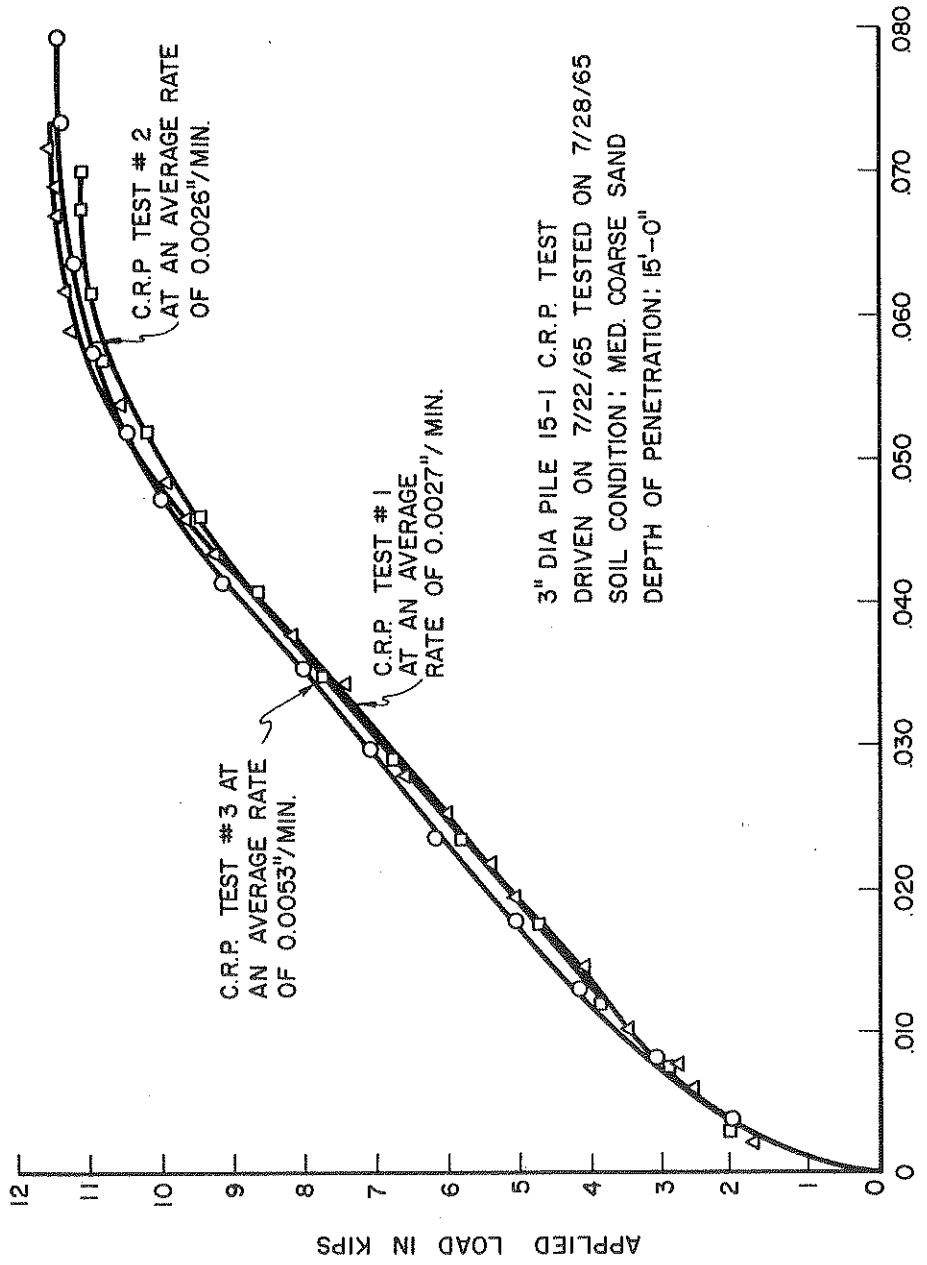

FIGURE 5.5

C.R.P. Test Results Performed on Model Pile No. 15-1 at Various Rates of Loading

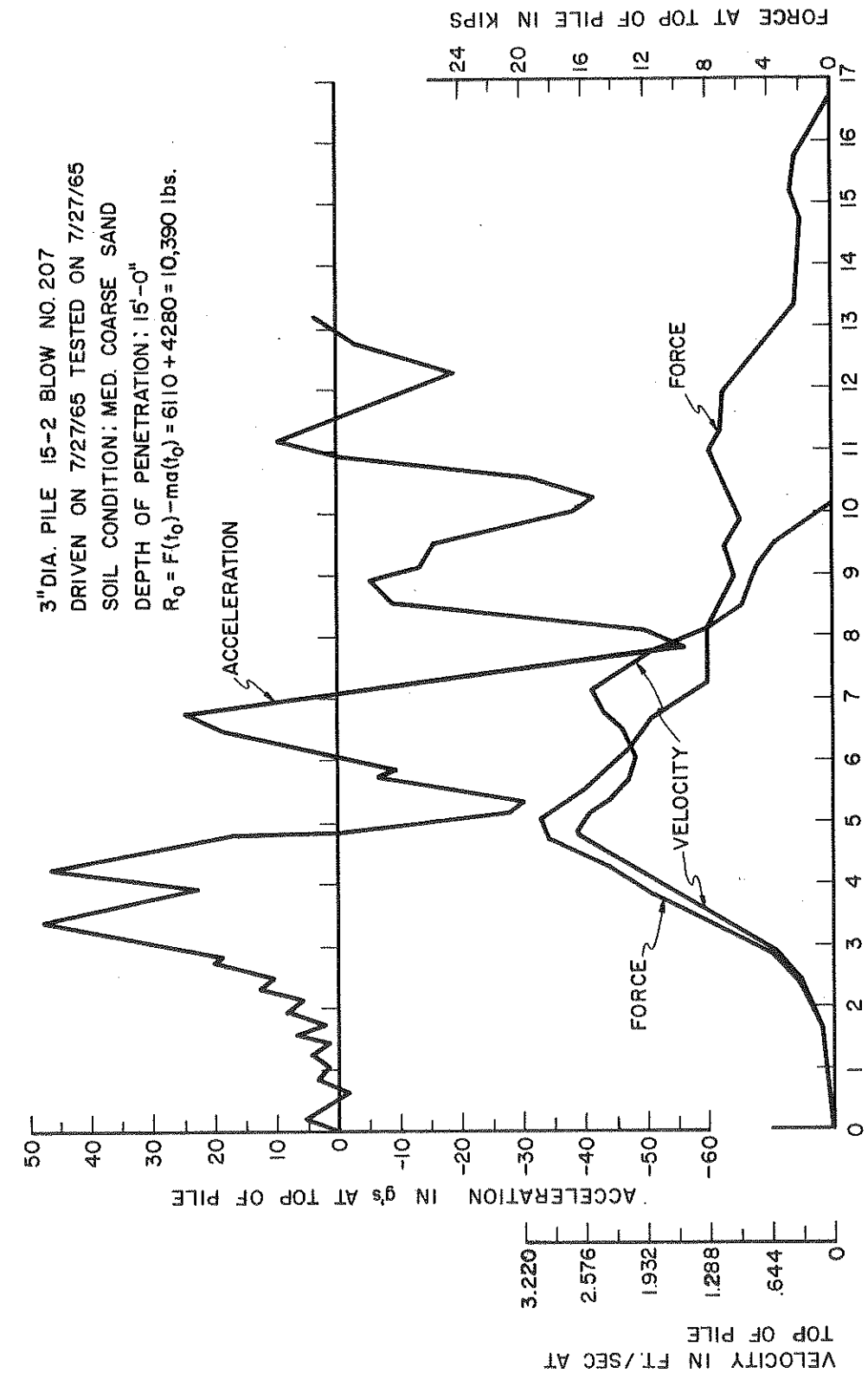

FIGURE 5.6

Dynamic Results of Model Pile No. 15-2 at the End of Driving, Blow No. 207

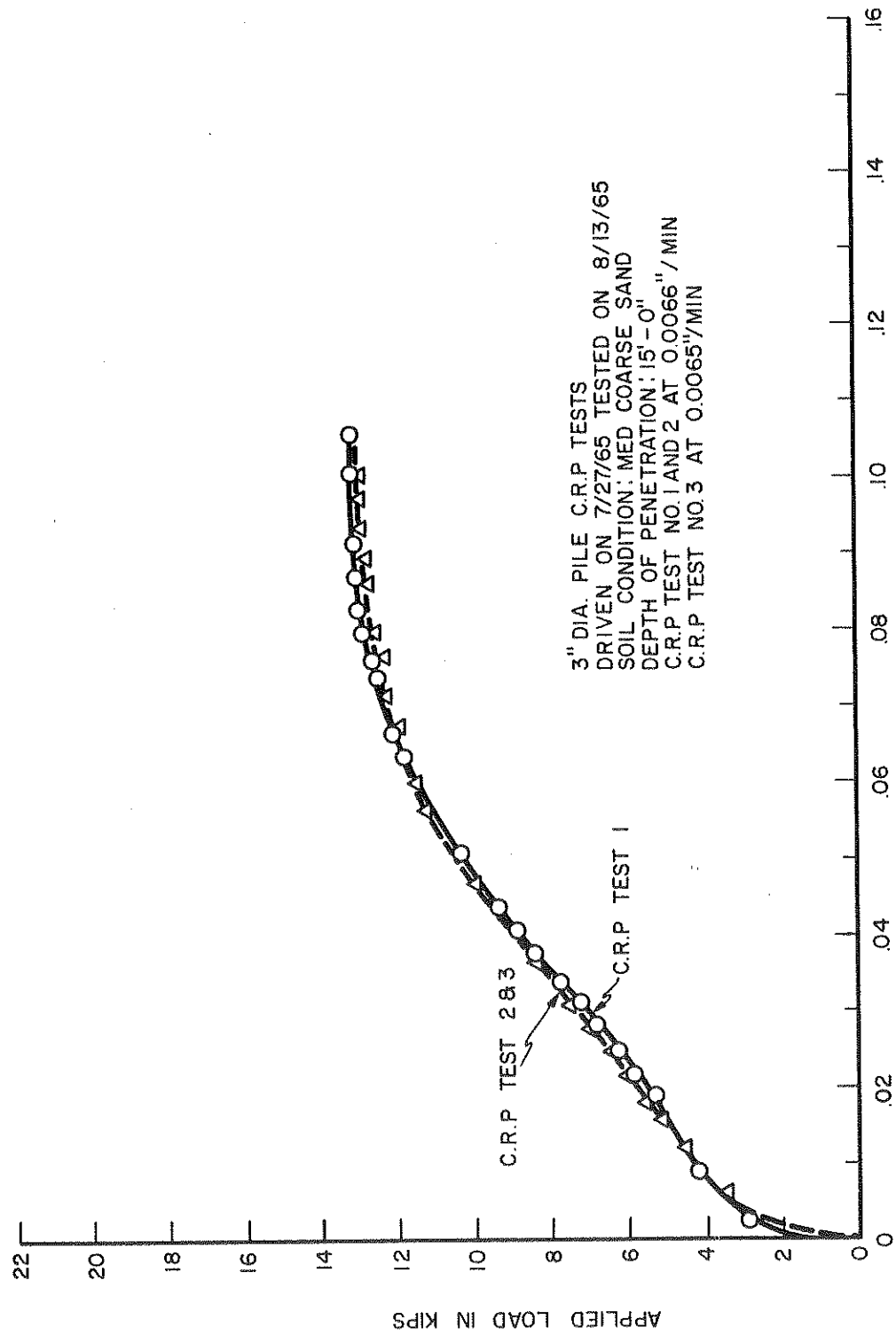

FIGURE 5.7

C.R.P. Test Results of Model Pile No. 15-2

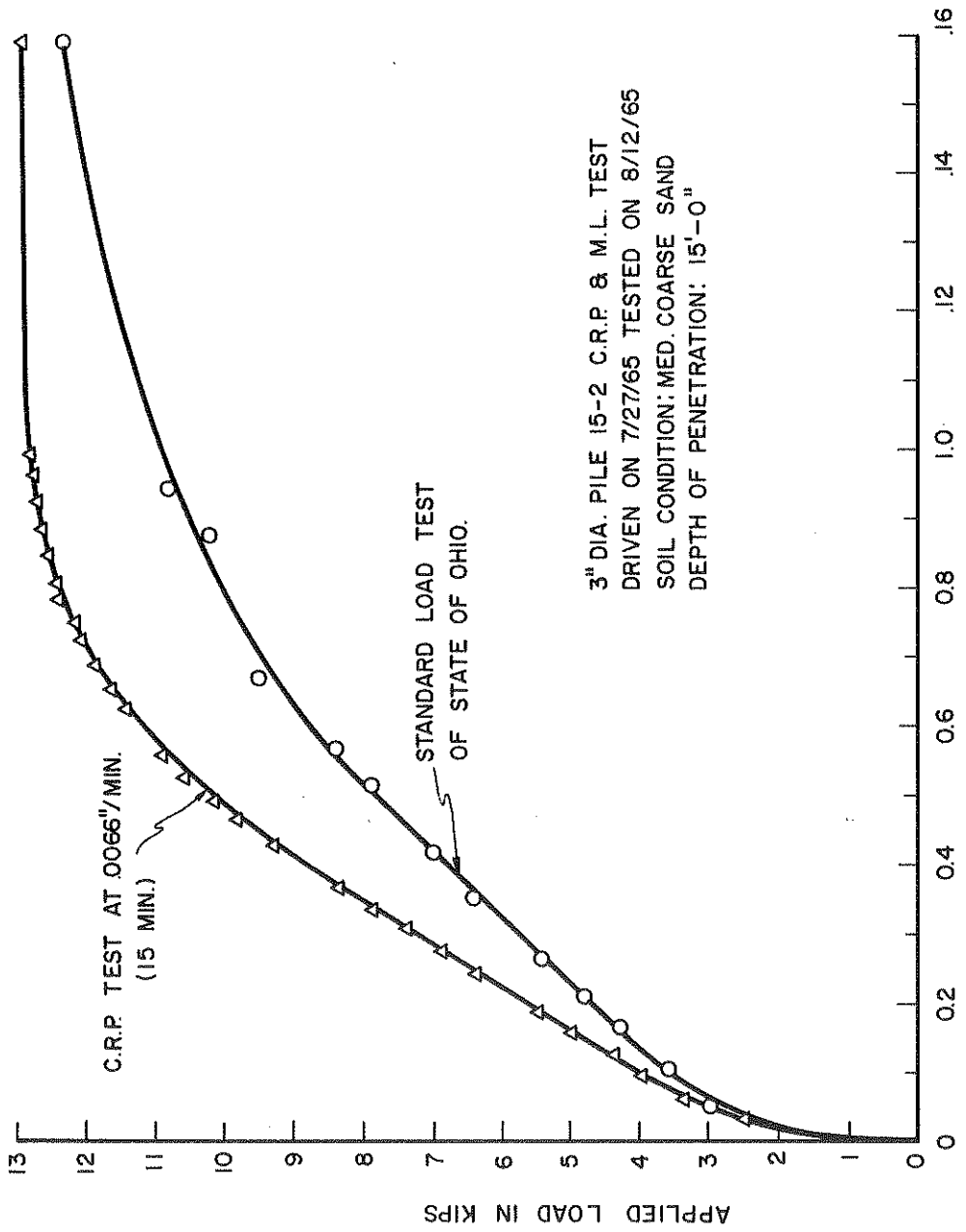

FIGURE 5.8

C.R.P. and M.L. Test Results of Model Pile No. 15-2

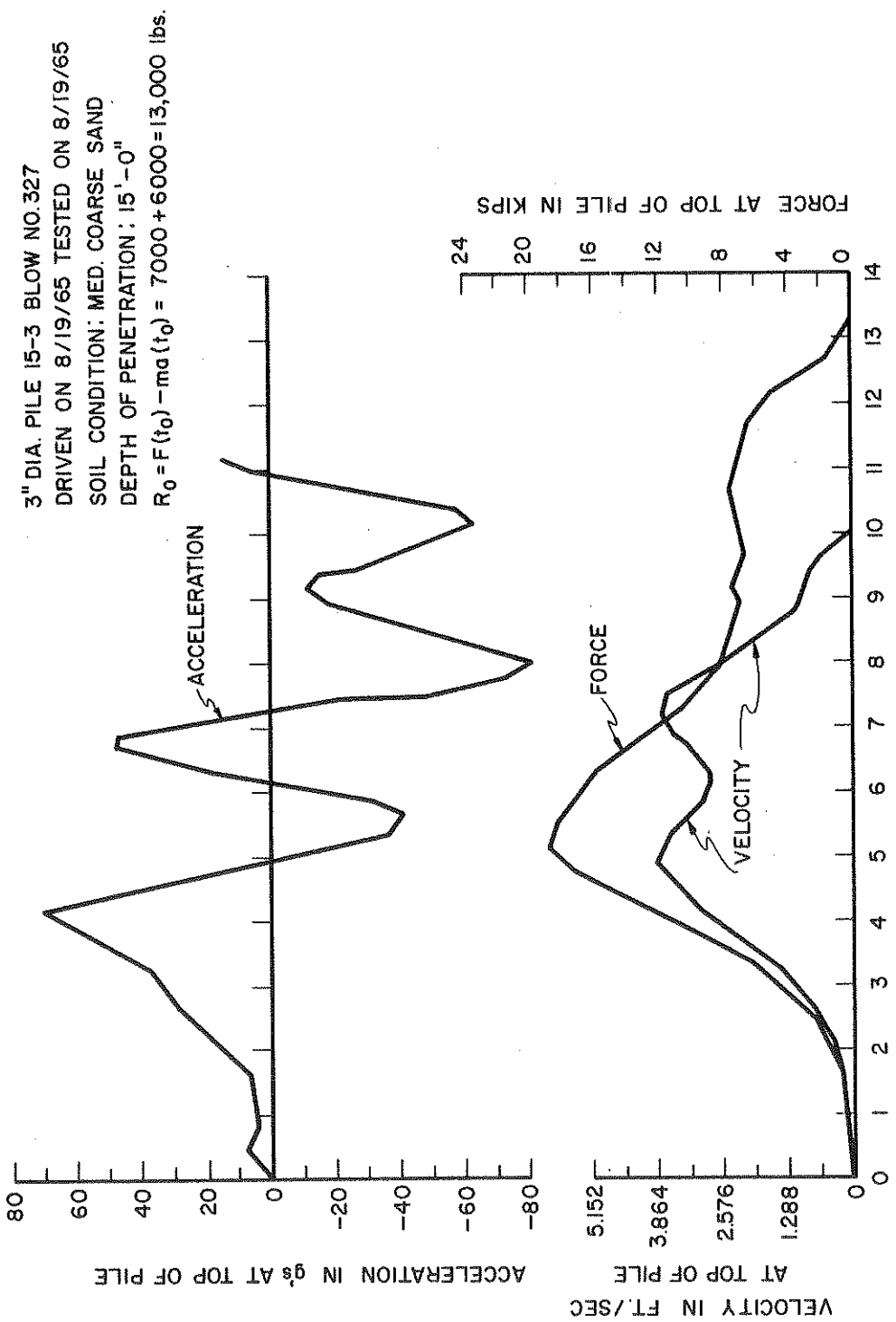

FIGURE 5.9

Dynamic Results of Model Pile 15-3 Blow No. 327 before 1st C.R.P. Test

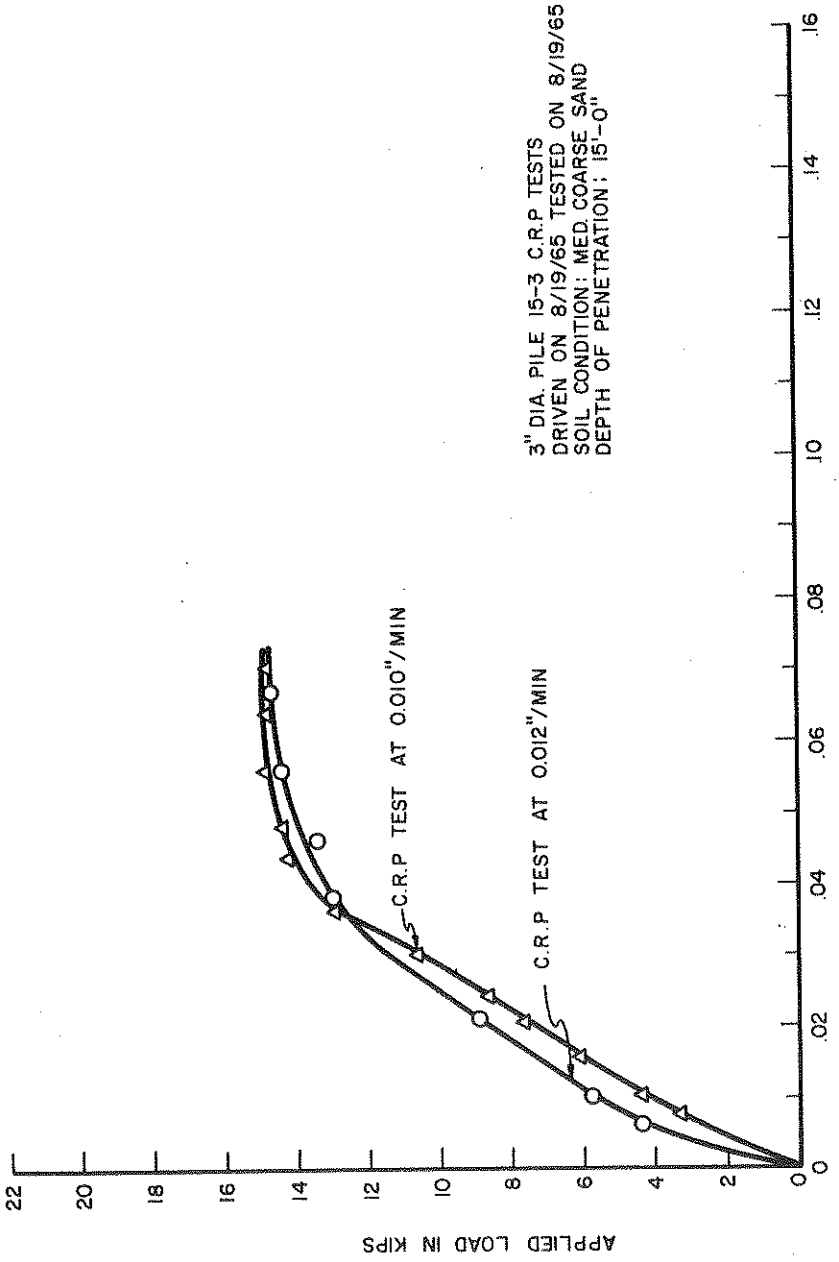

FIGURE 5.10

The C.R.P. Test Results of Model Pile 15-3, 3 hours after Initial Driving

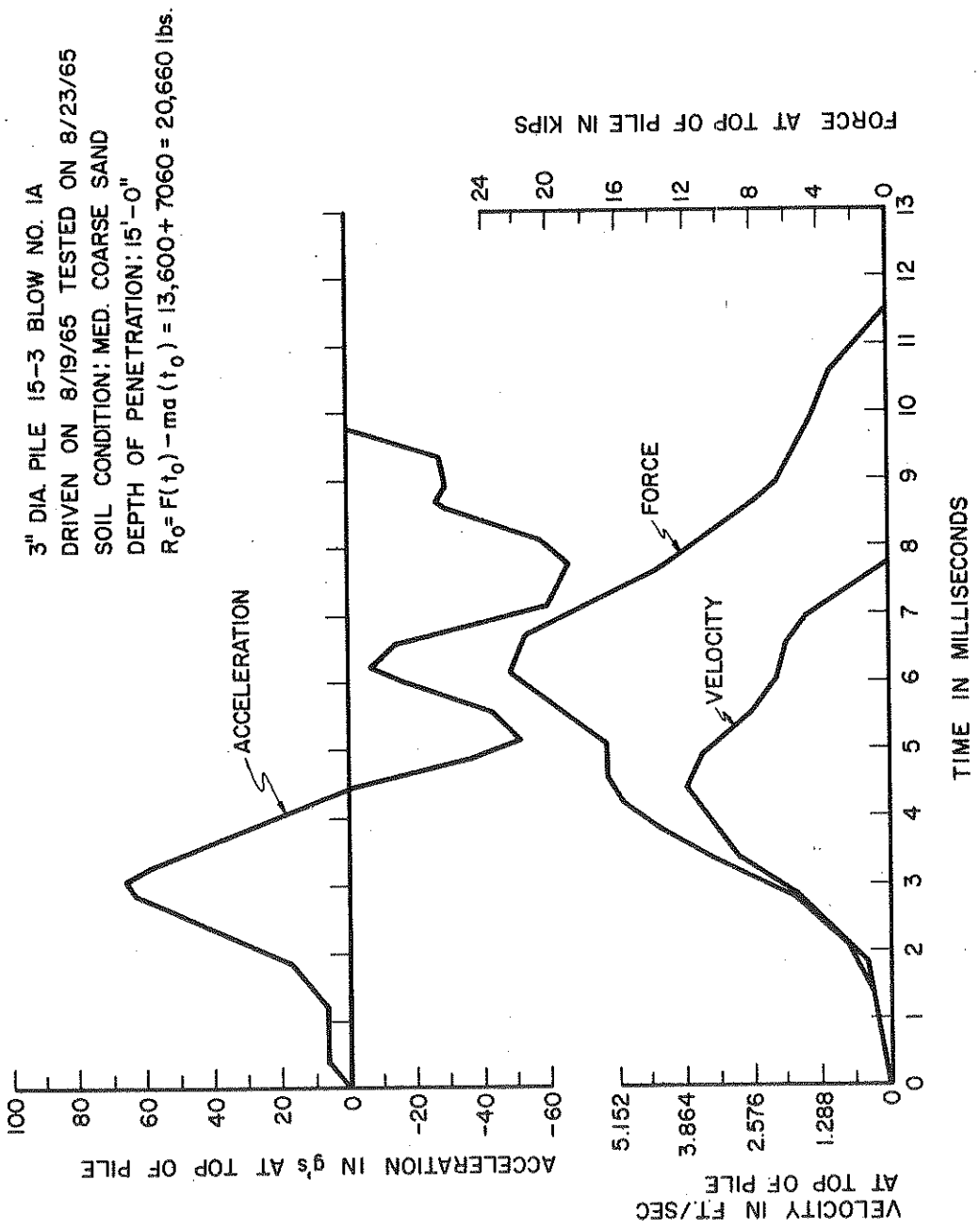

FIGURE 5.11

Dynamic Results of Model Pile 15-3 Blow No. 1A After C.R.P. Test

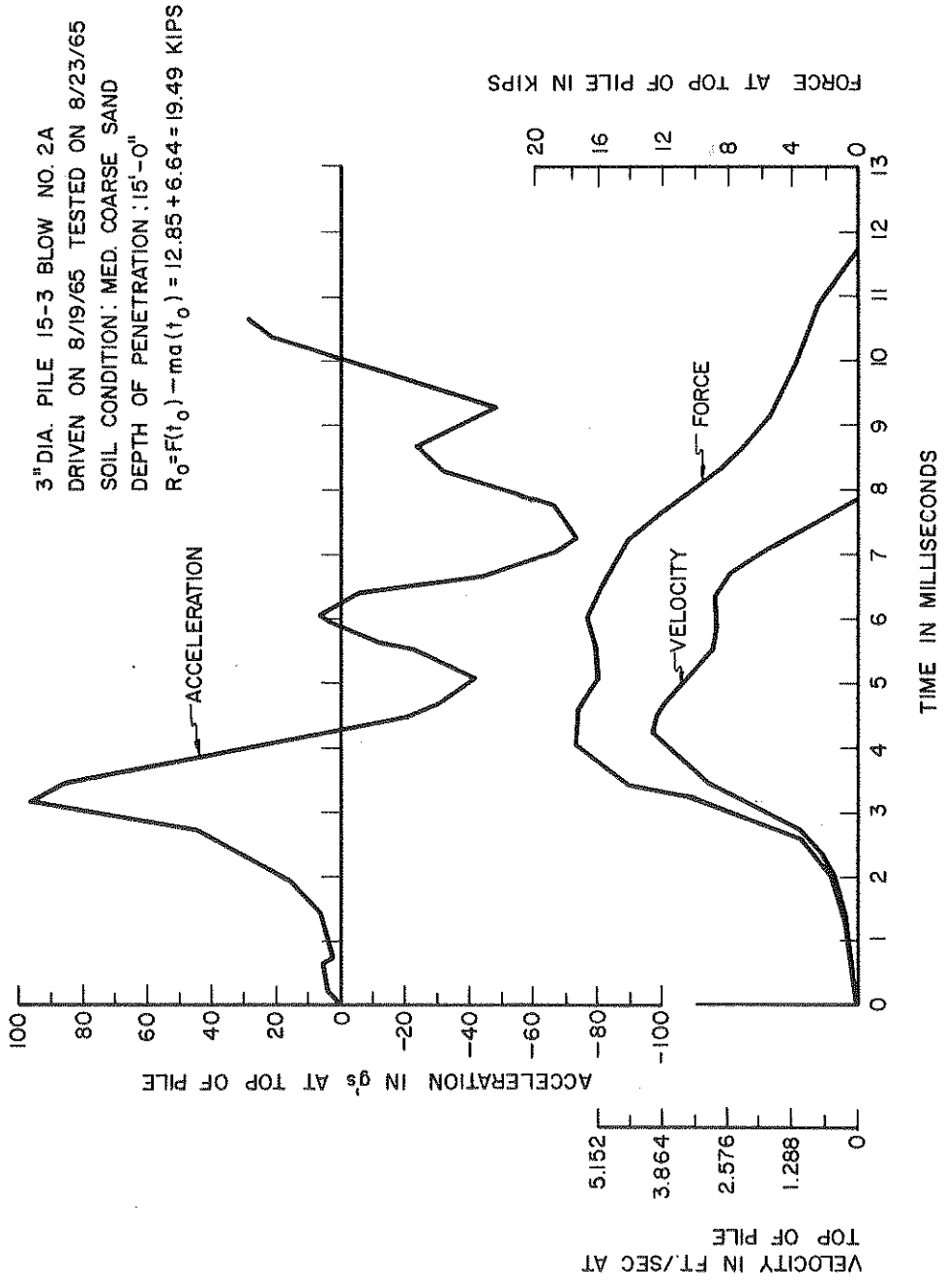

FIGURE 5.12

Dynamic Results of Model Pile 15-3 Blow No. 2A After C.R.P. Test

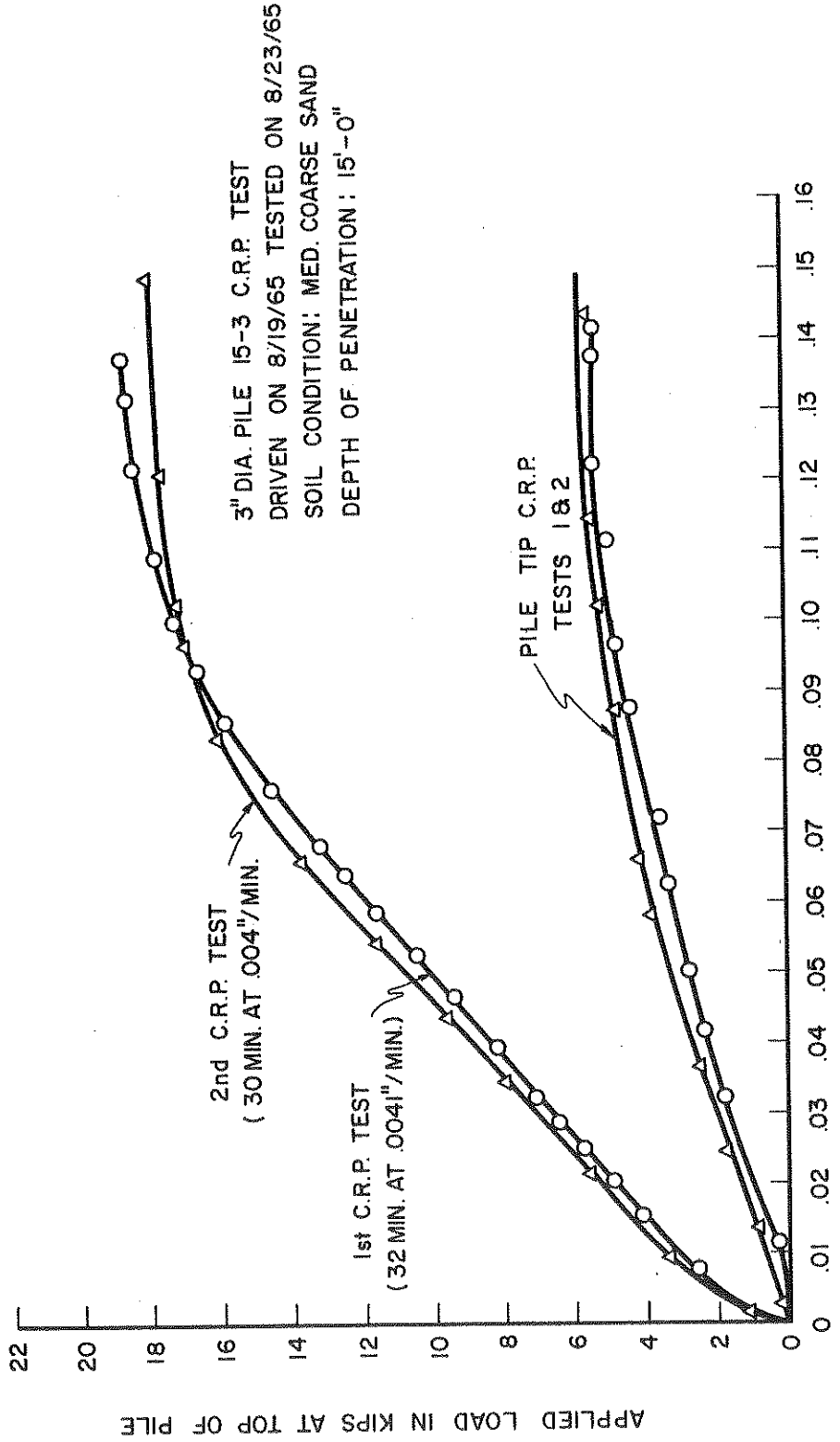

FIGURE 5.13

C.R.P. Test Results of Model Pile 15-3 After a 3-day Setup Period

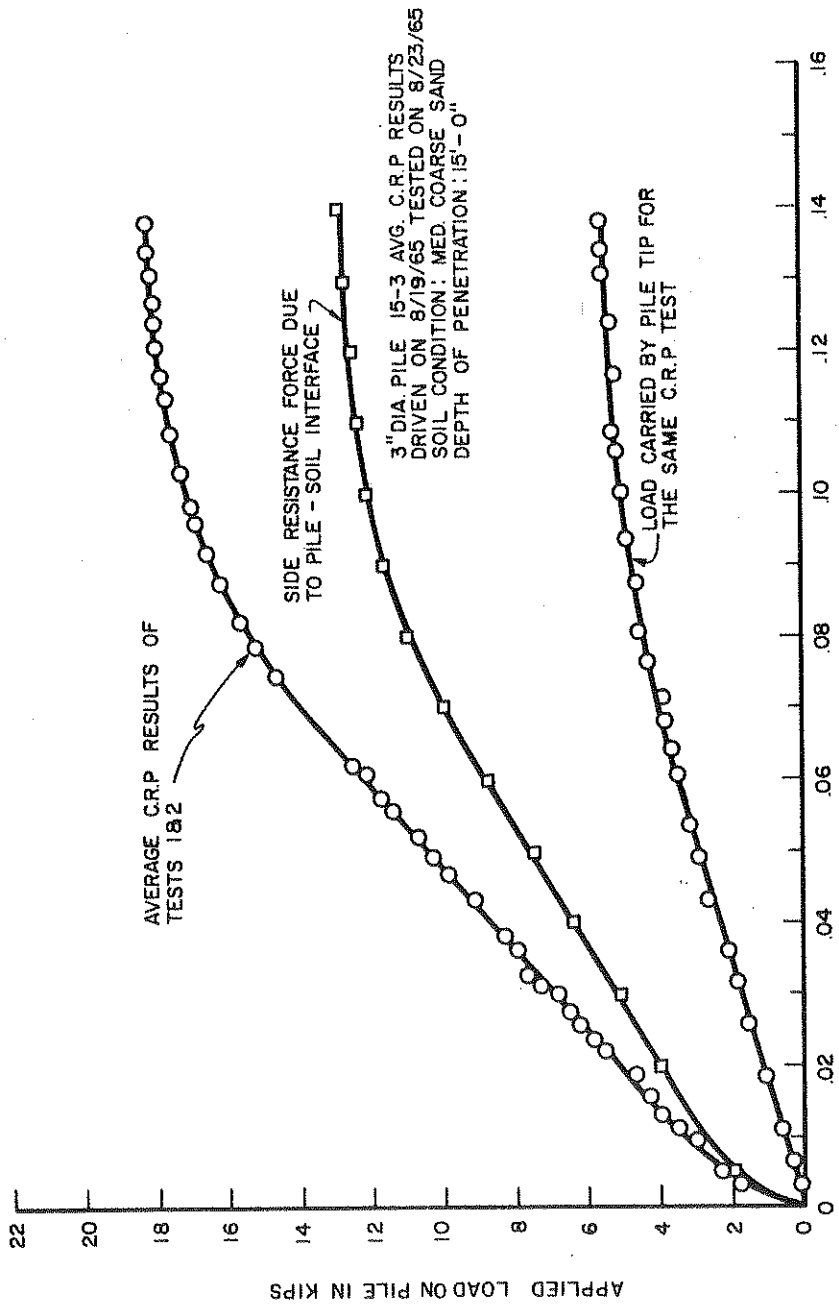

FIGURE 5-14

Average Results of C.R.P. Test of Model Pile 15-3 After a 3-day Setup

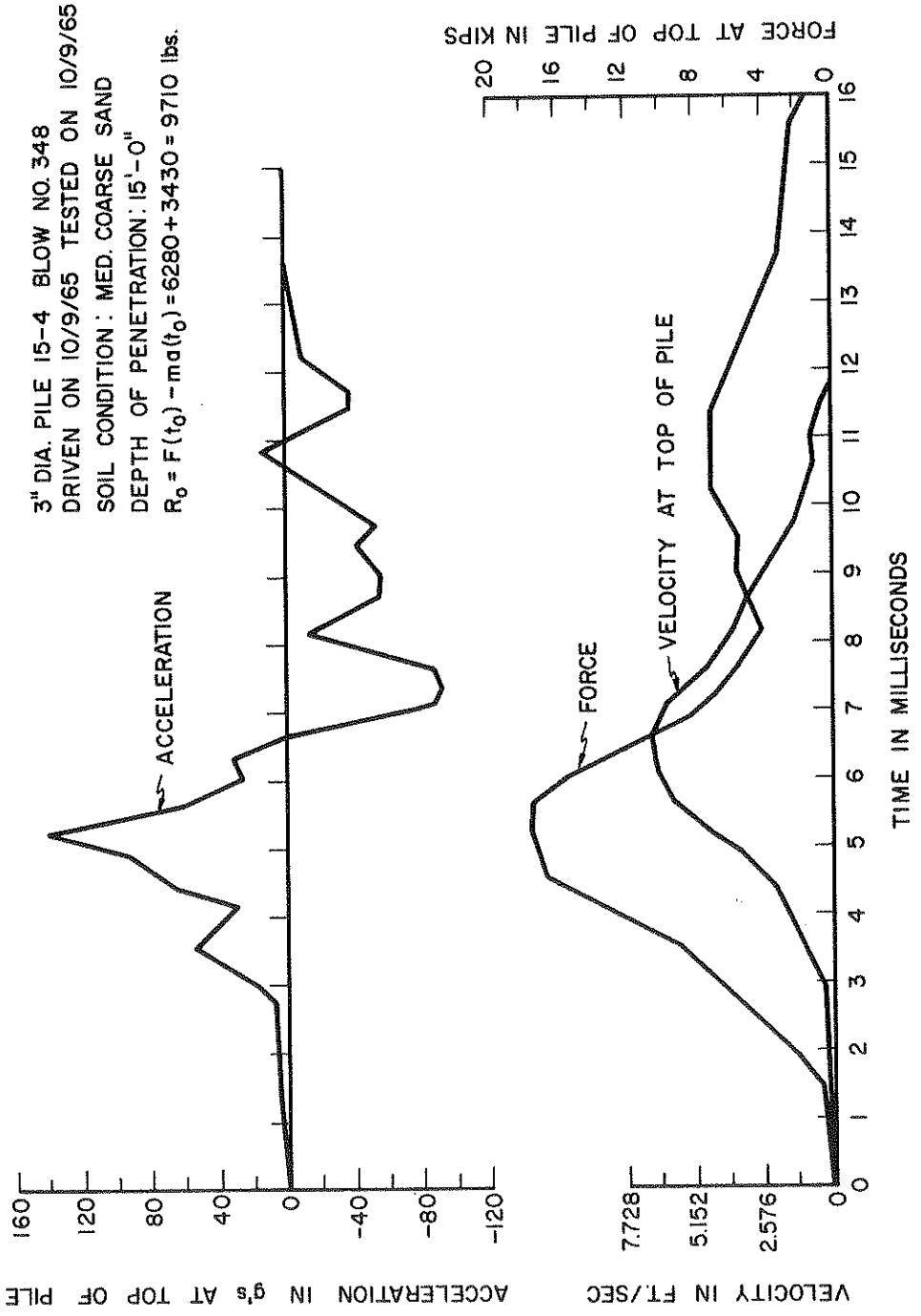

FIGURE 5.15

Dynamic Results of Model Pile No. 15-4 at the End of Driving, Blow No. 348

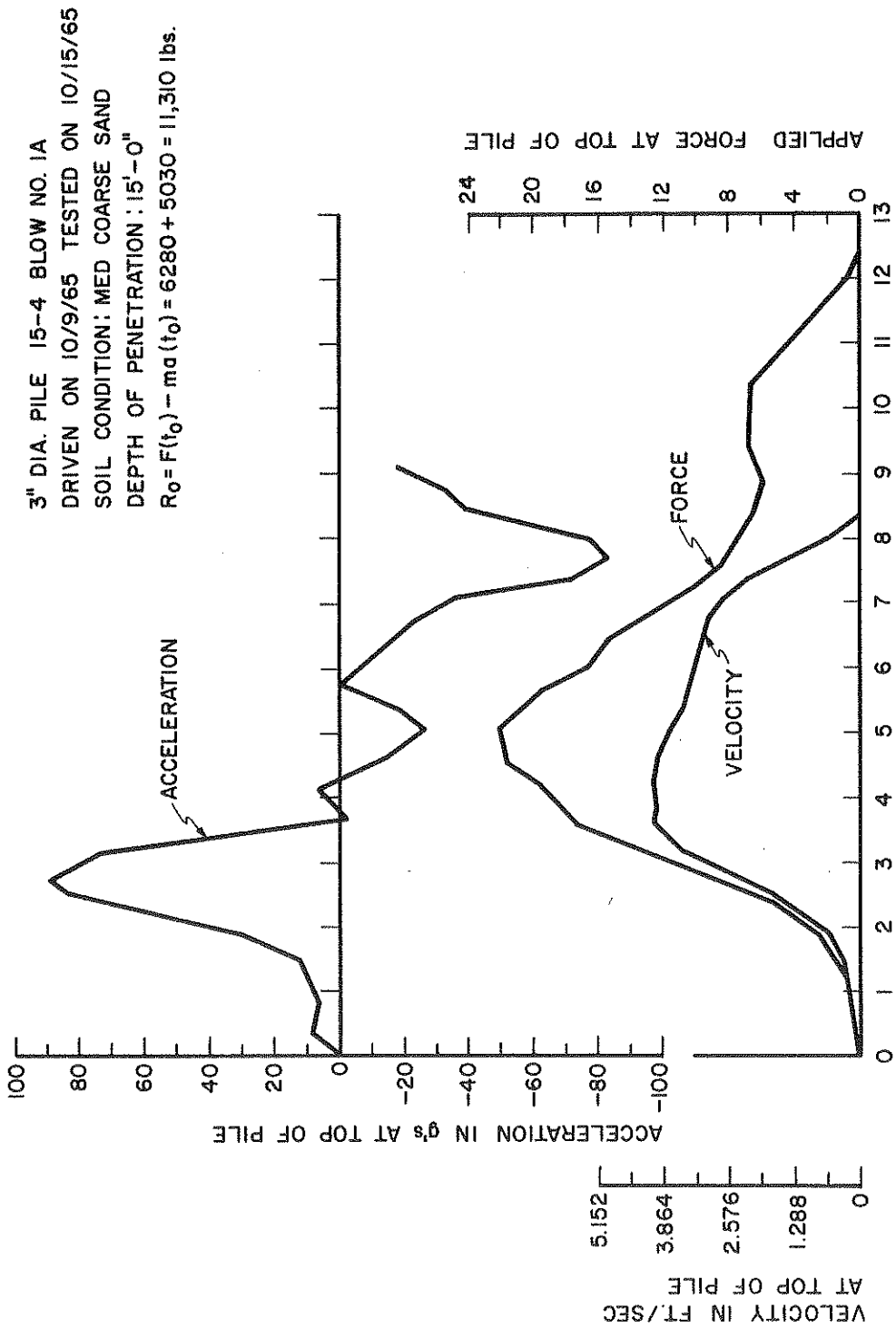

FIGURE 5-16

Dynamic Results After Setup Period for Model Pile No. 15-4, Blow No. 1A

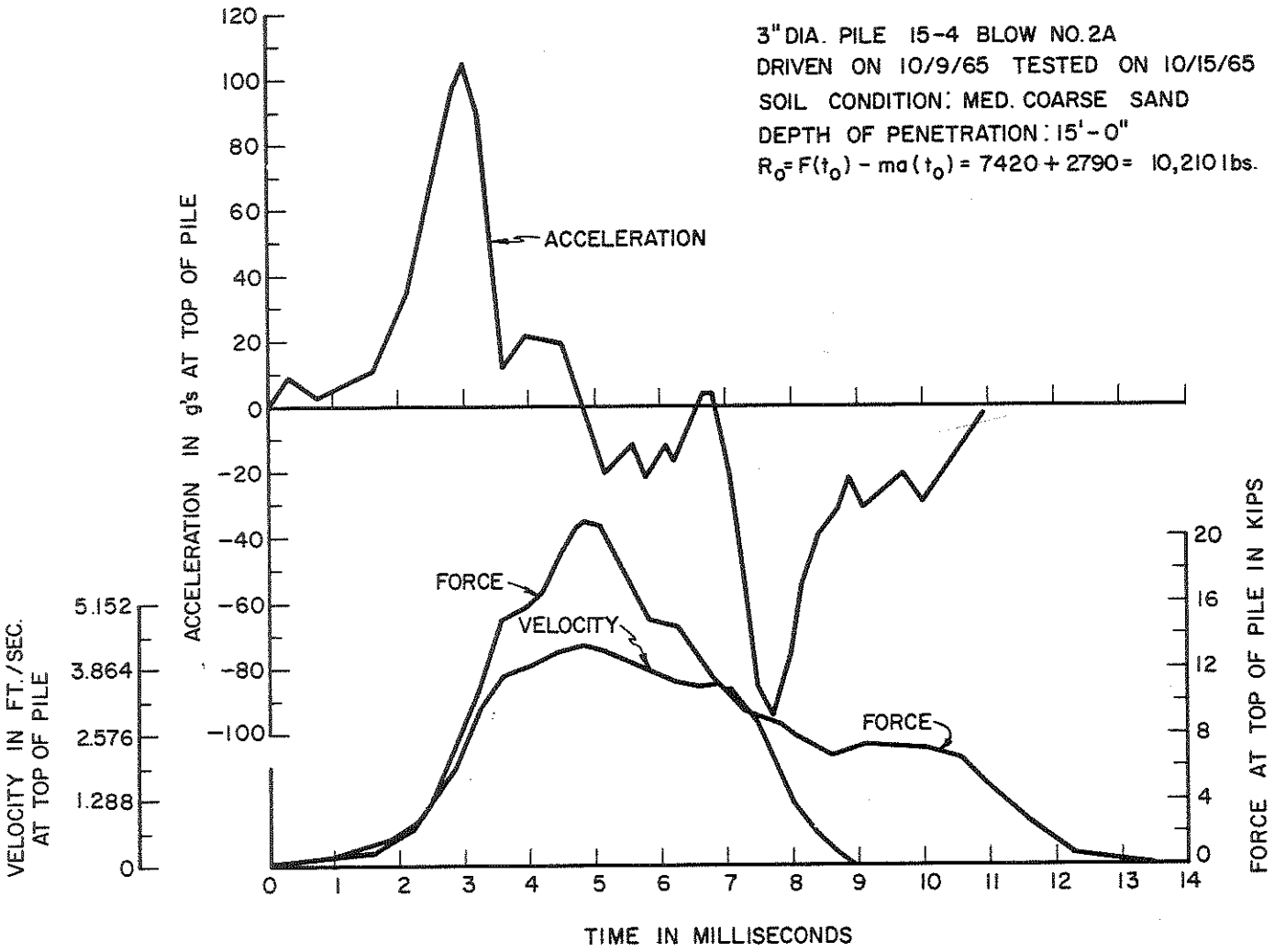

FIGURE 5-17

Dynamic Results After Setup Period, for Model Pile No. 15-4, Blow No. 2A

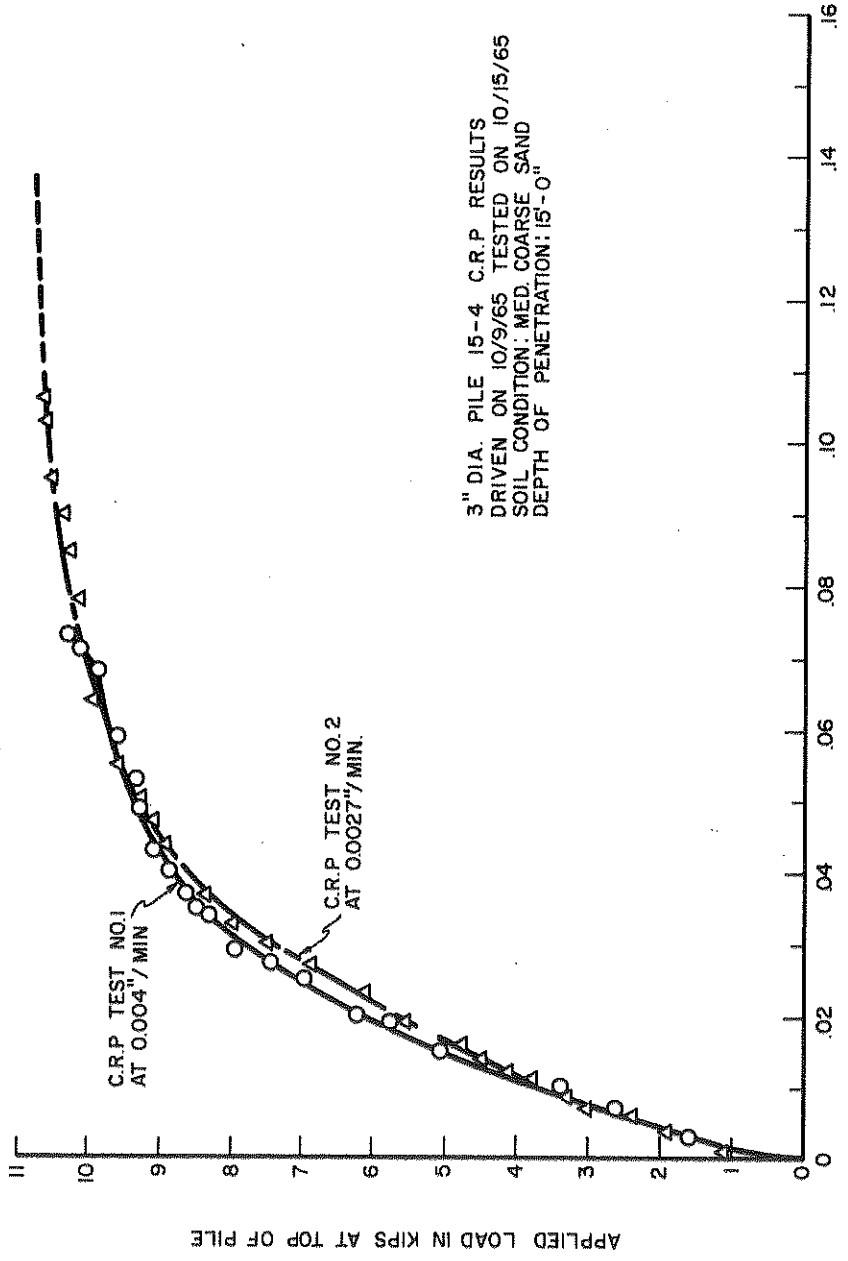

FIGURE 5.18

C.R.P. Test Results of Model Pile No. 15-4

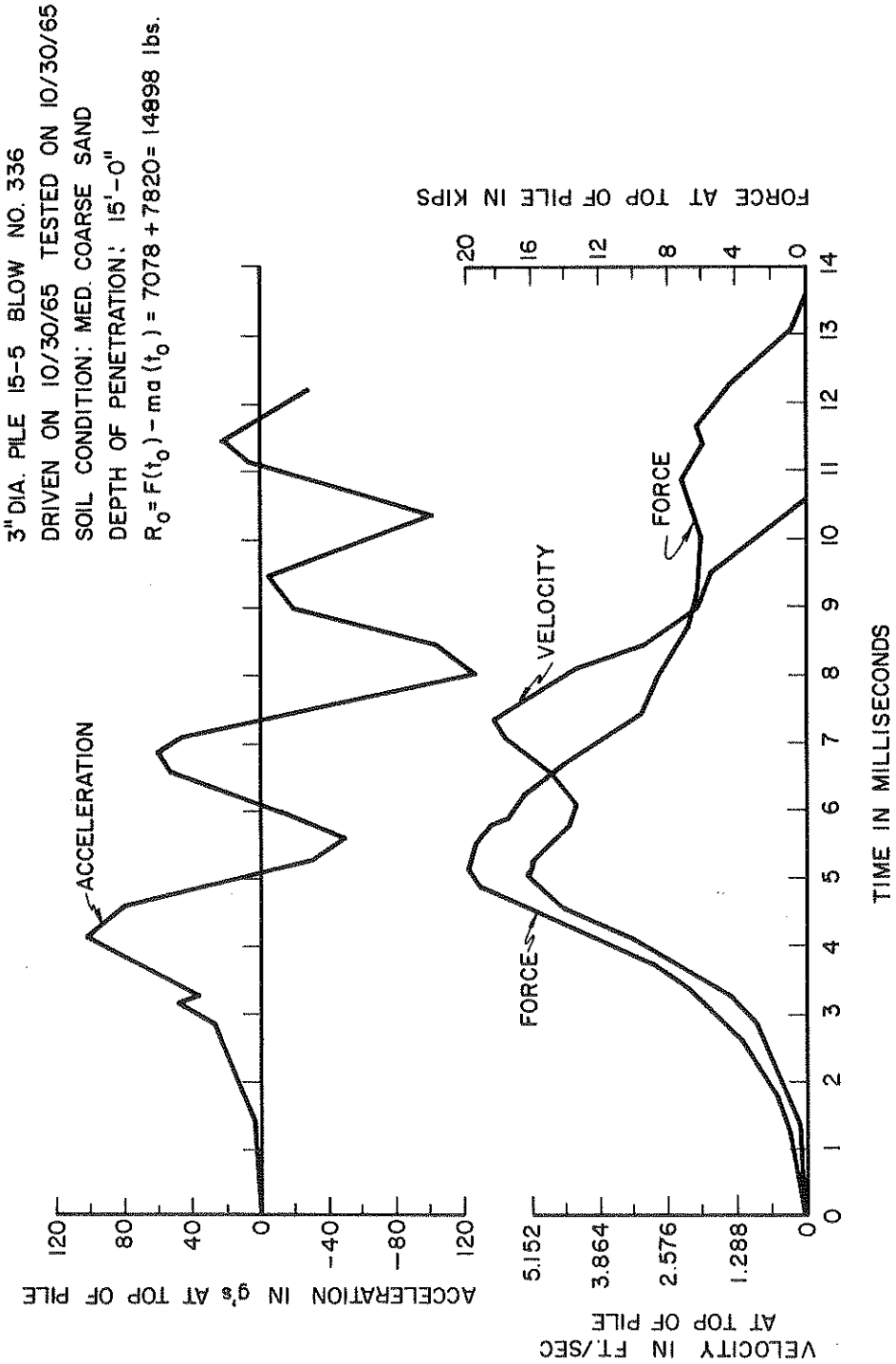

FIGURE 5.19

Dynamic Results of Model Pile No. 15-5 at the End of Driving Blow No. 336

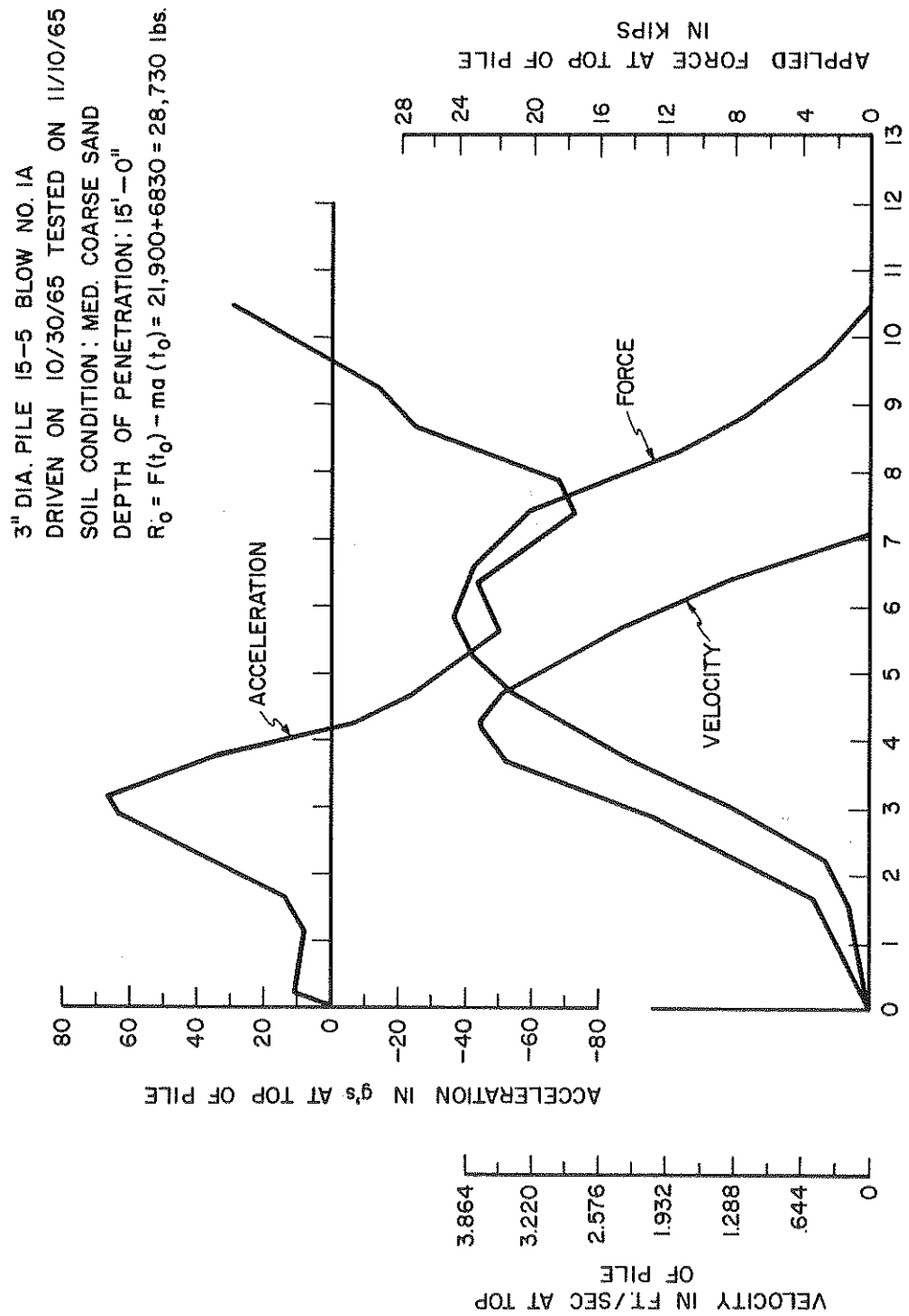

FIGURE 5-20

Dynamic Results of First Blow After Setup Period for Model Pile No. 15-5

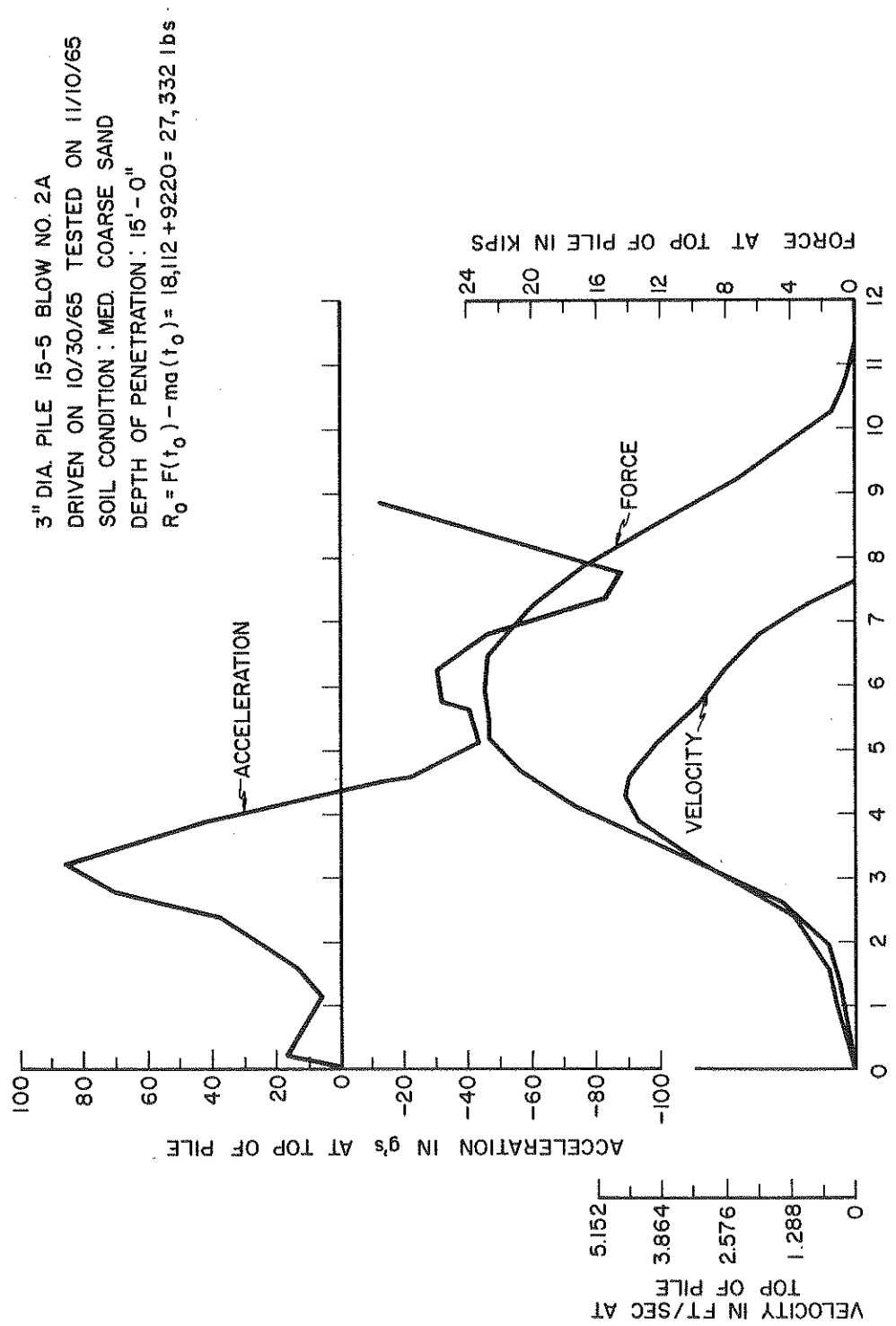

FIGURE 5-21

Dynamic Results of Second Blow After Setup Period for Model Pile No. 15-5

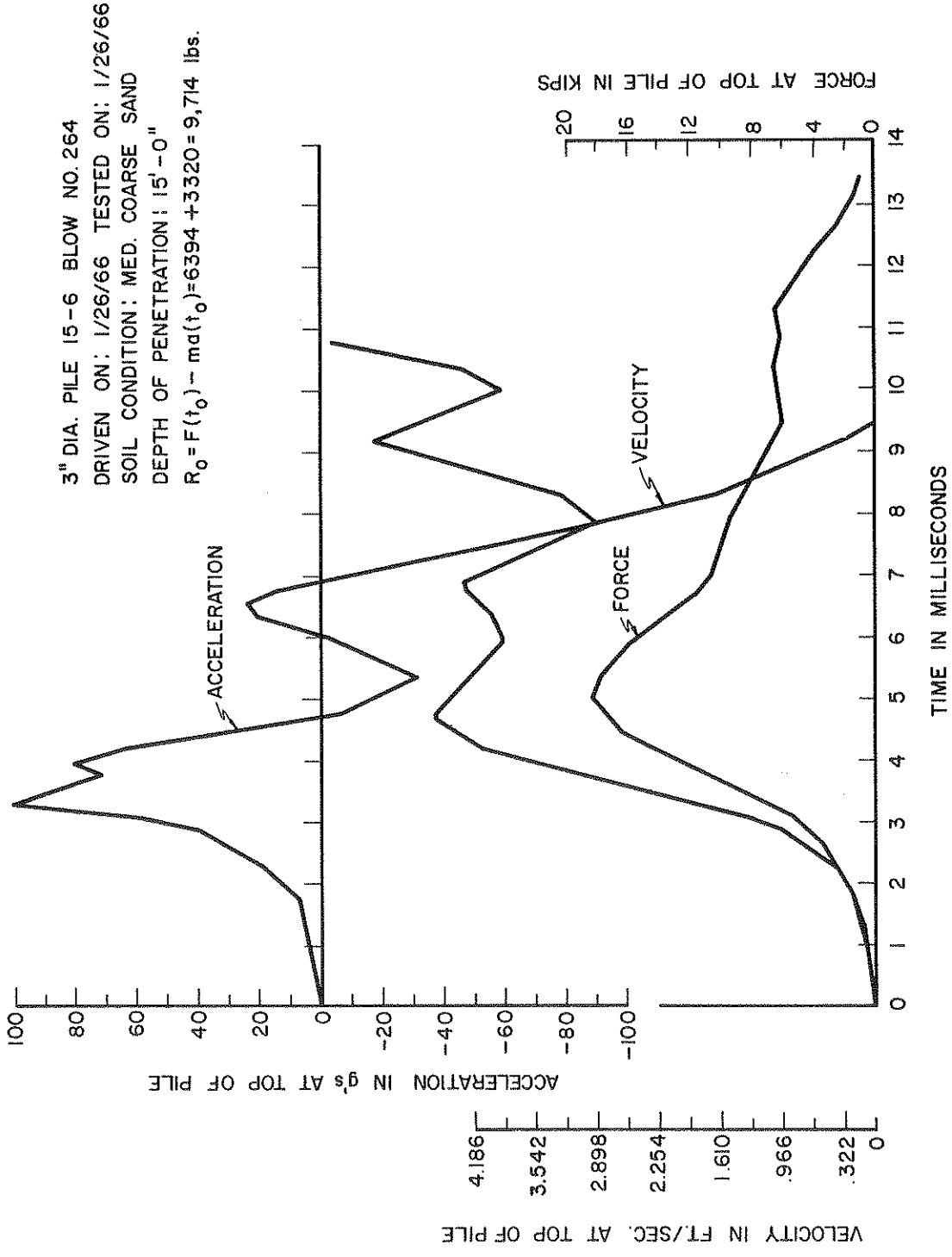

FIGURE 5-22

Dynamic Results of Model Pile No. 15-6 at the End of Driving, Blow No. 264

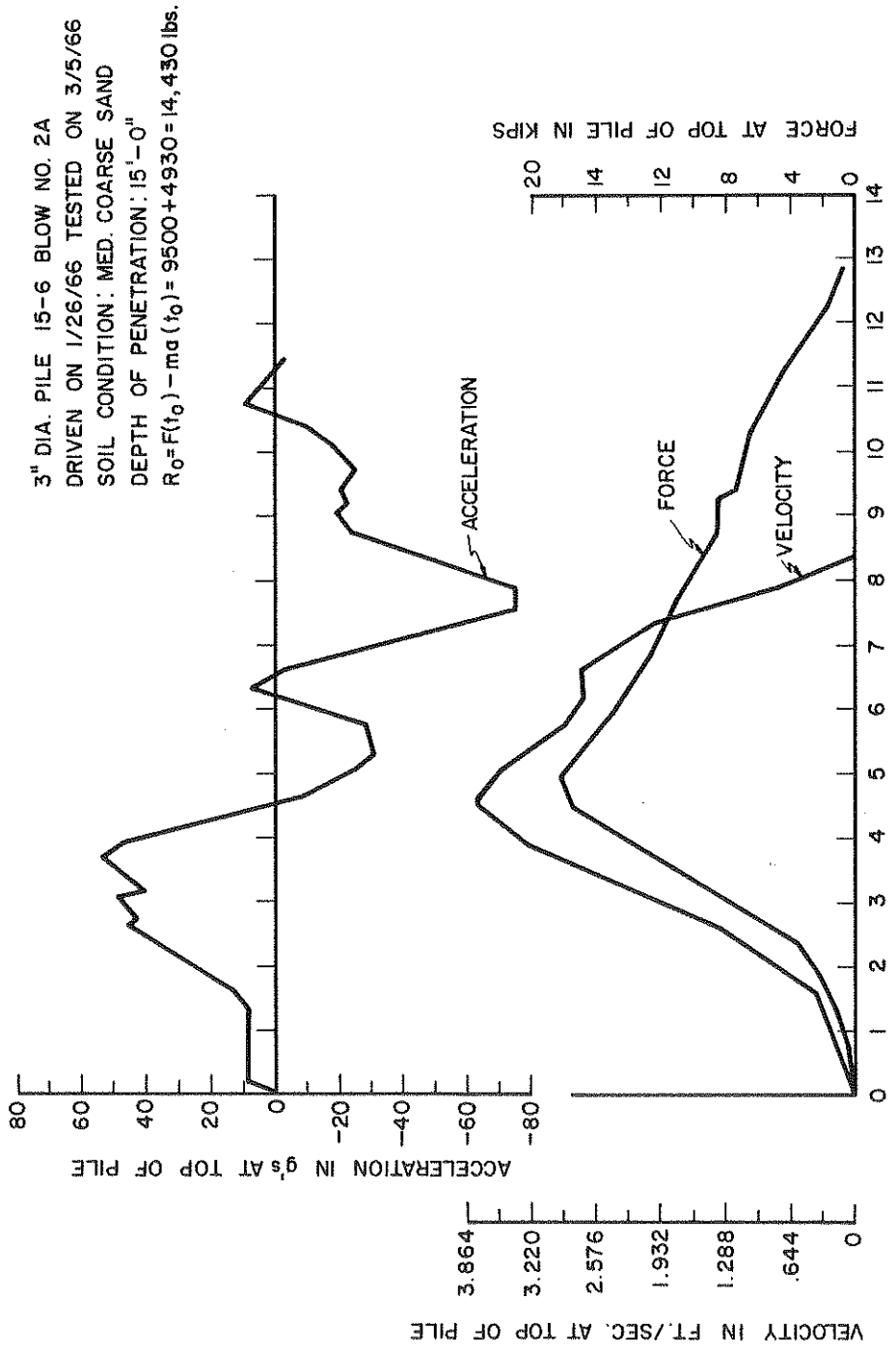

FIGURE 5-23

Dynamic Results After Setup Period for Model Pile No. 15-6 Blow No. 2A

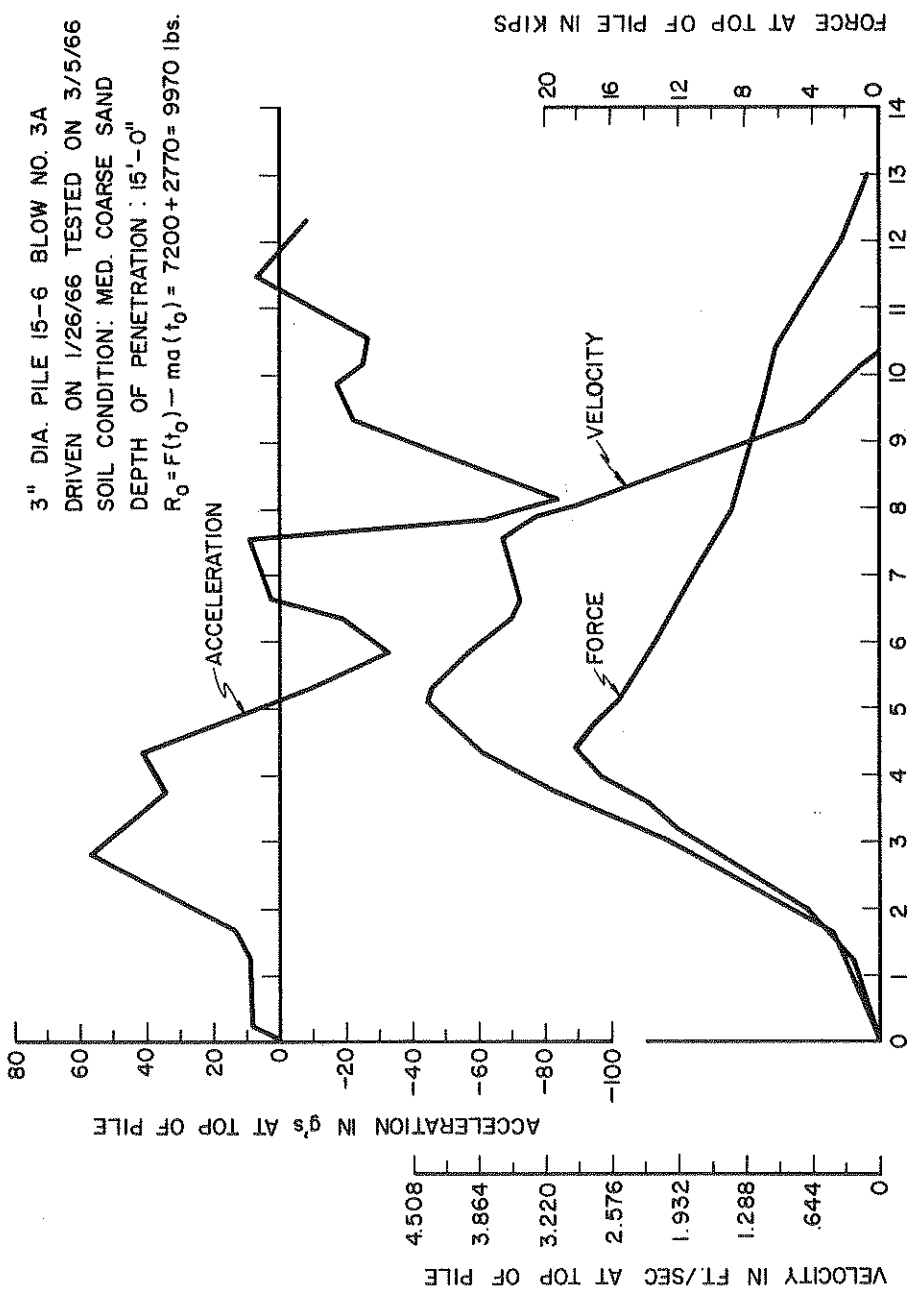

FIGURE 5-24

Dynamic Results After Setup Period for Model Pile No. 15-6 Blow No. 3A

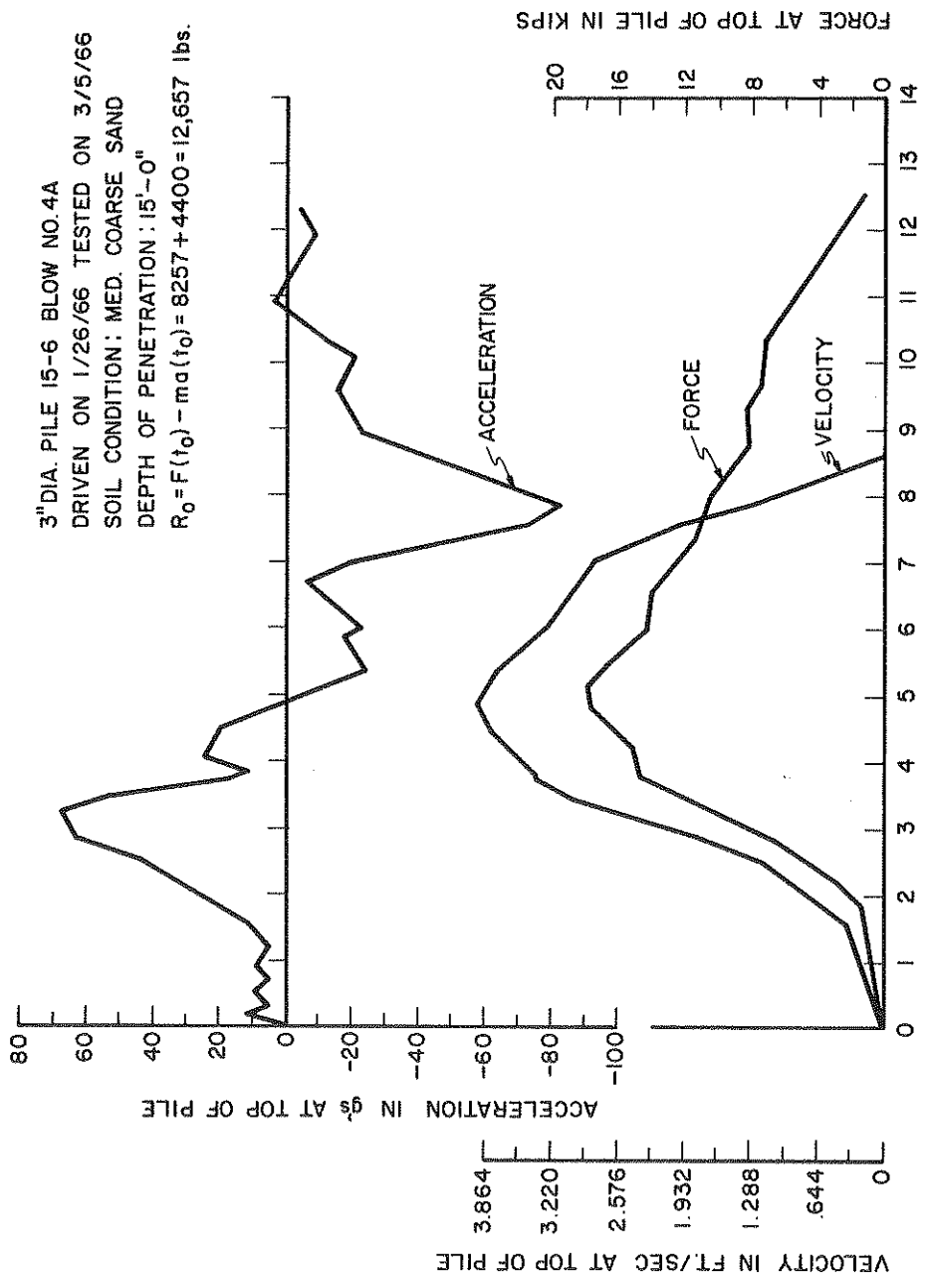

FIGURE 5-25

Dynamic Results After Setup Period for Model Pile No. 15-6, Blow No. 4A

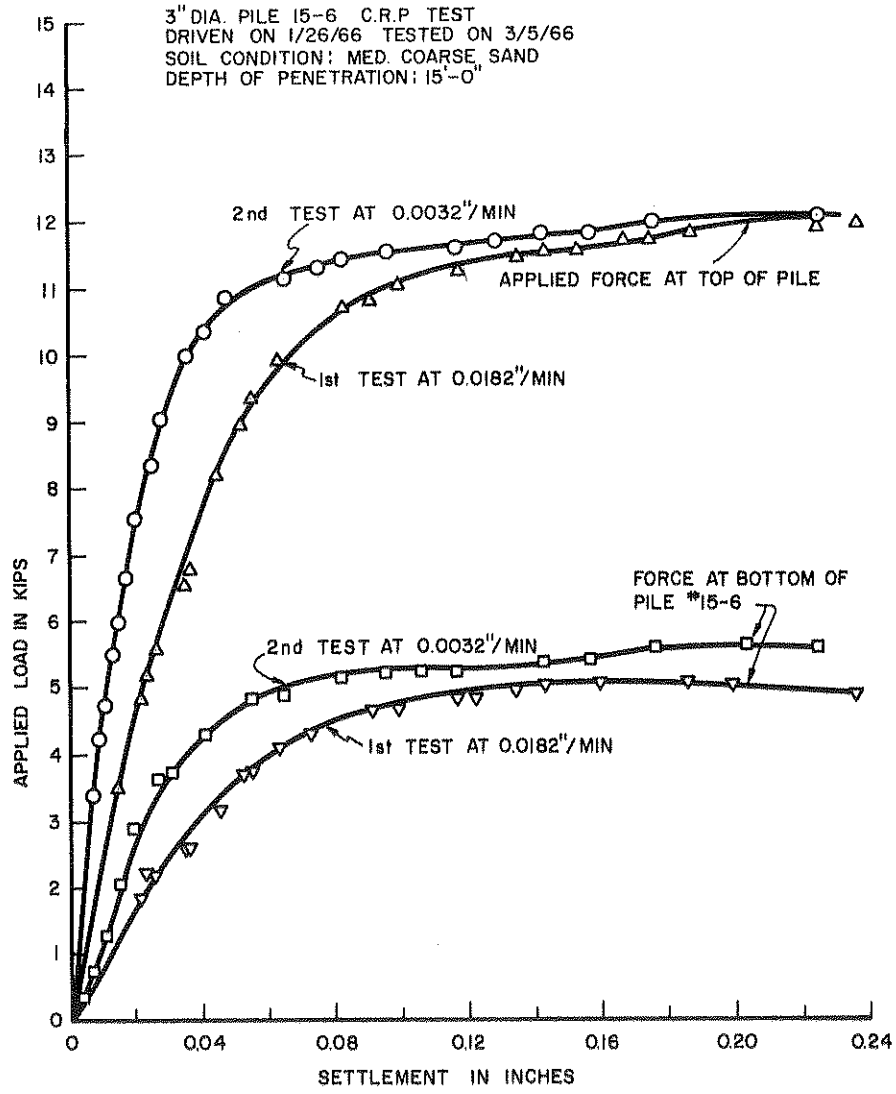

FIGURE 5.26

C.R.P. Test Results of Model Pile No. 15-6

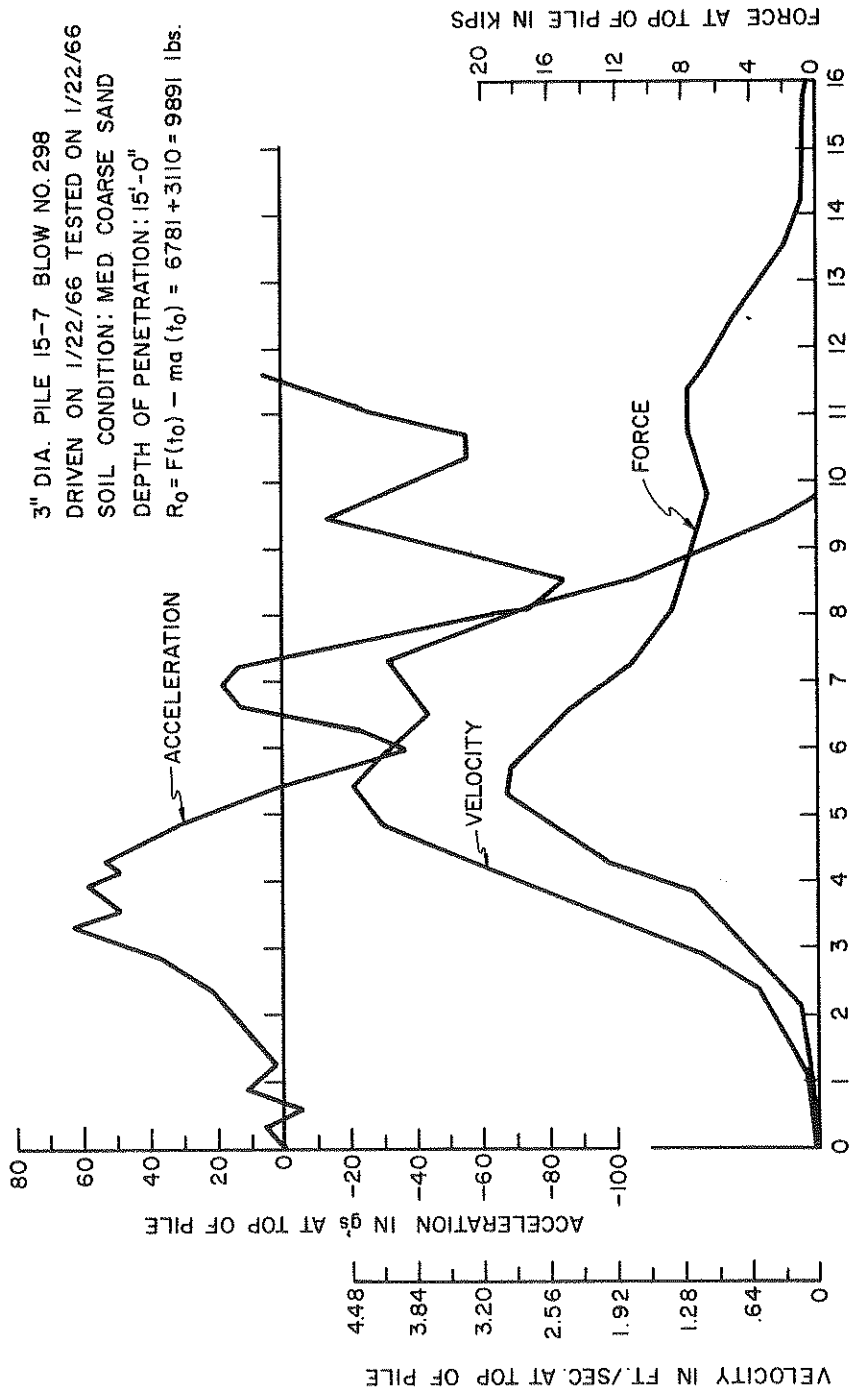

FIGURE 5-27

Dynamic Results of Model Pile No. 15-7 at the End of Driving, Blow No. 298

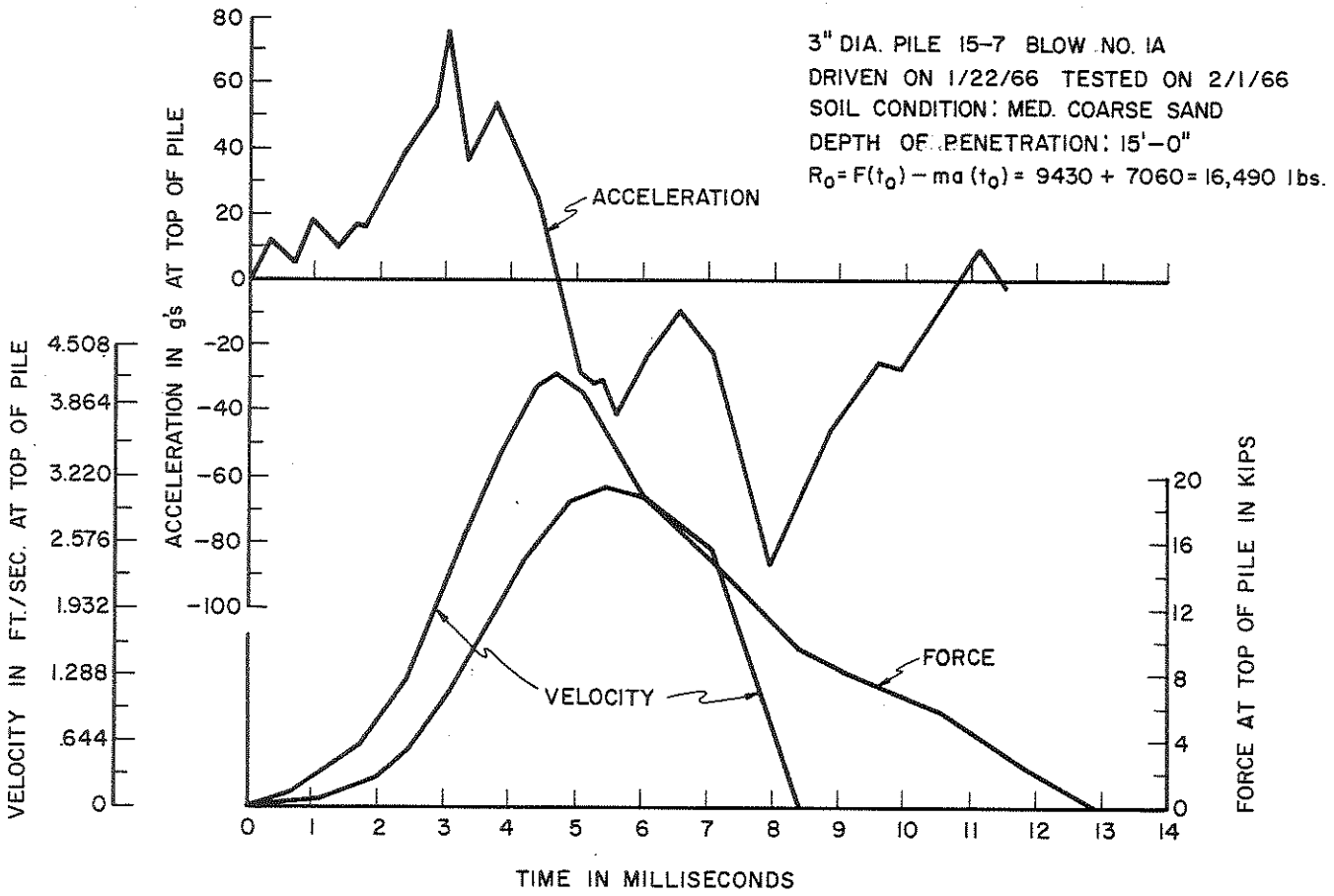

FIGURE 5-28

Dynamic Results After Setup Period for Model Pile No. 15-7, Blow No. 1A

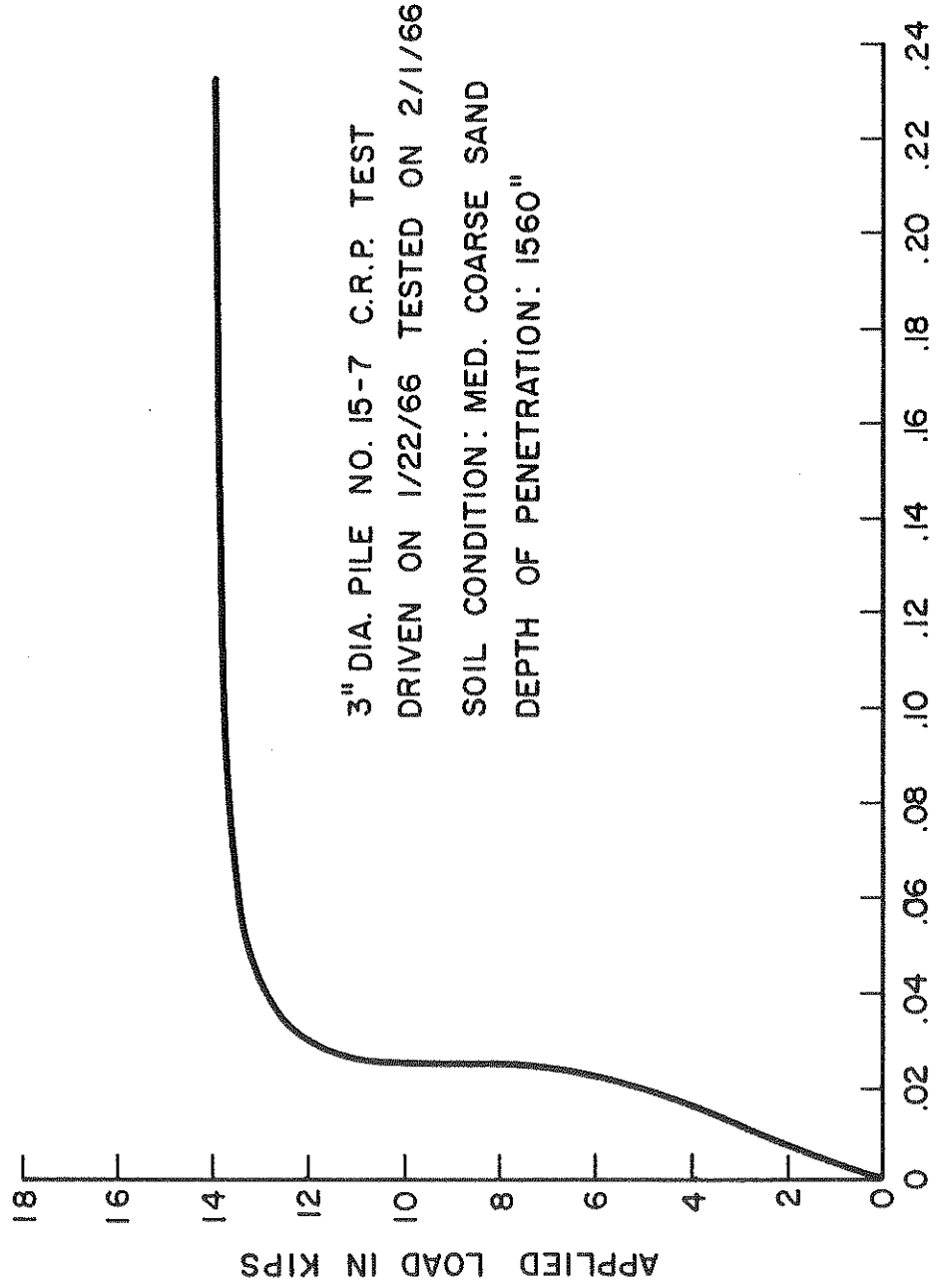

FIGURE 5-29

C.R.P. Test Results of Model Pile No. 15-7, After a 9-day Setup

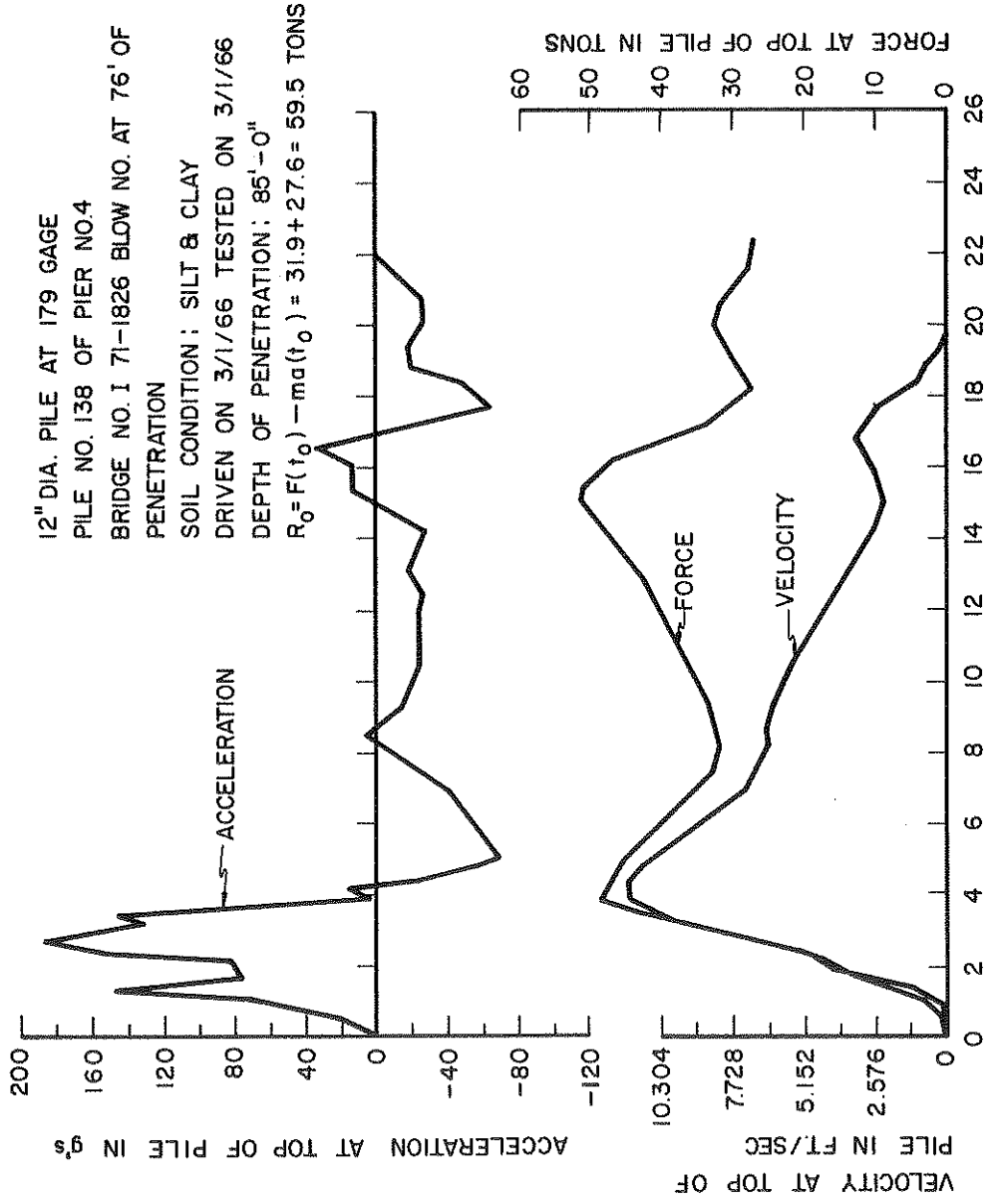

FIGURE 5-30

Dynamic Results of Full Scale Pile No. 138 of Pier No. 4 of Bridge No. I-71, 1826, Blow at 76' of Penetration

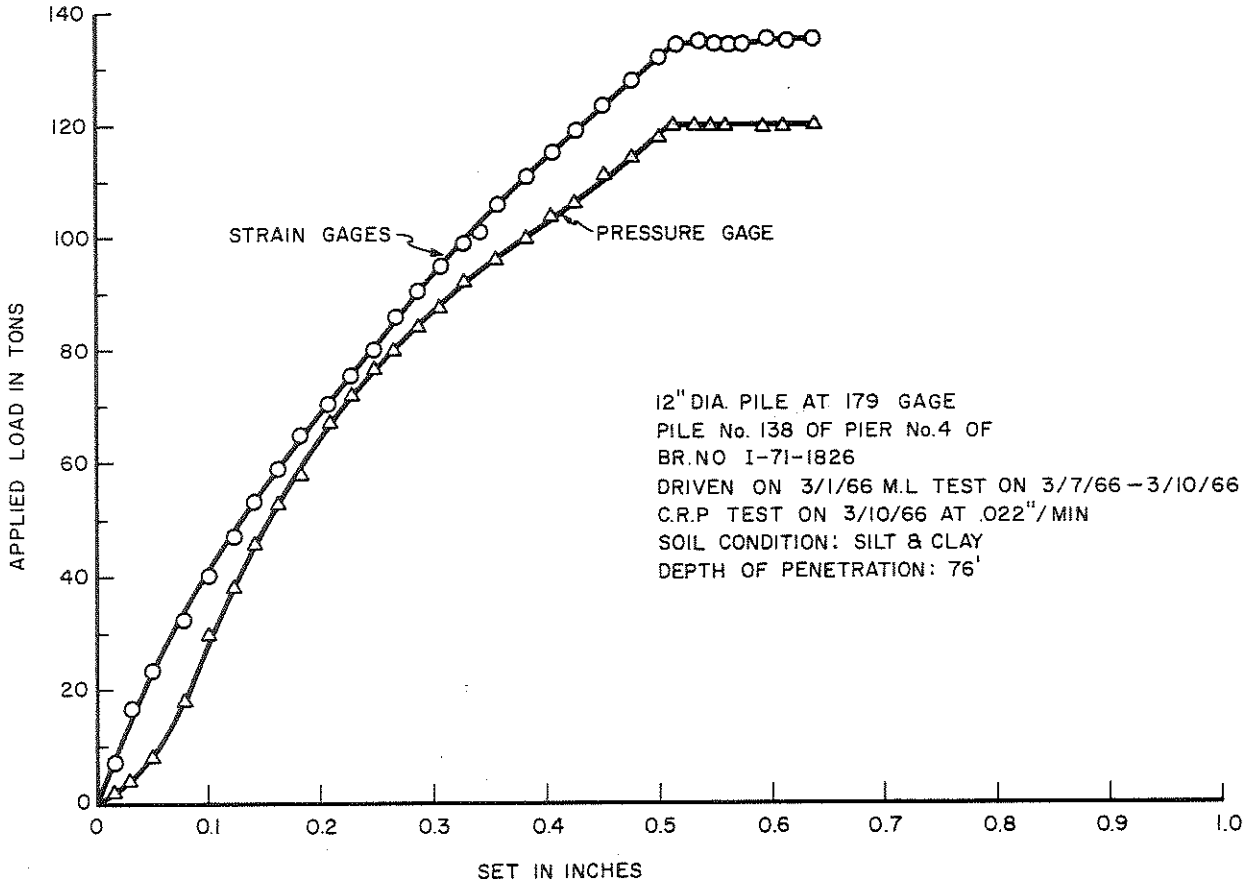

FIGURE 5-31

Comparisen of Load Obtained From Strain Gages and Pressure Gage Supplied by Contractor

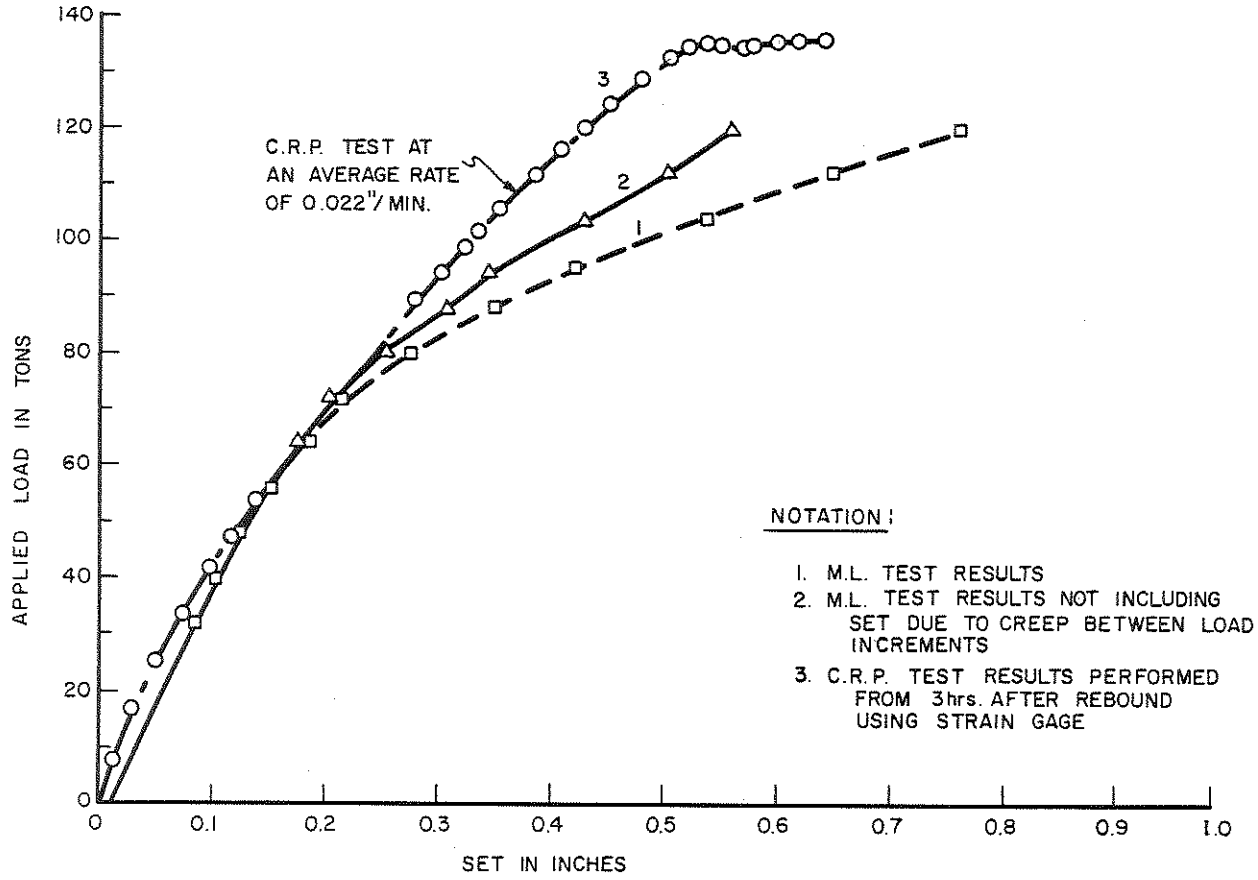

FIGURE 5-32

Comparison of C.R.P. Test and M.L. Test of Pile No. 138 of Pier No. 4, Bridge I 71-1826

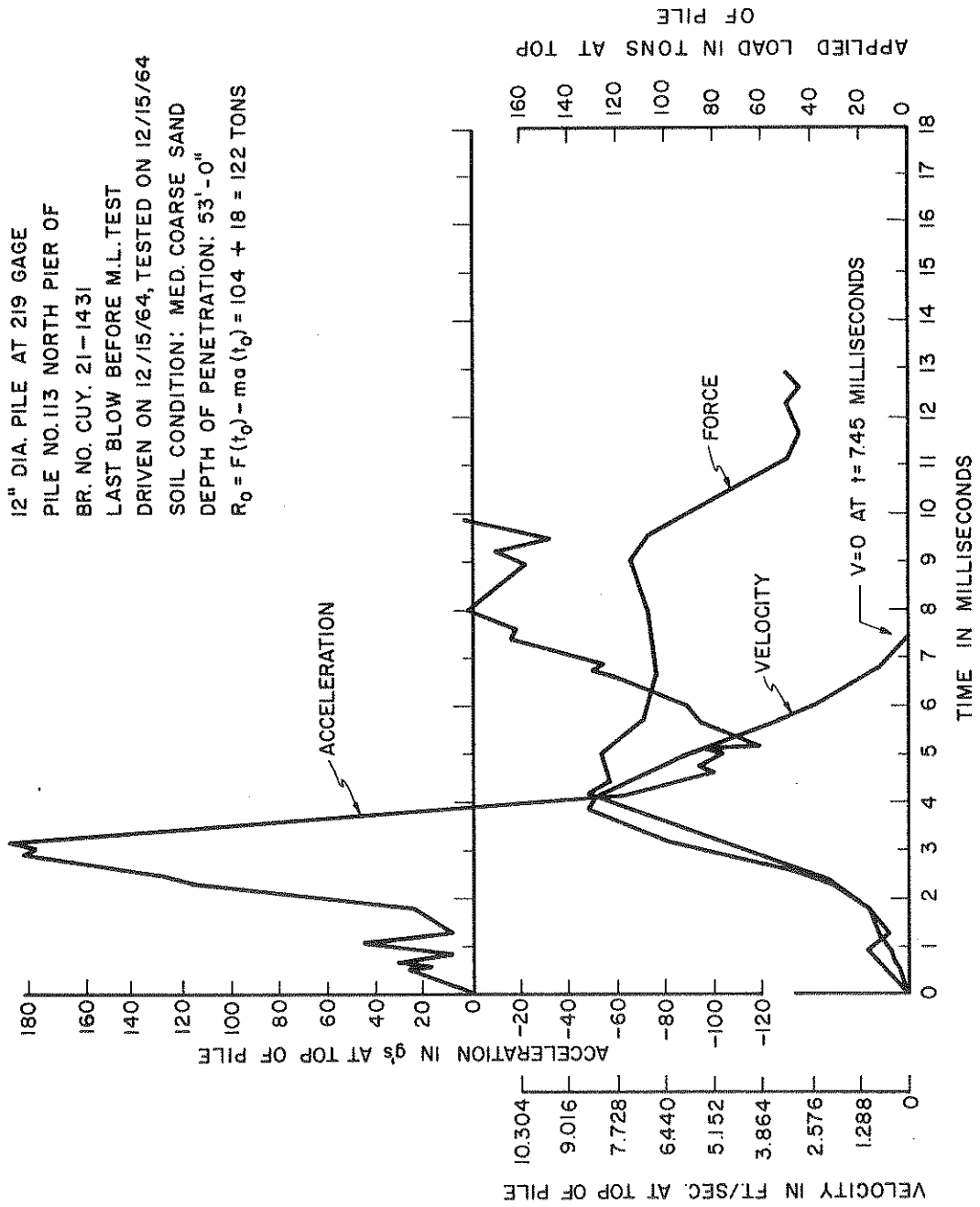

FIGURE 5.33

Dynamic Results of Full Scale Pile No. 113 North Pier of Bridge No. Cuy 21-1431

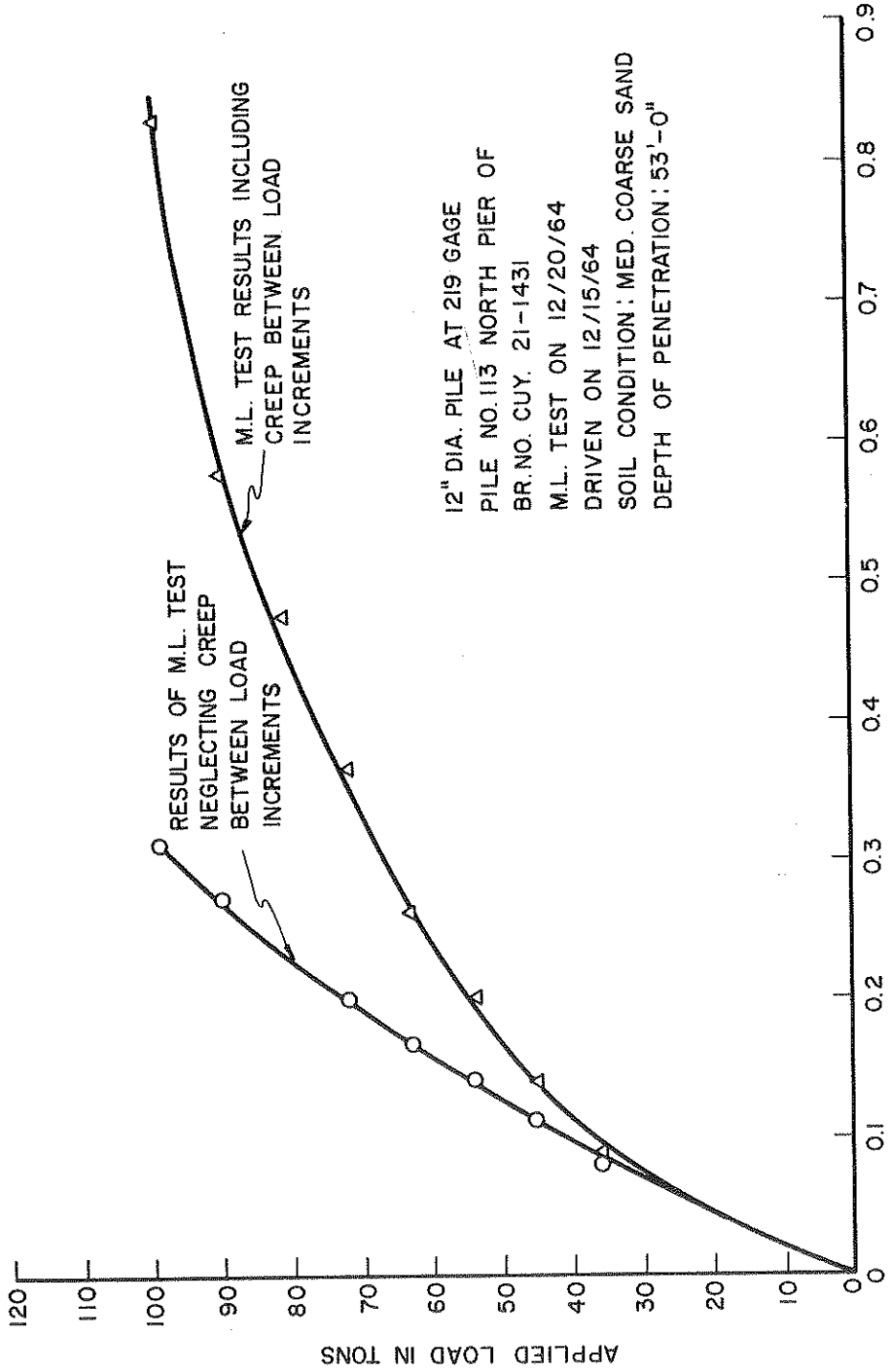

FIGURE 5.34

Results of M.L. Test Performed on Pile No. 113 North Pier of Bridge No. Cuy. 21-1431

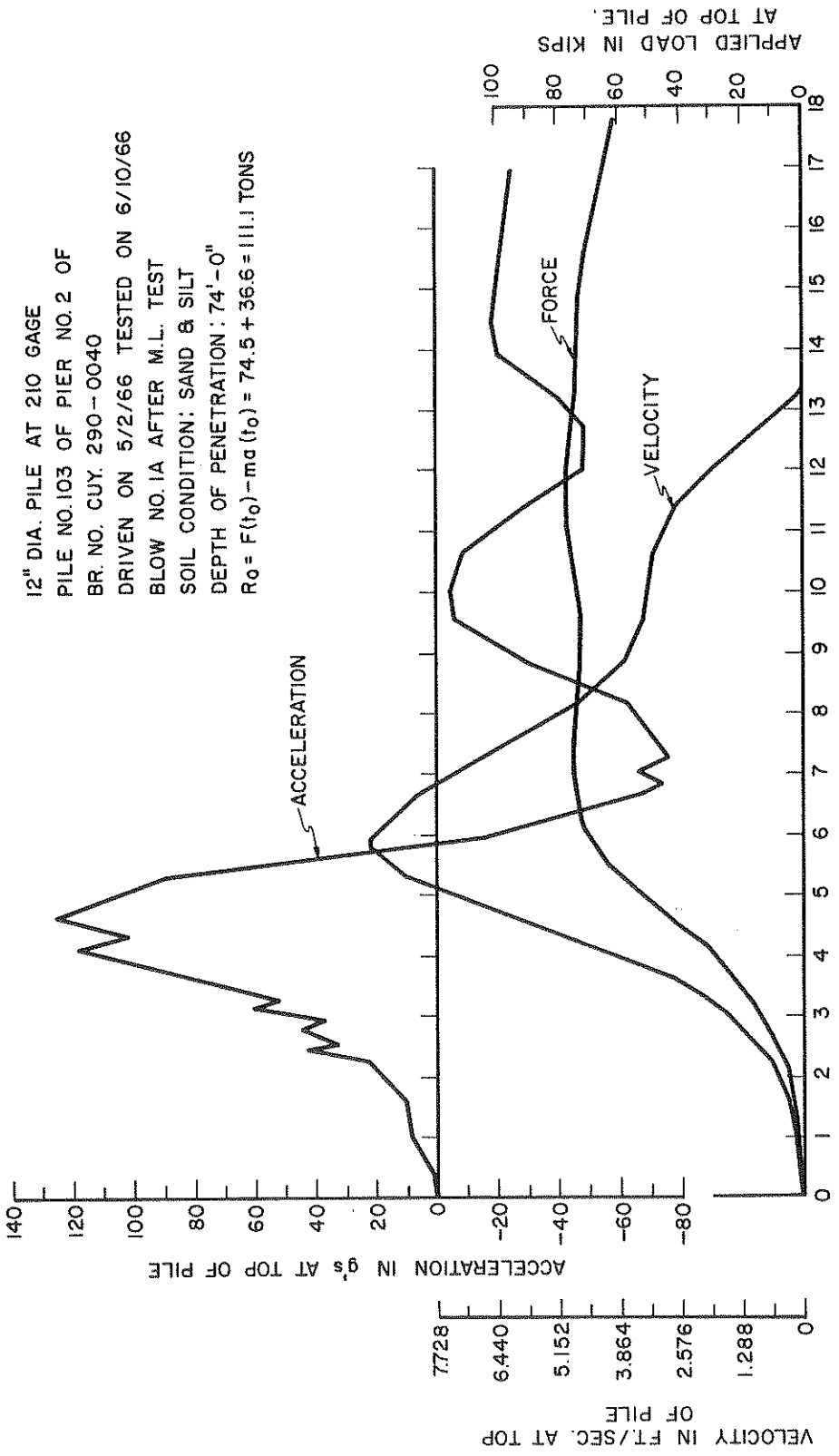

FIGURE 5-35

Dynamic Results of Full Scale Pile No. 103 of Pier No. 2, Bridge No. Cuy. 290-0040
Blow No. 1A After M.L. Test

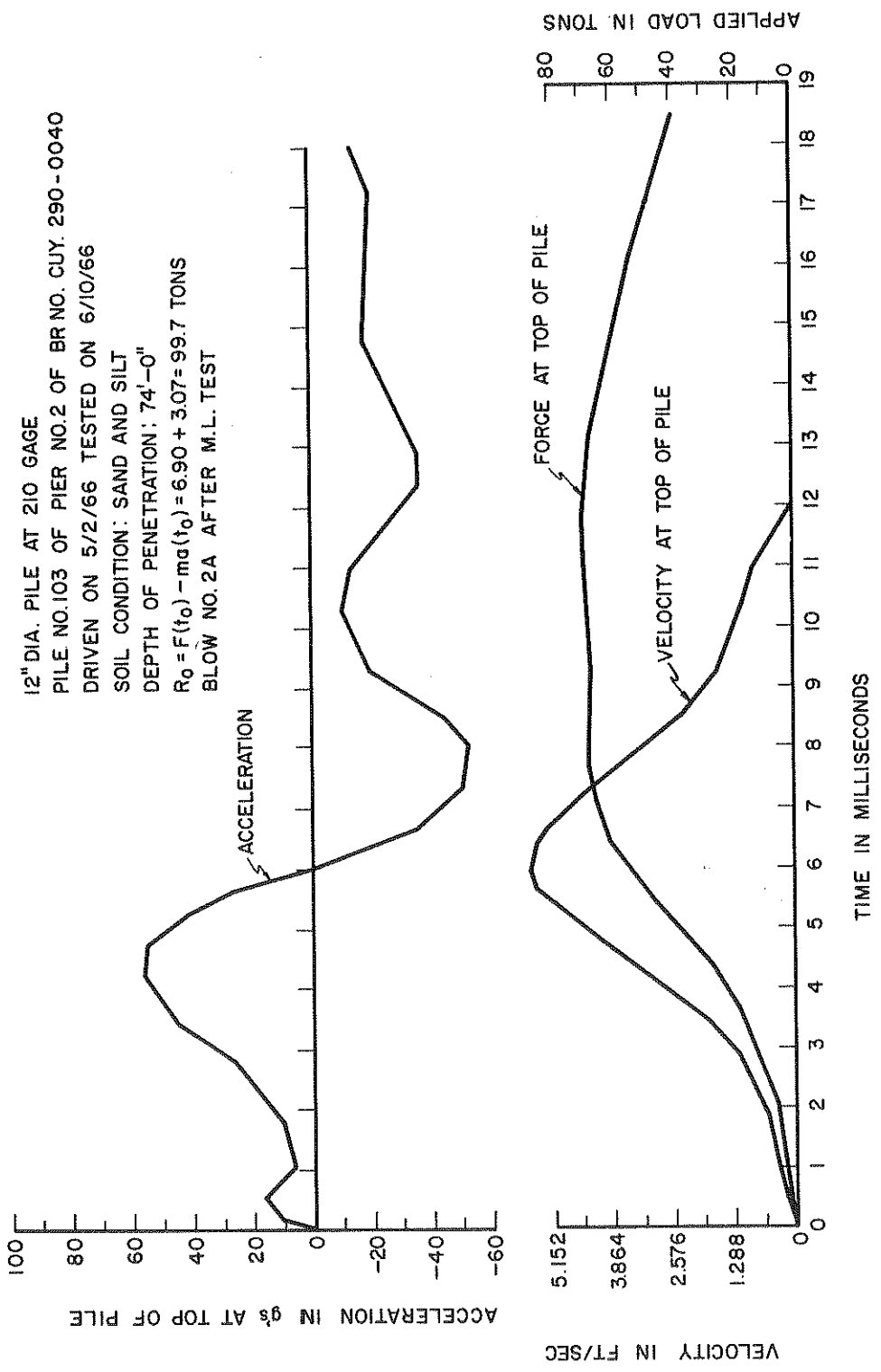

FIGURE 5.36

Dynamic Results of Full Scale Pile No. 103 Pier No. 2 of Bridge No. Cuy 290-0040, Blow No. 2A

After M.L. Test

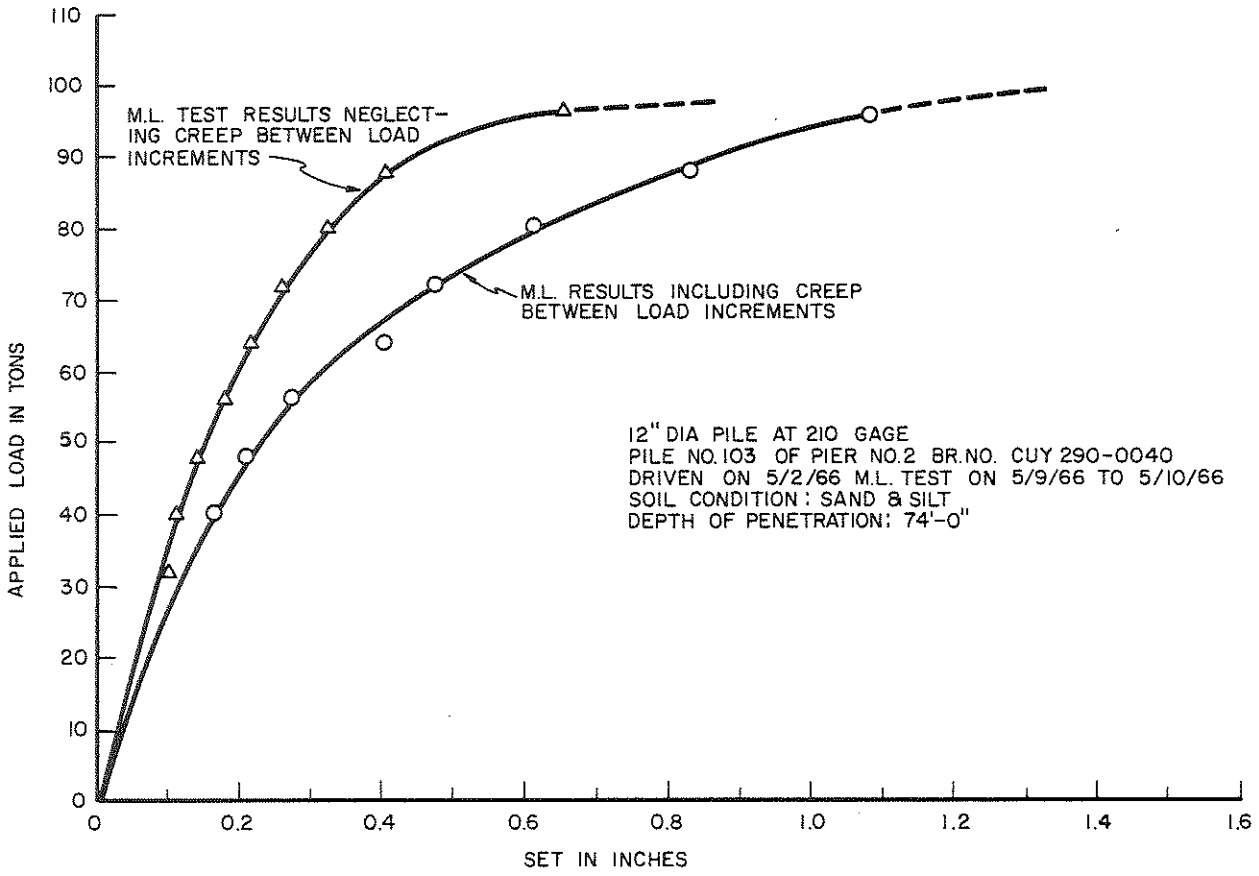

FIGURE 5.37

M.L. Test Results of Full Scale Pile No. 103, Pier No. 2 of Bridge No. Cuy. 290-0040

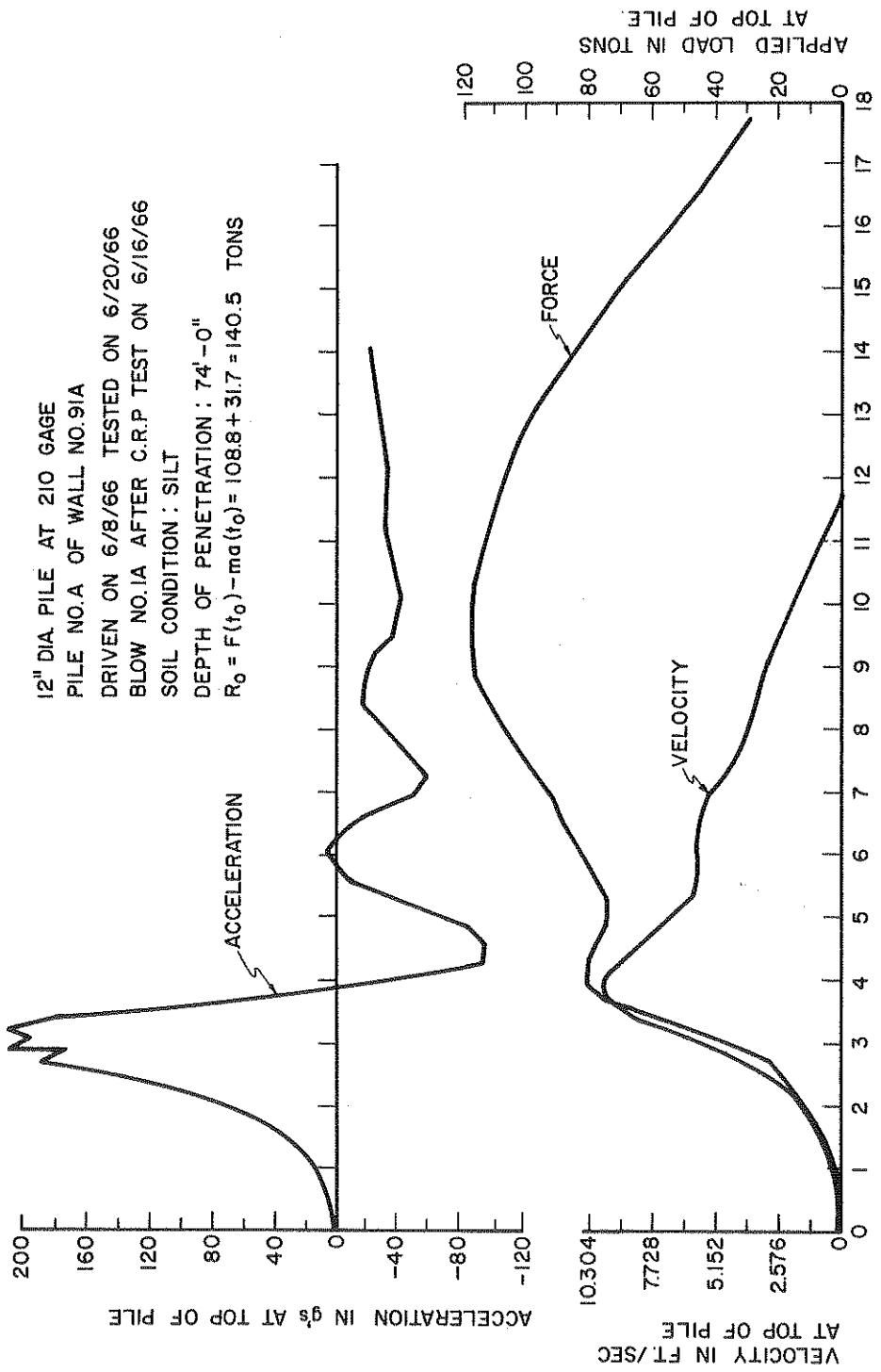

FIGURE 5.38

Dynamic Results of Full Scale Pile No. A of Wall No. 91A Blow No. 1A After C.R.P. Test

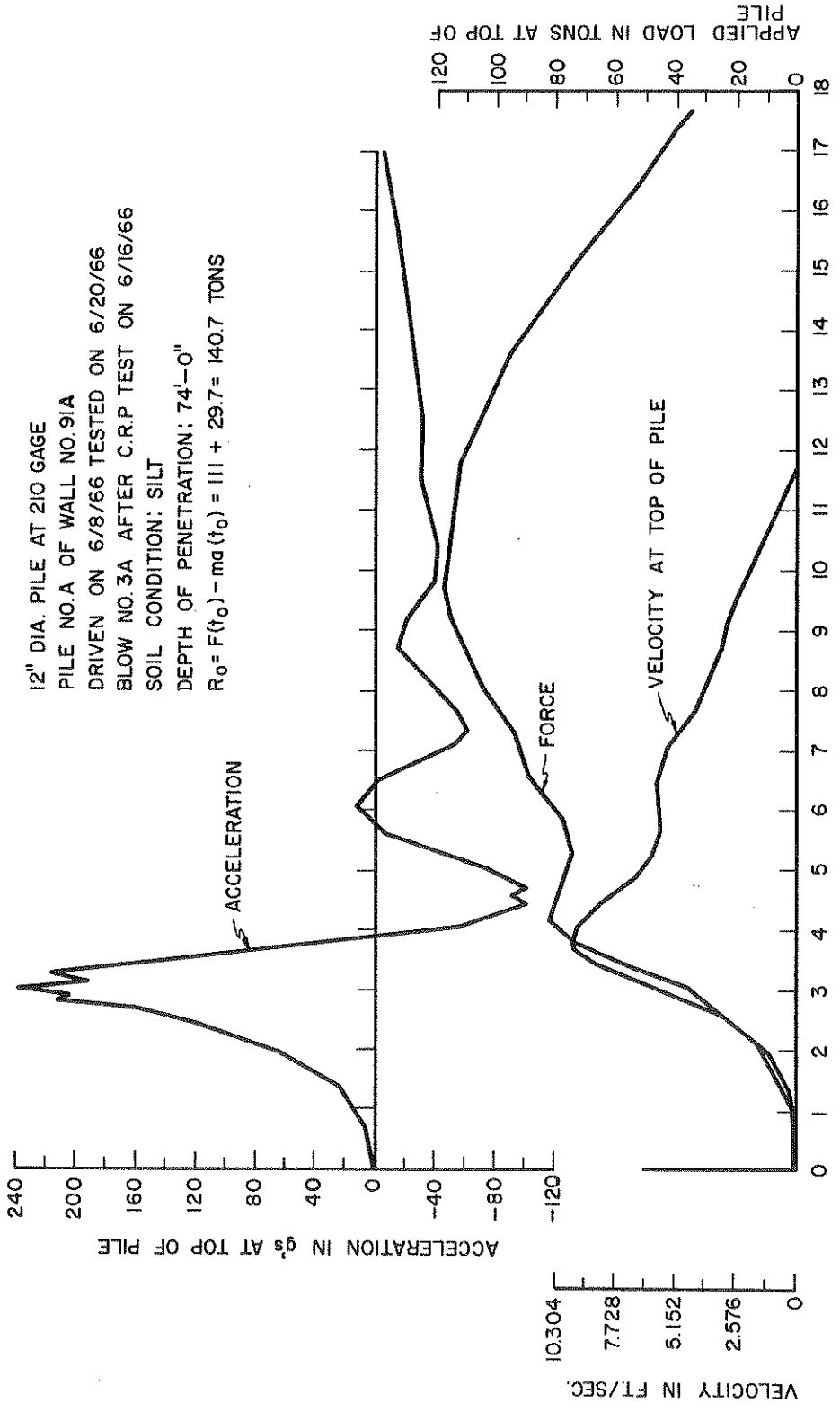

FIGURE 5.39

Dynamic Results of Full Scale Pile No. A of Wall No. 91A Blow No. 3A After C.R.P. Test

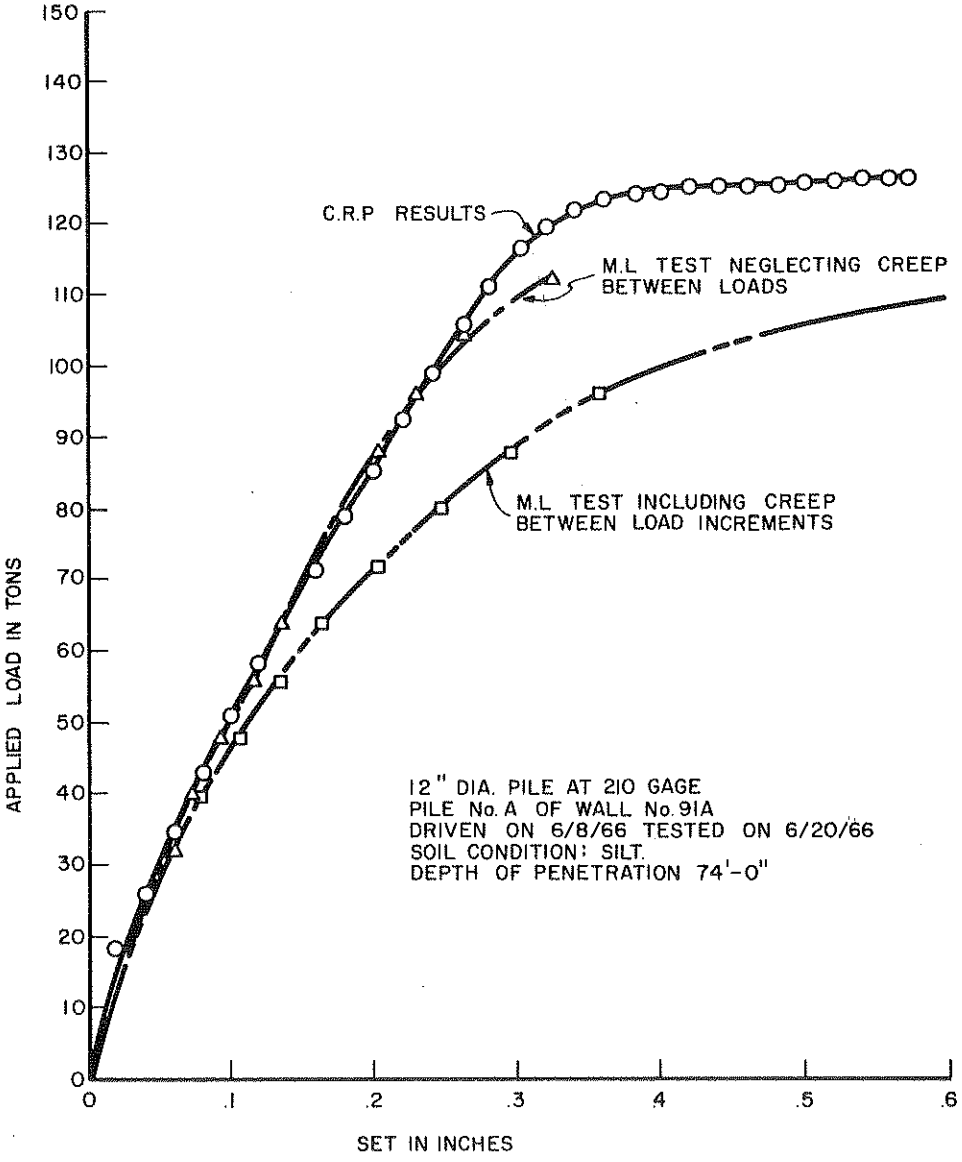

FIGURE 5.40

C.R.P. and M.L. Test Results of Full Scale Pile No. A of Wall No. 91A

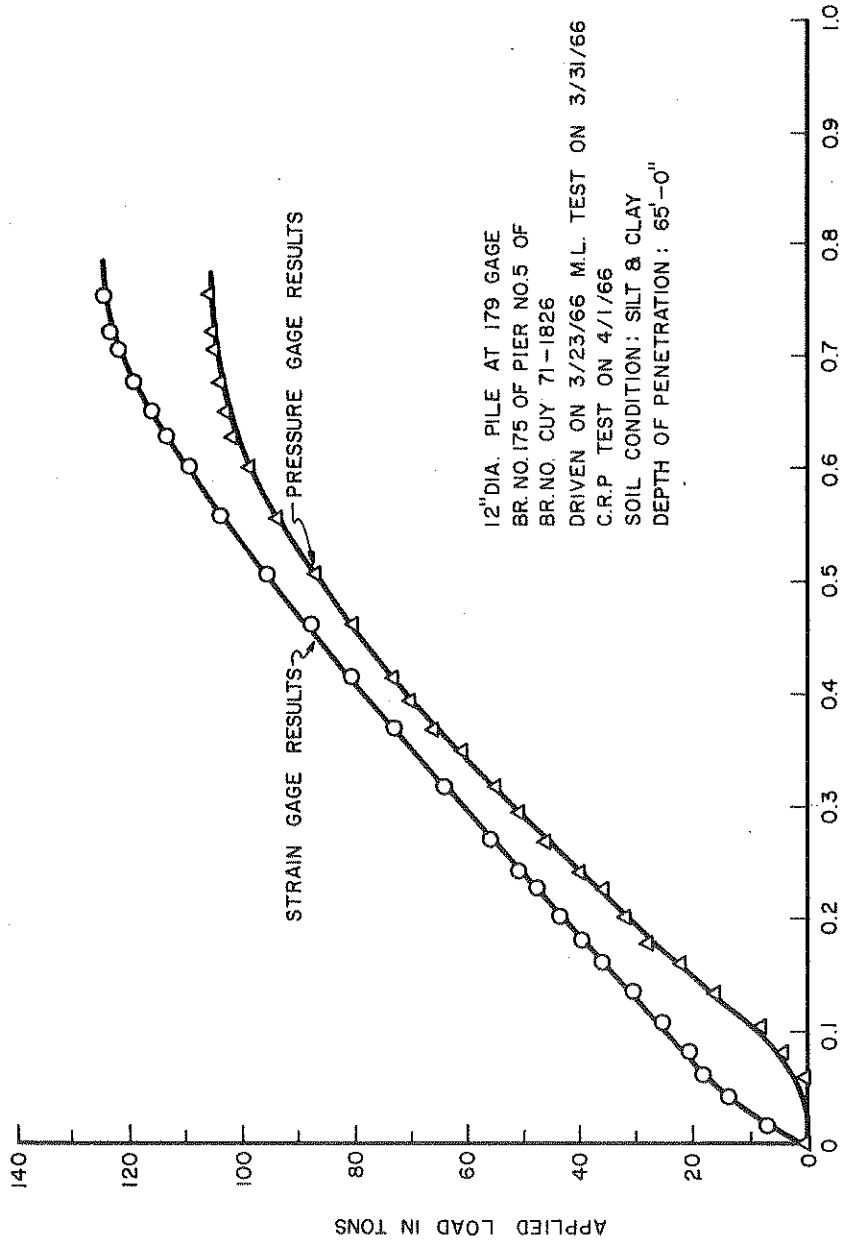

FIGURE 5.41

Comparison of Load Obtained From Strain Gages and Pressure Gage Supplied by Contractor

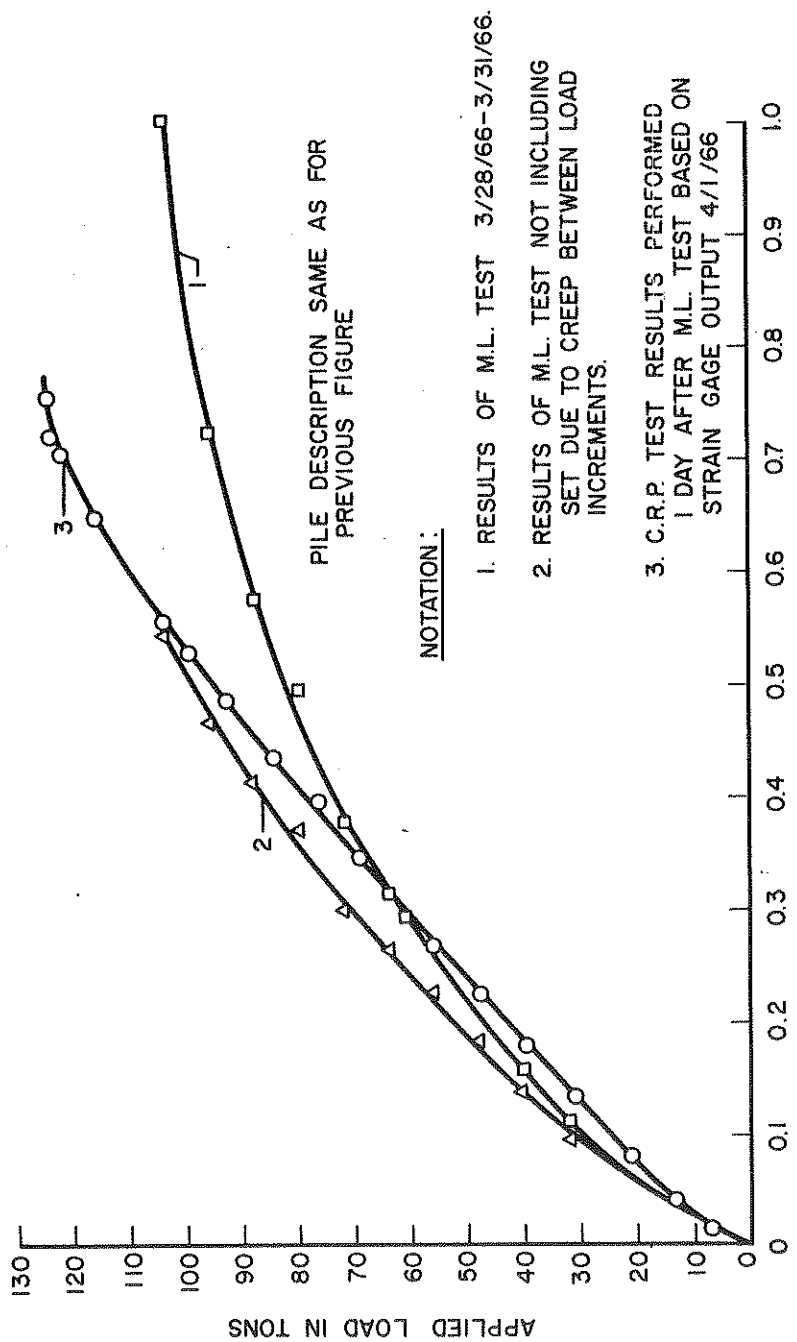

FIGURE 5.42

C.R.P. and M.L. Test Results Performed on Full Scale Pile No. 175 of Pier No. 5 of Bridge No. Cuy. 71-1826

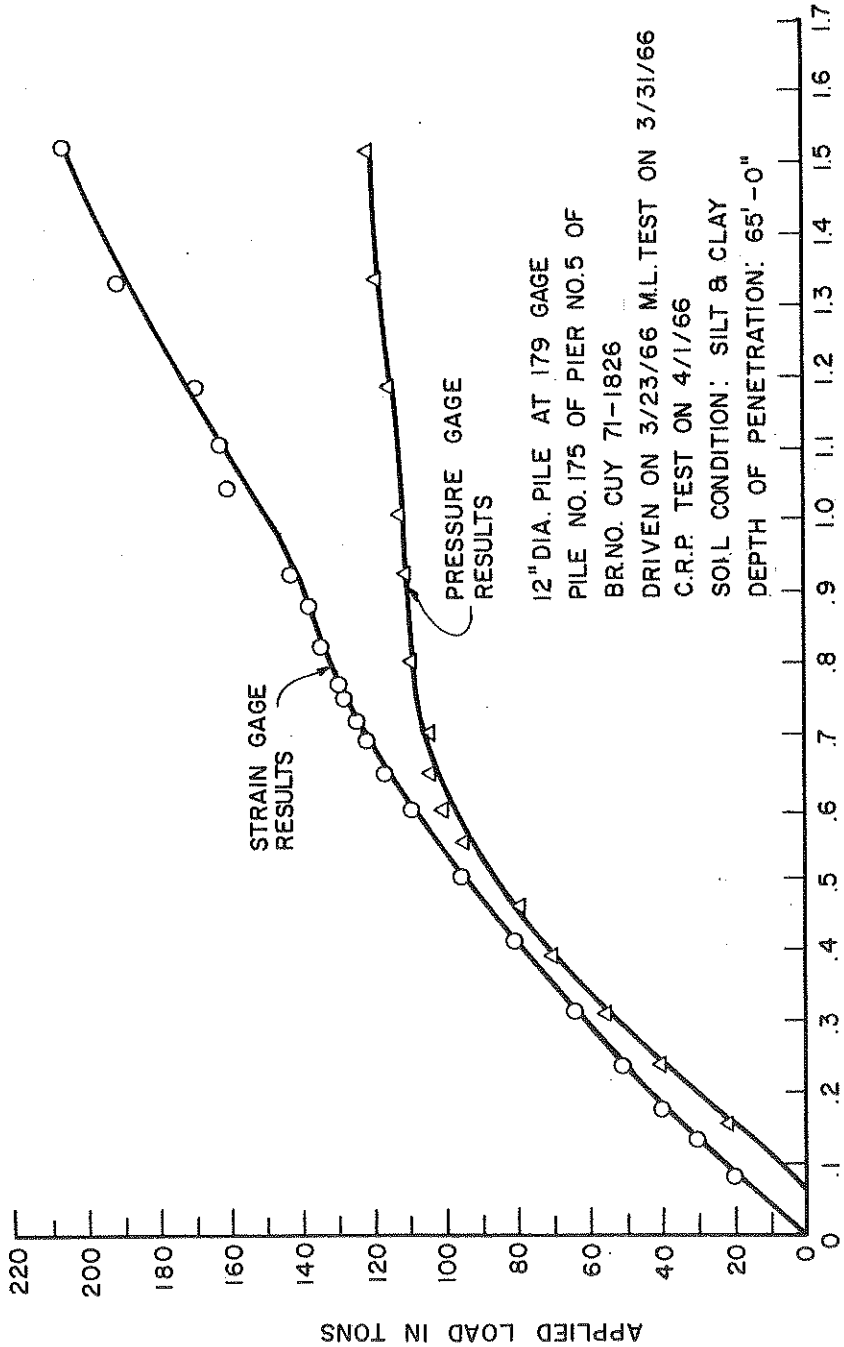

FIGURE 5-43

Comparison of C.R.P. Test Results Using Strain Gages and Pressure Gage Supplied by Contractor